WL-TR-93-7058

Kinetics and Mechanisms of Thermal Decomposition of Nitroaromatic Explosives

Thomas B. Brill
Kenneth J. James

Department of Chemistry and Biochemistry
University of Delaware
Newark, Delaware 19716

December 1993

FINAL REPORT FOR PERIOD APRIL 1990 - APRIL 1993

Approved for public release; distribution is unlimited.

WRIGHT LABORATORY, ARMAMENT DIRECTORATE
Air Force Materiel Command ■ United States Air Force ■ Eglin Air Force Base

REPORT DOCUMENTATION PAGE

Form Approved
OMB No. 0704-0188

1. AGENCY USE ONLY (Leave blank)	2. REPORT DATE	3. REPORT TYPE AND DATES COVERED
	20 April, 1993	20 April, 1990 to 20 April, 1993

4. TITLE AND SUBTITLE
Kinetics and Mechanisms of Thermal Decomposition of Nitroaromatic Explosives

5. FUNDING NUMBERS
C: F08635-C-0211
PE: 61102F
PR: 2302
TA: EW
WU: 13

6. AUTHOR(S)
Thomas B. Brill and Kenneth J. James

7. PERFORMING ORGANIZATION NAME(S) AND ADDRESS(ES)
Department of Chemistry & Biochemistry
University of Delaware
Newark, DE 19716

8. PERFORMING ORGANIZATION REPORT NUMBER

9. SPONSORING/MONITORING AGENCY NAME(S) AND ADDRESS(ES)
WL/MNME
Eglin AFB, FL 32542-5430

10. SPONSORING/MONITORING AGENCY REPORT NUMBER

11. SUPPLEMENTARY NOTES
unclassified; unlimited

12a. DISTRIBUTION/AVAILABILITY STATEMENT
Approved for Public Release; Distribution Unlimited

12b. DISTRIBUTION CODE

13. ABSTRACT *(Maximum 200 words)*

A critical examination of the kinetics and mechanisms of nitroaromatic explosives is made. The initiation reaction mechanisms differ with temperature. Shock initiation conditions produce mostly C-NO_2 bond homolysis. Impact initiation produces a mixture of C-NO_2 homolysis and reactions of the non-energetic substituents on the ring. Time-to-explosion for times longer than about 0.1 seconds is controlled mostly by catalysis from the decomposition products of the parent molecule. The explosive characteristics depend to a large extent on the relative proportions of the gaseous decomposition products that are generated in the initial reaction steps.

14. SUBJECT TERMS

TNT	Thermal decomposition mechanisms	Shock sensitivity
Aminonitrobenzene explosives	Nitroaromatic explosives	Time-to-explosion
Thermal decomposition kinetics	Impact sensitivity	

15. NUMBER OF PAGES
133

16. PRICE CODE

17. SECURITY CLASSIFICATION OF REPORT	18. SECURITY CLASSIFICATION OF THIS PAGE	19. SECURITY CLASSIFICATION OF ABSTRACT	20. LIMITATION OF ABSTRACT
unclassified	unclassified	unclassified	SAR

NOTICE

When Government drawings, specifications, or other data are used for any purpose other than in connection with a definitely Government-related procurement, the United States Government incurs no responsibility nor any obligation whatsoever. The fact that the Government may have formulated, or in any way supplied the said drawings, specifications, or other data, is not to be regarded by implication, or otherwise in any manner construed, as licensing the holder, or any other person or corporation; or as conveying any rights or permission to manufacture, use or sell any patented invention that may in any way be related thereto.

This report has been reviewed and is approved for publication.

FOR THE COMMANDER

Martin F. Zimmer

MARTIN F. ZIMMER
Technical Director, Munitions Division

Even though this report may contain special release rights held by the controlling office, please do not request copies from the Wright Laboratory/Armament Directorate. If you qualify as a recipient, release approval will be obtained from the originating activity by DTIC. Address your request for additional copies to:

Defense Technical Information Center
Cameron Station
Alexandria VA 22304-6145

If your address has changed, if you wish to be removed from our mailing list, or if your organization no longer employs the addressee, please notify WL/MNME, Eglin AFB FL 32543-5434, to help us maintain a current mailing list.

Do not return copies of this report unless contractual obligations or notice on a specific document requires that it be returned.

PREFACE

This program was conducted by personnel at the Department of Chemistry and Biochemistry, University of Delaware, Newark, Delaware, 19716, under contract FO8635-90-C-0211 with WL/MN, Eglin Air Force Base, Florida, 32542-5434. Dr. Robert L. McKenney, Jr, MNME, managed the program for the Armament Directorate. The program was conducted during the period 20 April, 1990, through 20 April, 1993.

TABLE OF CONTENTS

LIST OF TABLES

LIST OF FIGURES

GLOSSARY OF TERMS

TNT:	2,4,6-trinitrotoluene
NT:	nitrotoluene
DNT:	dinitrotoluene
MATB:	1-amino-2,4,6-trinitrobenzene
PA:	picric acid
DATB:	1,3-diamino-2,4,6-trinitrobenzene
TATB:	1,3,5-triamino-2,4,6-tinitrobenzene
TNB:	1,3,5-trinitrobenzene
RDX:	hexahydro-1,3,5-trinitro-s-triazine
HMX:	octahydro-1,3,5,7-tetranitrotetrazacine
Tetryl:	2,4,6-trinitrophenylmethylnitramine
HNS:	hexanitrostilbene
TACOT:	tetranitrodibenzo-1,3a,4,6a-tetrazapentalene
2,4-DNAn:	2,4-dinitroanthranil
DSC:	differential scanning calorimetry
DTA:	differential thermal analysis
GC-MS:	gas chromatography - mass spectroscopy
MS/MS:	tandem mass spectroscopy
CID:	collision induced dissociation
IDSC:	isothermal differential scanning calorimetry
EG:	evolved gas analysis
ESR:	electron spin resonance
EI/MS:	electron impact/mass spectroscopy
UV:	ultaviolet
IR:	infrared spectroscopy
MO:	molecular orbital
MNDO:	modified neglect of diatomic overlap
MINDO/3:	modified intermediate neglect of differential overlap
SCF-MO:	self consistent field approximation-molecular orbital
STO-3G:	Slater-type orbitals - 3-Gaussian
STO-5G:	Slater-type orbitals - 5-Gaussian
SCF-3-21G:	self consistent field approximation-3-21-Gaussian
CINDO:	complete intermediate neglect of differential overall
TTX:	time-to-exotherm (explosion)
E_a:	activation energy
D:	detonation velocity
XPS:	x-ray photoelectron spectroscopy
RDS:	rate determining step
ΔSPE:	shake-up promotion energy
ρN:	density of $-NO_2$ groups in the crystal lattice
ΔH_{ex}:	heat of explosion
OB_{100}:	oxidant balance
ΔH_f:	heat of formation
MW:	molecular weight
ρ:	density
MP:	melting point
ΔH_{vap}:	heat of vaporization
T_b:	boiling temperature
$K^{\ddagger}$:	equilibrium constant for activated complex
$\Delta S^{\ddagger}$:	entropy of activation

T:	temperature
A:	frequency factor
BDE:	bond dissociation energy
∂:	average bond length
R:	correlation coefficient
Atm:	atmosphere

SECTION I

INTRODUCTION

No critical review exists of the thermal decomposition mechanisms of polynitroaromatic explosives. This void is surprising in view of the fact that 2,4,6-trinitrotoluene (TNT) has been available as a pure material since about 1870 and is the most widely used explosive. For any explosive the thermal decomposition mechanisms and resultant products are important details because they affect the opportunity to predict systematically the feasibility of large-scale synthesis, the long-term stability for purposes of storage, and the sensitivity to various stimuli, such as heat and mechanical impact. Although safety and performance of explosives are intimately tied to the thermal decomposition process, knowledge of the mechanisms does not automatically enable improvements in safety and performance to be made. However, without mechanistic information, the behavior of explosives remains highly empirical.

Robertson and Yoffe (Reference 1) and Wenograd (Reference 2) were among the earliest to connect thermal decomposition processes to initiation phenomena. Moreover, the thermal decomposition mechanisms and products are believed to influence the performance of the explosive, such as the Chapman-Jouguet (C-J) pressure (the pressure at the rear of the reaction zone of the detonation front) and the detonation velocity. For example Cook, et al. (References 3 and 4) proposed that the initial reaction kinetics were important in determining the detonation velocity. Zeman and co-workers expanded this notion by attempting to correlate the thermal decomposition kinetics of polynitroaromatic explosives at lower temperature with molecular structure (Reference 5), heat of explosion (Reference 6), detonation characteristics (References 5 and 7), and thermal stability (Reference 8). The critical temperature of a thermal explosion is related to Arrhenius kinetics by the Frank-Kamenetskii model (References 9-12).

A very large number of polynitrobenzene derivatives are known, of course. All reasonable trinitrobenzene derivatives will explode if subjected to an energy input exceeding a threshold value. TNT achieves its special position partly because of its

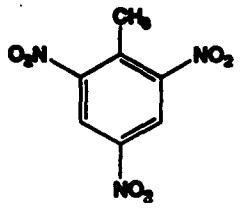

TNT

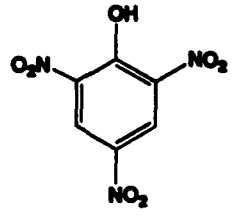

PA

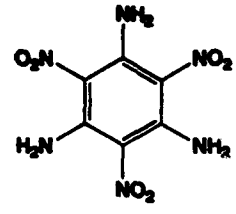

TATB

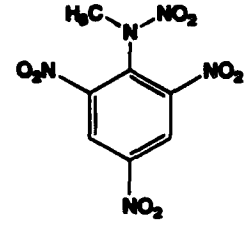

TERTYL

compatibility with other materials and low hygroscopicity, and partly because of its good thermal stability, relatively low sensitivity to impact and friction, and high explosion power. These characteristics influenced the German Army to adopt TNT in place of picric acid (PA), which is more hydroscopic, chemically reactive, and sensitive to impact. Other nitrobenzene derivatives having practical value as explosives are triamino-trinitrobenzene (TATB), 2,4,6-trinitrophenylmethylnitramine (Tetryl), hexanitrostilbene (HNS), and tetranitrodibenzo-1,3a,4,6a-tetrazapentalene (TACOT), which is used in two isomeric forms, Z and T, that differ in the position of the $-NO_2$ groups on the

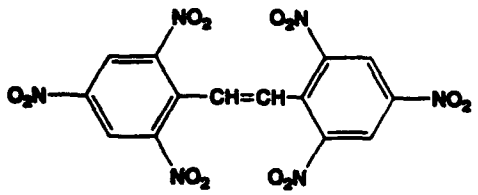

HNS

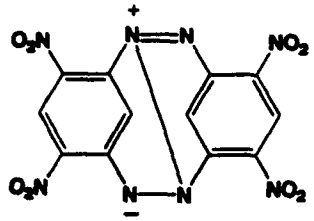

TACOT

the rings. TATB has excellent thermal stability and is especially noteworthy for its extreme insensitivity to impact. Likewise, TACOT has exceptional thermal stability. It is able to retain predictable explosive characteristics after ten minutes at 350°C making it useful for deep well oil exploration. Meyer (Reference 13) is a good source of practical aspects of explosives.

A large amount of work has been conducted on decomposition processes of polynitroaromatics. Of the many conclusions reached, some are contradictory, many are perplexing, some are in unavailable government documents, and others are in untranslated, poorly circulated (at least in the West) Russian literature. This article is an attempt to assess critically the literature of decomposition processes of polynitroaromatic explosives and to come to some conclusions about the dominant thermal mechanisms in the bulk phase.

First, it is necessary to outline why thermal decomposition mechanisms of explosives have produced divergent literature. Treacheries of the materials aside, the complications and realities of thermolysis processes of relatively large molecules in their bulk state and the restrictions on measurements are highlighted next in Sections II. 1-4.

SECTION II

SPECIAL CONSIDERATIONS OF EXPLOSIVE DECOMPOSITION CHEMISTRY

The results and, ultimately, the description of thermal decomposition of an explosive depend on the amount and configuration of the sample, the rate and magnitude of energy loading, the diagnostics employed, and the interpretative scheme. Experimental conditions are frequently dramatically different from one laboratory to another which complicates comparison of the data.

1. Decomposition Depends on the Conditions of Thermal Stimulus

The numerous decomposition reactions of a complex organic molecule in the bulk condensed phase each have their own rate constant and sensitivity to temperature. The temperature to which the bulk material is heated and the heating rate controls the time that the products have to form. At lower temperatures, processes with lower activation energies and greater exothermicity are favored. Time is available for stable products to grow in concentration via the complex reaction network and to serve as catalysts. At higher temperatures, the higher activation energy and more endothermic processes increase in importance. However, the products have a shorter time to form and may or may not be the same as products formed at lower temperature. At least the product distribution will be different. Consequently, descriptions of decomposition processes depend significantly on the temperature and the heating rate, a fact that has led to many contradictory assertions. Aside from the chemistry, the physical details about the material, such as its thermal conductivity, heat capacity, hardness, void volume, void size, etc., contribute to the details of the decomposition process, especially during mechanical stress. The conversion of mechanical energy into chemical effects (Reference 14) is being addressed at an increasingly sophisticated level (References 15-19).

a. Low Heating Rate/Low Temperature

Programmed heating over minutes or hours to a chosen temperature while monitoring the change of heat flow or pressure is the basis of differential scanning calorimetry (DSC), differential thermal analysis (DTA), and manometry. The decomposition rates extracted tend to apply to the lower activation energy processes and reflect the overall (global) process, rather than a particular step. Zeman and co-workers (References 5-8) claim that correlations exist between the activation energies during the induction period before autocatalysis takes over and detonation properties pertaining to high pressure and temperature, such as the heat of explosion (Reference 6), C-J pressure, and detonation velocity (Reference 7). They suggest that the rate of early decomposition process is

extendable to high temperature and pressure conditions. The products that are isolated by solvent extraction of TNT heated to a temperature characteristic of slow decomposition are numerous and frequently difficult to identify (References 20 and 21).

b. Moderate Heating Rate/High Temperatures

Heating times in the range of 20 - 500 μsec to a chosen high temperature can be achieved by T-jump methods (References 2,22). Wenograd (Reference 2) quotes heating rates of an explosive packed into a hypodermic needle at 2.5 x 10^7 K/sec. These rates are undoubtedly optimistically fast because models indicate that the rate of heat transfer to the explosive cannot keep pace with the heat that is believed to be supplied (Reference 23). Heating times of <1000 μsec to a chosen temperature are important because they simulate conditions that exist during mechanical impact and during combustion. In fact, a frequently used index of the sensitivity of an explosive to mechanical impact is the drop weight impact test. The impact sensitivity is the height, H_{50}, that a weight of given mass must be dropped onto the sample to produce an explosion 50% of the time. The duration of heating during impact is 200 - 300 μsec (Reference 24) and the pressure achieved is 7 - 15 kbar. In addition to the chemical reactions, h_{50} is affected by a score of other variables including the particle size, hardness of the crystals, the defect number, the defect volume, the crystal size distribution, the atmospheric conditions, and the operator technique. Given the many factors that influence the impact sensitivity, numerous shots are averaged while holding constant as many of the variables as possible. Not surprisingly, some scatter in the data occurs.

Robertson and Yoffe (Reference 1) concluded that chemical decomposition during impact is very similar to that at less rapid heating rates. This notion was extended by Wenograd (Reference 2) who found that the impact sensitivity of a series of diverse explosives roughly correlated with the temperature to which the sample could be raised in 250 μsec. Thereby, he too concluded that impact sensitivity was linked to thermally induced chemistry. The temperature achieved by several explosives, including TNT, in this time exceeded 1000°C. It should be emphasized that this result does not link thermal stability with impact sensitivity, because thermal stability is controlled by lower activation energy reaction branches which become de-emphasized in favor of higher activation energy branches at higher temperatures.

The drop weight impact test does not provide chemical details about the thermal processes. To achieve this information, a technique such as T-jump/FTIR spectroscopy (Reference 22) can be used. This technique is able to separate and detect some of the dominant reaction branches during rapid heating, and to determine the temperature dependence of some of these branches (References 22,25).

c. High Heating Rate/High Temperature/High Pressure

The use of a shock wave to heat a material affords a heating time to a high temperature of less than 1 μsec. For example, the chemical peak corresponding to 95% decomposition TNT in a stationary detonation has a duration of 0.4 μsec (Reference 26). Pressures for shocked condensed phase materials are in the range of 30 - 200 kbar. The shock sensitivity of many, but not all, polynitroaromatics for which data are available follows the same trend as the impact sensitivity (Reference 27) suggesting that the shock initiated chemistry is similar to impact initiated chemistry. However, a considerable body of Russian literature indicates that this is not always the case (Reference 28).

An up-to-date overview of shock and detonation physics of explosives is available elsewhere (Reference 29). In practice shock compression of a solid or liquid can be induced in a number of ways that usually employ a flyer plate. The most common method is to use a standard explosive to transmit a shock wave through a buffer plate to the explosive of interest. Tests known as "wedge" and "gap" are well-known to workers in the field. For example, the Navy small scale gap test uses a booster explosive in a standard configuration to transmit a high pressure shock wave through a Plexiglas attenuator to the explosive packed at a particular density compared to the theoretical maximum density. The shock sensitivity is determined by the pressure at which an explosion occurs 50% of the time. For example, P_{90} would be the initiation threshold pressure for an explosive packed at 90% theoretical maximum density. A comparison of various detonation sensitivity tests is given by Urizar, et al. (Reference 30). Electric spark sensitivity has also been compared to shock and impact sensitivity (Reference 31).

For studies of unimolecular reactions in the gas phase at low pressure, a laser pulse (Reference 32) or a shock wave created by a burst of gas pressure (References 33,34) can be used to heat molecules to a high temperature in ≤1 μsec. Temperatures in excess of 800°C can be achieved by shock tube and laser pyrolysis. Lower and higher activation energy processes can be expected to compete effectively with one another under these conditions.

In summary, the reaction temperature and the heating rate play an important role in how the thermal decomposition process of a complex molecule occurs. Some reactions can be expected to be present over a wide range of temperatures while others will not. Consequently, considerable care is needed when comparing the merits of reaction pathways derived from measurements made under diverse conditions.

2. Experimental Diagnostics for Chemistry of Explosives

Interpretations of the chemistry that is important in an explosive depend on the diagnostic method, because the time resolution, the pressure, the temperature, the sample quantity, and the phase are major variables. The relatively high vapor pressure of many nitroaromatic compounds makes them amenable to study by gas phase as well as condensed phase analytical techniques.

a. Dynamic Analysis

Ideally the course of the reactions could be followed directly in real time. When this condition is achieved for an explosive (Reference 35), the spectral window is narrow and the amount of detailed information is limited. More commonly, simulation of conditions is required to optimize the chemical detail.

Manometry is used extensively in Russia, especially by Maksimov, to determine the rate of gas evolution as a function of temperature for many nitroaromatic compounds. Typically, a 15 - 20 cm^3 glass vessel fitted with a Bourdon-type compensation manometer is immersed in a thermostated bath. Evaporation of the compound is sought so that the decomposition rate can be measured in the gas phase. However, transfer of heat from the glass surface to the nitroaromatic molecule at the temperatures used is primarily by conduction. The molecule must collide with the wall where heterogeneous catalysis can be appreciable. Nevertheless, a large percentage of the rate data for aromatic nitrocompounds has been obtained by this method.

DSC and DTA have been applied extensively to obtain rate data for the condensed phase decomposition of energetic nitroaromatic compounds. These techniques extract the rate of the processes from the overall heat flow at relatively low temperatures and heating rates. Details of the kinetics are sometimes over-shadowed by the fact that energetic materials can generate heat rapidly and the instrument is limited by its ability to detect heat changes instantly. As a result, the rate data are sensitive to the sample size. As with manometry, the global reaction rate is measured. The reactions that are responsible for the rate must be inferred.

Mass spectrometry is more broadly applicable to the study of thermal decomposition mechanisms of nitroaromatic compounds than it is for many other energetic materials. The foundation of this notion lies in the extensive work of Fields and Meyerson (References 36,37), who investigated the mass spectra of numerous nitroaromatic compounds and concluded that the early fragmentation patterns closely resemble the thermal decomposition routes. This finding can not be applied broadly to other energetic materials.

With nitramines, for example, the species produced by thermal routes and those generated by electron impact must be carefully differentiated (Reference 38).

Electron impact mass spectrometry yields only the fragments and not their mechanism of formation (Reference 39). Tandom mass spectroscopy (MS/MS) used in conjunction with collision induced dissociation (CID) elucidates the fragmentation pathways of individual ions. The principle is that mass selected primary ions are fragmented in a reaction cell as a result of collisions with an inert gas. These daughter ions are then analyzed by a second MS, thereby enabling determination of the individual fragmentation pathways of the parent ions (Reference 40).

Electron spin resonance potentially yields mechanistic information, but it is sensitive only to radicals that form and degrade during thermal decomposition in the condensed phase. Very low concentrations ($< 10^{-4}$ M) are readily detected. There is no way to prove that the radicals observed are the key species in the decomposition mechanism. Non-radical and ionic pathways are always possible. Assignment of structure and composition of the species is sporting, especially for complicated condensed phase decomposition reactions that produce closely related radicals.

b. Post Reaction Analysis

Rapid-scan FTIR spectroscopy is a near real-time analytical technique with a wide spectral window. The gaseous decomposition products at sub-atmospheric and super-atmospheric (~100 atm) can be determined at heating rates up to 2×10^{4}°C/sec (Reference 22). Structure/decomposition relationships can be developed (Reference 41) and the sequence of product formation outlines the decomposition mechanism (References 22,25). The products detected are not the elementary radicals, but the more thermally and kinetically stable species.

Unimolecular decomposition in the gas phase can be induced at high temperature by use of a pulsed laser (References 32,42) or a shock impulse (References 33,34). The quenched products can be analyzed by a variety of techniques, such as by GC-MS.

Essentially the full range of analytical techniques can be applied to analyzing species in a quenched sample that have been generated by heating or mechanically abusing the material. The caveat is that the most reactive intermediates which are central to the decomposition mechanism at elevated temperature will rearrange and react further upon cooling and during time delayed analysis. The thermodynamically and kinetically more stable species therefore are always detected. These species are only a historical record of the most relevant dynamic processes.

3. Complexity of Thermal Decomposition in the Condensed Phase

Unperturbed unimolecular decomposition kinetics can be determined only for molecules in the gas phase at low pressure. Materials that are useful as explosives or propellants almost always begin to react in the condensed phase. Thus, while gas phase studies of individual molecules can be useful guides to the behavior in other phases, the most important reactions arise when the molecules are in the condensed phase in the presence of like molecules. For instance, by using the oxidation of hydrocarbons as an analogy, the liquid phase reaction is rarely unimolecular, but the propagation steps can be similar in the liquid and the gas phase (Reference 43).

Qualitative accounts of the decomposition process of bulk TNT and TATB indicate that determination of the mechanisms of polynitroaromatic derivatives in the presence of neighboring molecules is an extraordinary difficult problem. Robertson (Reference 44) described the behavior of TNT when heated to a constant temperature in a closed ampule. TNT melted at 81°C and partially volatilized, followed by a quiescent period with no gas evolution. Next, gas evolution began accompanied by darkening followed by more rapid gas evolution and then explosion. During the period of darkening, the amount of gas is small (about 1 mole per mole of TNT) and catalysts form (Reference 20). Catalano and Crawford (Reference 45) observed that exothermic decomposition of TATB begins at about 302°C and found that the reaction stage in the 342 - 357°C range necessitated the use of five different rate expressions. These observations are stark reminders that the aggregation of many time-dependent chemical and physical processes occurs during the thermal decomposition of a material in the condensed phase. Despite the complications, major temperature segments of the decomposition regime follow Arrhenius behavior, equation 1. E_a is the activation energy, A is the frequency factor, and k is the reaction rate.

$$k(T) = Ae^{-E_a/RT} \qquad (1)$$

The major perturbations to the elementary decomposition reactions of an isolated polynitrobenzene molecule when the molecule is part of a bulk condensed phase are:

(1) Bimolecular reactions (References 46,47) and intermolecular associations (Reference 48);

(2) Homogeneous and heterogenous (References 32,49,50) catalysis (References 20,34,44,51) by reaction products;

(3) Heterogeneous catalysis by the supporting surface and the reactor walls (References 7,32,44,48,49,52-56).

Intermolecular association and atom transfer have been proposed by Maksimov (Reference 48) to be responsible for the fact that the rate of decomposition of TNT in the melt phase is about ten times faster than in the gas phase or in solution. The reverse is true of most other energetic molecules, such as nitrate esters, hexahydro-1,3,5-trinitro-s-triazine (RDX), and octahydro-1,3,5,7-tetranitrotetrazacine (HMX) (Reference 48). In fact, the specific rate constants for many condensed phase decomposition reactions of polynitroaromatics are 10^5 - 10^{10} sec^{-1}, which is below the limit of 10^{12} sec^{-1} for many unimolecular reactions and is suggestive of bimolecular processes (Reference 48).

An important factor contributing to the faster rate of condensed phase reactions compared to the gas phase is catalysis by the reaction products. For this reason virtually every kinetic study of decomposition of polynitroaromatic explosives in the condensed phase since an early report (Reference 57) has found that an autocatalytic expression is required to fit the rate data. Of course, very small amounts of catalyst can markedly influence the rate of most reactions. In fact, Maksimov (Reference 58) proposed that impurities in the original sample sharply change the rate of decomposition of nitroaromatic compounds. Irrespective of the impurities, many compounds (References 20,44,51,59,60) including essentially any source of H• or other radicals, accelerate the rate of decomposition of TNT (Reference 51). TNT and most of its decomposition products produce radicals at the 10^{-4} M level (Reference 61) when heated below 300°C. Several specific decomposition products of TNT have been tested and are found to catalyze decomposition of TNT. These include 2,4,6-trinitrobenzaldehyde (Reference 20), 2,4-dinitroanthranil (2,4-DNAn) (References 51,59), an ill-defined explosive "coke" from long-term thermal degradation (Reference 20), and elemental carbon (Reference 62). The role of catalysis by low levels of decomposition products is not readily separable from the role of intermolecular associations (Reference 48) mentioned above. Therefore, catalysis rather than intermolecular associations may be responsible for the faster rate of decomposition of TNT in the condensed phase compared to the gas phase.

The influence of catalysis by the walls of the reactor and the supporting surface of the sample has been mentioned by many authors as a potential factor in the reaction rate (References 7,32,44,48,49,52-54,63), but has been investigated systematically in only a few studies. For example, Maksimov (Reference 53) found that increasing the surface area of the glass reaction vessel with the aid of capillaries greatly accelerated the initial rate of decomposition of trinitrobenzene derivatives in the vapor phase. Since the wall and bulk phase decomposition mechanisms are thought to be the same (References 46,53,63), it is difficult to separate the role of catalysis by the decomposition products from the role of surface catalysis.

One of the more helpful empirical insights for sorting out thermal decomposition schemes of trinitrobenzene derivatives in the condensed phase is the observation that initial fragmentation patterns in the EI mass spectrum seem to parallel thermal decomposition schemes in the gas phase (References 36,37,64,65). Moreover, it is helpful that the early thermal decomposition products found in the gas phase closely resemble the stable intermediates formed by heating the condensed phase. While the elementary steps leading to these molecules are undoubtedly altered somewhat by the phase, the similarity of the stable species in the gas phase and the stable intermediates in the condensed phase supports a role for them in the decomposition sequence, at least under certain conditions. However, because of catalysis by the decomposition products and intermolecular interactions as noted above, there is no reason to assume that the reaction details of a nitrobenzene derivative in the gas phase or in dilute solution will be the same as the bulk material.

4. Uncertainty about Determining Molecular Control over Explosive Behavior

It was noted in Section I that there are strong reasons to believe that thermochemistry is in some way connected to impact and shock initiation of explosives (References 1-12,27,66). The desire to understand the controlling molecular mechanisms of impact and shock sensitivity of an explosive has led to many published correlations of explosive data with molecular properties. The most extensive of these compilations for nitroaromatic compounds are by Kamlet and Adolph (Reference 24), Zeman (References 5-8,54), and Storm, et al. (Reference 27). A number of other correlations of molecular and crystal parameters with explosives behavior have been noted for the limited, but attractively related, set of the four compounds TNB, MATB, DATB and TATB. However, this series is also an excellent illustration

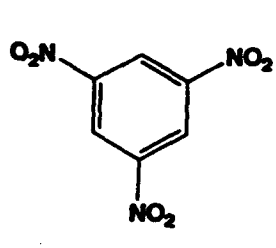

TNB

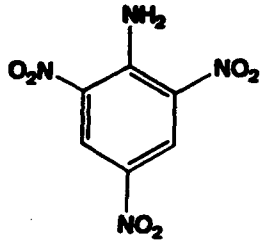

MATB

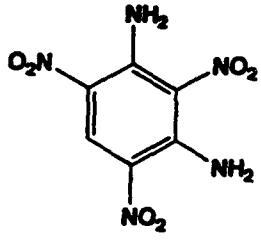

DATB

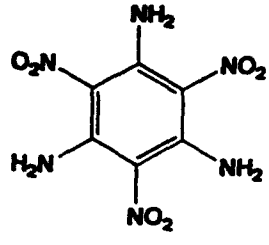

TATB

of the problems of correlating of molecular variables with explosive properties in an attempt to find the controlling mechanism. For TNB, MATB, DATB and TATB these variables are categorized according to whether the basis is predominantly the

explosive characteristics (Table 1), the composition and crystal properties (Table 2) or the molecular and electronic structure (Table 3). Most of the entries are self-explanatory, but a few require brief description. The impact sensitivity, H_{50}, the shock initiation threshold pressure, P_{90}, and the Chapman-Jouguet pressure, P_{CJ}, were defined in Sections I and II.1. ΔH_{ex} is the heat of explosion. In Table 2, ρN is the density of $-NO_2$ groups in the crystal lattice defined by equation 2 (Reference 72) where

$$\rho N = \frac{ZM}{V} \tag{2}$$

Z is the number of molecules in the unit cell, M is the molecular

$$OB_{100} = \frac{100\,(2N_O - N_H - 2N_C - 2N_{COO})}{M} \tag{3}$$

weight, and V is the unit cell volume. The oxidant balance, OB_{100}, is defined according to equation 3 as the number of equivalents of oxygen in 100 gms of a CHNO explosive required to convert all of the H to H_2O and C to CO. N is the number of atoms of each element in the formula. The melting point is partly a reflection of the intermolecular cohesive forces. In Table 3, the electrostatic potential calculated at the mid-point of the $C-NO_2$ bond, V_{mid}, determined by a Mulliken orbital population analysis at the level of CINDO (Reference 73) and ab initio SCF-MO with STO-3G (Reference 74) or STO-5G (Reference 75) basis sets. The number of aromatic π electrons was calculated at the STO-3G level (Reference 67). The shake-up promotion energy separation, ΔSPE, of N(1s) of the $-NO_2$ groups was obtained by x-ray photoelectron spectroscopy (Reference 76). The average bond distances were obtained from the crystal structures (Reference 68-71).

Perusal of the columns of Tables 1-3 and of the Tables relative to one another reveals that a trend exists in all columns. To emphasize the similarity, the correlation coefficient, R, (Reference 2) and the confidence level of statistical significance according to the t test (Reference 77) equation (4), are given in Table 4 for all columns plotted versus the impact sensitivity, H_{50}. To exceed 95% confidence, the value of t for four data points (n) must exceed 3.18. In all cases

$$t = R\left(\frac{n-2}{1-R^2}\right)^{1/2} \tag{4}$$

except one, this confidence level is achieved. In fact, twelve data sets exceed 99% confidence ($t > 5.84$). The only case that fails 95% exceeds 90% confidence ($t > 2.35$). Furthermore, two sets of data that are linearly related to a third are linearly related to each other. Therefore, among the 18 sets of data in Tables 1-3, there are 153 positive correlations. A few of course

Table 1. Sensitivity and Performance Parameters

Compound	H_{50}, cm	P_{90}, kbar[c]	P_{CJ}, GPa[d]	ΔH°_{ex}, kJ g^{-1}
TNB	100[a]	15	22.9	4.734
MATB	177[a]	28	24.7	4.263
DATB	320[a]	46	26.7	4.138
TATB	490[b]	70	29.3	3.990

a. Reference 24
b. Estimated, but frequently used, see References 27 and 72.
c. Reference 5
d. Reference 7
e. Reference 6

Table 2. Compositional and Crystal Parameters

Compound	MW, g mol^{-1}	ρ, g cm^{-3}	ρN^{e}, g cm^{-3}	ΔH°_{f}, cal g^{-1}	mp, K	OB_{100}
TNB	213	1.688[a]	0.653	-41.8	396	-1.46
MATB	228	1.760[b]	0.646	-78	461	-1.75
DATB	243	1.837[c]	0.628	-122.6	559	-2.06
TATB	254	1.938[d]	0.623	-143	623[f]	-2.33

a. Reference 68
b. Reference 69
c. Reference 70
d. Reference 71
e. Reference 72
f. Not well characterized.

Table 3. Molecular and Electronic Parameters

Compound	$\bar{V}$mid, au			No. πe^-	ΔSPE,[e]	$\bar{d}$, Å		
	STO-5G[a]	STO-3G[b]	CINDO[c]		ev	C-NO_2	N-O	C-C
TNB	0.208	0.197	0.012	5.96[d]	0	1.482[f]	1.199	1.380[f]
MATB	0.174	0.168	-0.018	6.16	0.8	1.469[g]	1.219[g]	1.393[g]
DATB	0.146	0.130	-0.048	6.36	2.1	1.454[h]	1.233[h]	1.411[h]
TATB	0.103	0.102	-0.063	6.54	2.7	1.419[i]	1.243[i]	1.442[i]

a. Reference 75

b. Reference 74

c. Reference 73

d. Reference 67

e. Reference 76

f. Reference 68

g. Reference 69

h. Reference 70

i. Reference 71

Table 4. The Coefficients of Correlation and the Confidence Level based on the "t test" for Plots of all Entries in Tables 1-3 versus the Impact Sensitivity Index, H_{50}.

Parameter	Correl. Coeff, R^2	t (equation 4)[a]
P_{90}	0.998	31.6
P_{CJ}	0.992	15.75
ΔH_{ex}	0.773	2.61
W	0.952	6.30
ρ	0.991	14.83
ρN	0.927	5.04
ΔH_f	0.931	5.20
mp	0.972	8.33
OB_{100}	0.971	8.18
V_{mid}, STO-5G	0.982	10.45
V_{mid}, STO-3G	0.972	8.49
V_{mid}, CINDO	0.919	4.76
ΔSPE	0.950	6.17
No. π e^-	0.968	7.78
$\bar{\sigma}_{C-NO2}$	0.981	10.17
$\bar{\sigma}_{N-O}$	0.955	4.55
$\bar{\sigma}_{c-c}$	0.994	18.2

a. Significant at confidence level 90% $\geq$ 2.35; 95% $\geq$ 3.18; 99% $\geq$ 5.84.

are dependent or, at least, interconnected. The density and C-J pressure are related through the detonation velocity, D, by equation 5. The molecular weight enters into OB_{100} by equation 3.

$$P_{CJ} = 0.25\rho D^2 \quad (5)$$

The increase in the average C-C and N-O distances is paralleled by the decrease in the average C-NO_2 distance as -NH_2 groups are added. In some cases the correlations are pure folly even though R (Reference 2) is high. For example, melting point vs. shake-up promotion energy separation, heat of formation vs. density, molecular weight vs. the C-NO_2 mid-point electrostatic charge are among the more chemically ridiculous correlations.

On the other hand, several of the correlations of the columns in Tables 1-3 have been proposed to identify crystal and molecular factors that influence the impact and shock sensitivity of TNB, MATB, DATB and TATB. The correlation of H_{50} in Table 1 with the shake-up promotion energy separation (References 76,78) (Table 3) was proposed as evidence of the importance of excited states in determining the impact sensitivity (Reference 78). Correlation of H_{50} with V_{mid} in Table 3 has been suggested to show that the C-NO_2 bond strength and homolysis play a role (References 74,75) or are rate-controlling (Reference 73) in the impact and shock sensitivity of the TNB, MATB, DATB, TATB series. Table 4 reveals that the C-NO_2 bond distance correlates as well or better with H_{50} than V_{mid}. In fact, all of the trends in Table 3 are principally the result of systematic ground state electronic and structural trends along this series. That is, the C-C, C-NO_2 and N-O bond distances are no more or less "controlling" of the sensitivity than any other factor at this level of analysis. Systematic differences in the bond distances figure importantly into the computed electrostatic potentials and measured relative orbital energies.

Other correlations of data in Table 2 with H_{50} have been made. Odiot (Reference 72) noted that the density of -NO_2 groups in the crystal correlated with H_{50}. Kamlet and Adolph (Reference 24) correlated OB_{100} with the log H_{50} for TNB, MATB, DATB and TATB and other compounds. The trends implied that the oxidizing potential of the molecule may be important. Table 3 reveals that for this series of compounds, H_{50} correlates as well with OB_{100} as does log H_{50}. Storm, et al. (Reference 27) noted that within Table 3, H_{50} and P_{90} correlate well. Rogers, et al. (Reference 67) proposed that the increasing amount of intermolecular hydrogen bonding as -NH_2 groups are added is responsible for the decrease in shock sensitivity. As intermolecular hydrogen bonds increase in number, they absorb energy from the shock front and prevent it from being localized in the molecule (Reference 67). Although difficult to quantify with the data available, a qualitative indication of the trend in intermolecular association in the series is the melting point, and, possibly, the density. Both

increase as $-NH_2$ groups are added to the ring and the shock sensitivity, P_{90}, decreases.

An inescapable conclusion of Tables 1-4 is that single column correlations of the molecular, lattice, and explosive properties for TNB, MATB, DATB and TATB are not especially helpful for identifying the primary chemical mechanisms of shock and impact sensitivity. Correlations within a given Table are the soundest. It is especially risky to pick a column of one table and correlate it with a column in another table. For example, any column of Table 3 is as justifiable as any other to correlate with H_{50} in Table 1. As a result, previous conclusions about molecular features that control shock and impact sensitivity in this series of compounds are contradictory: excited electronic states (Reference 78) vs. $C-NO_2$ electrostatic potential (References 73-75) vs. intermolecular hydrogen bonding (Reference 67) vs. oxidant balance (Reference 24). With 153 positive correlations among the data, single correlations are unlikely to provide the true factors. Perhaps all of these factors (or none of them) contribute to the sensitivity to some degree.

Given the enormous barriers to obtaining meaningful data on the condensed phase decomposition mechanisms of nitroaromatic explosives (temperature effects, pressure effects, shortcomings of diagnostics, catalysis, bimolecular processes, rapid heat generation, parallel properties, etc.), it is not surprising that contradicting data and interpretations are common. In the following sections the merits of kinetics and mechanistic models of thermal decomposition are evaluated.

SECTION III

GLOBAL KINETICS OF THERMAL DECOMPOSITION

Most knowledge about the thermal decomposition kinetics of explosives is obtained from rate measurements at relatively low temperature (< 400°C). Kinetic data for TNT are cited in this section along with some discussion of the merits of measurement methods. These kinetic data are used in later sections as an aid in determining the reactions mechanisms.

As mentioned in Section II.3, the decomposition process of bulk TNT involves a solid-to-liquid phase change. Reactions in the liquid phase lead to a small amount of gas and non-volatile intermediate products, followed by other reactions that produce a large quantity of lower molecular weight gases. It is widely agreed (References 44,79,80) that the overall process in the liquid phase is modeled by a first-order rate expression (6),

$$\ln(1-\alpha) = k(T)\,t \qquad (6)$$

where α is the amount of sample decomposed and t is time. Autocatalysis and self-heating complicate the interpretation of the kinetics. Therefore, attempts to measure k(T) are usually made under adiabatic or isothermal conditions whose relationship to k(T) for a first-order process is given by the heat balance equation (7) (Reference 9). λ Is the thermal diffusivity, C is the specific heat, and Q is the heat of reaction. The first term of equation (7) accounts for heat loss to the surroundings. The second term is the heat accumulated by the explosive. The sum of these two terms equals the heat generated by the thermal decomposition. Equation (7) can not be solved under non-

$$-\lambda\nabla^2 T + \rho C(dT/dt) = \rho Q A(1-\alpha)\,e^{-E_a/RT} \qquad (7)$$

isothermal non-adiabatic conditions. However, under adiabatic conditions ($\lambda\nabla^2 T = 0$), such as time-to-explosion or time-to-exotherm (TTX) experiments (References 11,44,81) the apparent activation energy can be calculated from equation (8), where t_e is

$$\ln t_e = \frac{E_a}{RT} + \gamma \qquad (8)$$

the time-to-exotherm at temperature T. Under isothermal conditions (dT/dt = 0), such as is achieved by evolved gas and DSC methods, Arrhenius constants are obtained from equation (1).

Figure 1, which is an idealized representation of the DSC thermogram of TNT, can be subdivided into three regions (Reference 82). Based on equation (7), the induction period represents the

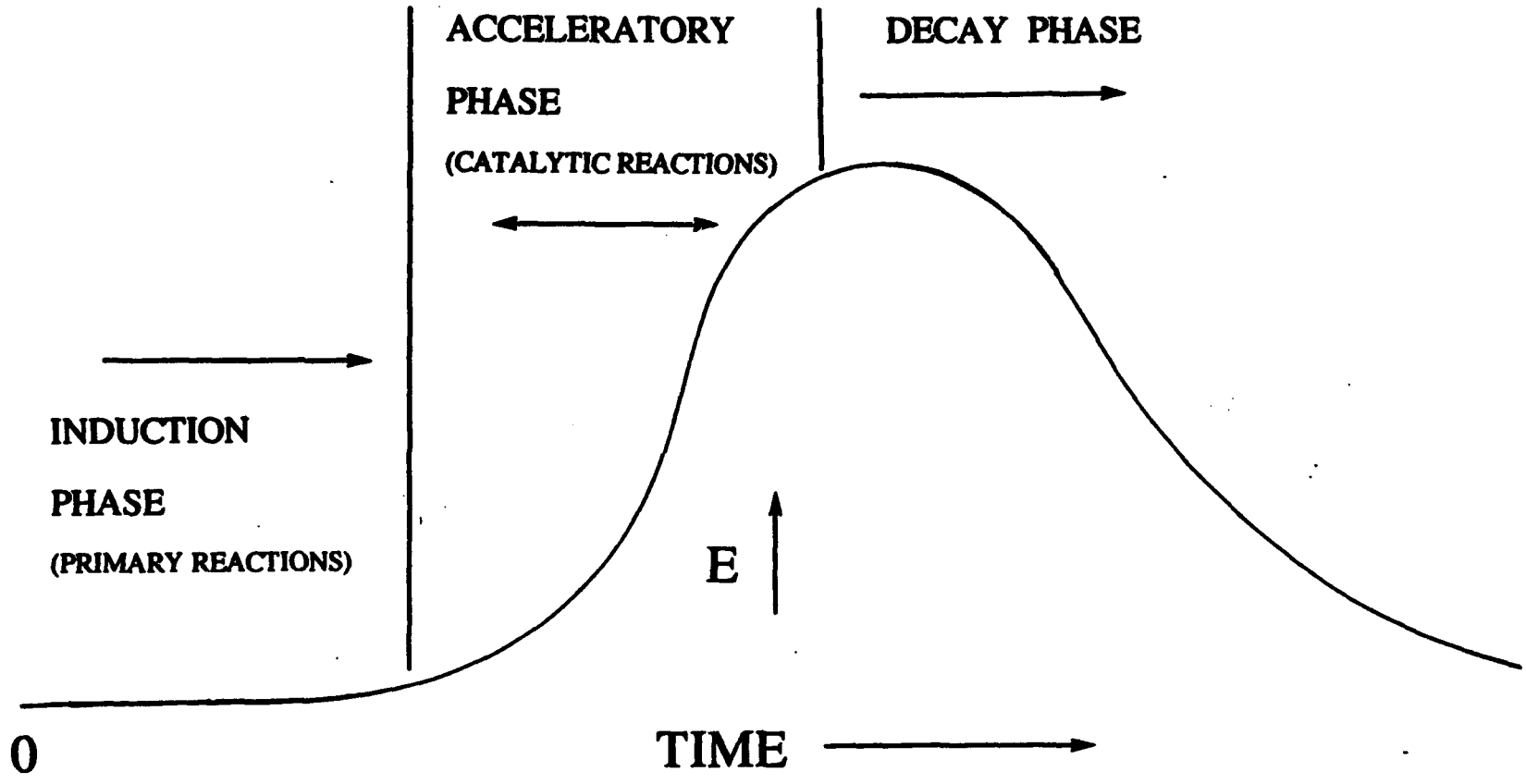

Figure 1. The Energy Release Trace for Slow Decomposition of a Nitroaromatic at a Relatively Low Temperature.

length of time that the sample is thermally quiescent afterheating toa set temperature. Activation energy determined during this period may have the best chance of being related to the structure of the parent molecule, since it reflects the earliest reaction events. The acceleratory stage is the time during which catalysis and self-heating dominate the rate of decomposition. The decay phase is the time when later stage decomposition products react. In reality, the kinetics of decomposition of a bulk sample of an explosive are also sensitive to the mass and geometry of the sample. One reason is that the rate of heat transfer into and out of the sample can not keep pace with the chemical reaction. Hence, the heat changes detected are partly a measure of the reaction rate and partly a measure of the heat transfer rate. Mass transport may also occur at a different rate than the reaction rate. Under these circumstances, agreement among measured rate parameters obtained by different techniques is unlikely. Moreover, association of the rate of the process during any of the phases in Figure 1 with a specific reaction is necessarily tentative.

The Arrhenius parameters for TNT are compiled in Table 5, and fall into three groups according to the stages shown in Figure 1. These data apply below 400°C and are not necessarily representative of the chemistry at high temperature which is initiated by shock and impact. Considerations of mechanisms at higher temperature are discussed in more detail in Section IV. Most publications in the past 15 years mention the stage of Figure 1 that is believed to be studied. If not noted, the data were grouped according to the E_a value. Older literature rarely discusses the reaction stage. The Arrhenius constants of the induction phase tend to be higher than the other stages perhaps because they are most closely related to a bond breaking step. Maksimov (Reference 84) attributes his data in this range to unimolecular processes. In the acceleratory stage, the Arrhenius constants are smaller perhaps because of catalysis by the decomposition products. Maksimov (Reference 84) attributes his rate data in this range to bimolecular processes. The measurement by Urbanskii and Rychter (Reference 85) gives the lowest E_a value of all probably because the temperature exceeds the boiling point of TNT (345°C) (Reference 44). In this case, heat of evaporation is mixed with the activation energy. The value of Brill and James (Reference 87) was obtained at a high heating rate and under 30 atm Ar to suppress evaporation. Wenograd's low value of E_a was determined at high temperature and high heating rate on a semi-confined sample. It is nearly impossible to achieve sufficiently rapid heat transfer and temperature sensing under Wenograd's conditions to obtain an accurate value of E_a (Reference 23). In fact, global activation energies determined at high heating rates and high temperature almost always tend to be smaller than those at lower heating rate and lower temperature (References 88,89). The one measurement (Reference 82) of Arrhenius parameters that is clearly stated to be of the decay phase is similar to, but

Table 5. Arrhenius Parameters for Thermal Decomposition of TNT. Data are Arranged Qualitatively According to the Stage of the Process Measured.

T, °C	E_a, kcal/mol	A, sec^{-1}	Method[a]	Ref.
	Induction Phase			
203 - 283	40.9 ± 1.6	-	ESR	80
298 - 490	41.4	$10^{13.2}$	TTX	81
237.5 - 276.5	43.4 ± 0.8	$10^{12.19 \pm 0.32}$	EG	79
140 - 180	46 ± 3.7	-	EG	83
220 - 260[b]	46.5	$10^{12.9}$	EG	84
245 - 269	46.5 ± 1.5	-	IDSC	82
240 - 255	50.7 ± 2.4	-	DTA	55
	Acceleratory Phase			
390 - 450	14	-	TTX	85
500 - 720	18	$10^{6.6}$	TTX	2
~300	27	-	TTX	57
203 - 283	30.2 ± 0.6	-	ESR	80
275 - 310	32.0 ± 2.5	-	TTX	44
275 - 310	34.4 ± 2.5	-	EG	44
280 - 320	34.5	-	EG	53
190 - 270	34.6	-	EG	86
220 - 260[b]	35.6	10^{9}	EG	84
390 - 407	37.4	-	TTX	87
	Decay Phase			
245 - 269	29.4 ± 1.4	$10^{9.9}$	IDSC	82

a. EG = Manometric measurement of evolved gas; TTX = time-to-explosion (exotherm); IDSC = isothermal differential scanning calorimetry; DTA = differential thermal analysis.
b. However, rate data in Figures of reference 84 are given at 280-330°C.

phase is similar to, but slightly less than, the acceleratory phase.

The methods of measurement of the Arrhenius data in Table 5 reflect all of the complications of kinetics determinations of thermal decomposition of bulk phase explosives. Manometric measurement of the rate of gas evolution from nitrobenzene explosives has been used extensively in Russia especially by Maksimov and co-workers. They described manometry as measuring decomposition in the vapor phase, but noted that substituted nitrobenzene compounds occasionally form a brown residue on the reactor wall (Reference 53). As noted in Section II.3., catalysis by this residue contributes to the reaction rate. Use of the manometric method for rate measurements has been critized (References 20,80-82) because the amount of gas generated by trinitrobenzene derivatives depends on the amount of non-volatile residue that forms and the mechanism of the reaction. Moreover, many substituted trinitrobenzene explosives have significant vapor pressure at elevated temperature (Reference 90). The vapor pressure equation for TNT is given by equation (9) (References 44,91). Fortunately, knowledge of the vapor pressure enables the sample size to be chosen to ensure that all of the decomposition

$$\log P(mm\ Hg) = 9.11 - 3850/T \qquad (9)$$

occurs in the vapor phase. Table 5 reveals that the activation energies from manometry are similar to those obtained by other techniques. Consequently, criticisms of manometry, while probably valid, do not disqualify the data and do not strengthen confidence in any other method of kinetics measurement.

Various methods of measuring the time-to-exotherm (explosion) involve sensing the time of violent release of heat or explosion. Equation (8) is used to determine the apparent activation energy. Numerous studies employ this method and a characteristic of most data is curvature (References 2,80,81,92-95) in the plot of $\ln t_e$ vs. 1/T. The inability to control the heat transfer rate and to know the true temperature makes the value of E_a sensitive to the assumed temperature. Perhaps the best-controlled method for measuring the length of the induction period is isothermal DSC.

Measurement of the rate of growth of the ESR signal of a paramagnetic species has been used to determine the rate of the induction and acceleratory phase of TNT decomposition (Reference 80). Following the concentration of a particular species in this way is sounder than EG or DSC measurements of the global rate, but assumes that the reaction involving the paramagnetic species occurs at the same rate as the overall decomposition process.

In sum, there is no completely unambiguous method to measure the rate of decomposition of an energetic material in the bulk state. Fortunately, rough agreement exists among measurements on

TNT made by several different methods. Rate data exist for decomposition of other nitroaromatic compounds (References 5,6,8, 47,50,52,53-56,84,86,96-106) some of which are used later in this report.

SECTION IV

EARLY THERMAL DECOMPOSITION REACTIONS

Several of the thermal decomposition reactions of polynitroaromatic compounds result from simple bond scission or rearrangements of the substituents on the ring. These are among the first few reactions and thereby initiate all subsequent steps in the complex decomposition scheme. This section evaluates these reactions beginning with the nitro group and concluding with reactions of other substituents on the benzene ring, particularly those ortho to the $-NO_2$ group. A notable feature of these reactions is the fact that the aromatic ring remains intact. Destruction of the aromatic ring is a later stage process described in Section VI.

1. $C-NO_2$ Homolysis

Simple homolysis of the $C-NO_2$ bond to form an NO_2 radical and an aromatic radical by equation (10) is a logical reaction on the

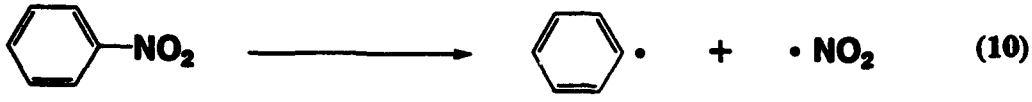

(10)

basis of the importance of the analogous reaction in nitroaliphatics, nitramines (R_2NNO_2), and nitrate esters ($RONO_2$) (Reference 107). For these latter compounds the $X-NO_2$ bond is frequently the weakest bond in the molecule. Two observations suggest, however, that simple extension of this analogy to nitroaromatic compounds requires qualification. First, the bond dissociation energy (BDE) of nitrobenzene derivatives is known to be about 71 kcal/mol (Reference 32) and is altered by only 1 - 4 kcal/mol by adding an $\alpha-CH_3$ group (Reference 32), an additional $-NO_2$ group (References 32,52), or Cl, Br, I, NH_2, and OH, (Reference 52) to the ring. The $C_6H_5-NO_2$ BDE is significantly larger than that of an aliphatic carbon-bound $-NO_2$ group (about 60 kcal/mol), a nitramine (about 50 kcal/mol), and a nitrate ester (about 40 kcal/mol) (Reference 108). Second, although $NO_2(g)$ has been reported from decomposition of nitrobenzene at 275°C (Reference 109) and from pyrolyzed 1,3-dinitrobenzene (Reference 110), 1,4-dinitrobenzene (Reference 110), and 1,3,5-trinitrobenzene (Reference 111) by MS, $NO_2(g)$ is rarely observed from decomposition of substituted nitrobenzene compounds in the bulk state. This behavior sharply contrasts with the behavior of nitroaliphatics, nitramines, and nitrate esters, where $NO_2(g)$ is a readily detected product (Reference 107). Both of these observations suggest that nitroaromatic compounds may have alternate decomposition channels whose activation energies lie below that of $C-NO_2$ homolysis, especially when other substituents are present on the ring.

Table 6 lists Arrhenius parameters for C-NO_2 homolysis from unsubstituted nitroaromatic compounds (equation 10) in the gas phase. The process is first-order (Reference 52). Earlier literature values of E_a for thermal decomposition of nitrobenzene of 51-52 kcal/mol (References 113,114) appear to be in error. The values of E_a in Table 6 are very similar to the BDE of C_6H_5-NO_2, which is good evidence that the activation energy corresponds to C-NO_2 homolysis (Reference 115). As noted above, pyrolysis of 1,3- and 1,4-dinitrobenzene (Reference 110), and 1,3,5-trinitrobenzene (Reference 111) in the gas phase produces ions corresponding to the successive loss of NO_2. The rate constants for decomposition of these three compounds in the gas phase at 330°C are in the ratio 1:20:34 (Reference 53). The primary loss of NO_2 from these molecules leaves the aromatic fragment with the vibrational and electronic internal energy to drive additional reactions (Reference 111).

C-NO_2 homolysis by equation (11) is a dominant decomposition channel of 3- and 4-nitrotoluene, and also occurs for 2-nitrotoluene, (References 32-34,36,52,96,116). Table 7 list the Arrhenius data for equation (11). While only rough agreement exists among these data, the E_a values are similar to the BDE of C-NO_2. The relatively large A factor is characteristic of

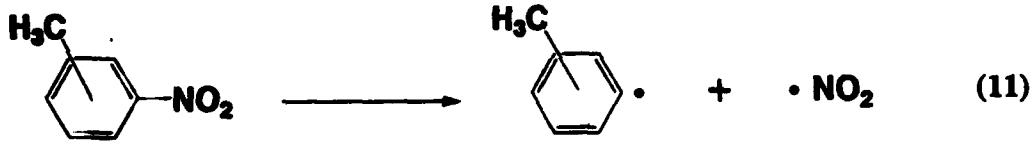

(11)

unimolecular bond scission and produces a positive entropy of activation. Using Maksimov's data (Reference 96) $\Delta S^{\ddagger}$ is about 20 cal/deg for 3-NT and 14.5 cal/deg for 4-NT. C-NO_2 homolysis has been suggested to be initial reaction of para-substituted nitrobenzene compounds on the basis of DSC and accelerating rate calorimeter data where the temperature at the onset of decomposition roughly correlates with the electron withdrawing and donating effect of the substitutent (Reference 116a).

In the gas phase C-NO_2 homolysis in 1,2-NT completes with other reactions. These reactions have been addressed by Tsang and co-workers (References 33,34), and McMillen and Golden and co-workers (References 32,42). Equation (12), the formation of

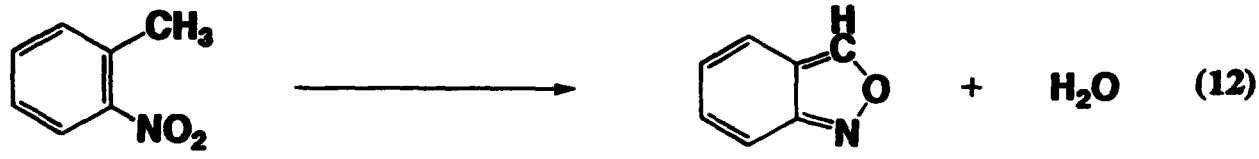

(12)

Table 6. Arrhenius Data for C-NO_2 Homolysis of Mono-, Di- and Trinitrobenzene Compounds

Compound	T, °C	E_a, kcal/mol	A, sec^{-1}	Ref.
$C_6H_5NO_2$	410 - 480	69.7 ± 1.4	$10^{17.3 \pm 0.3}$	52
	455 - 530	67.3 ± 4.7	-	112
	797 - 907	65.7	$10^{15.3}$	33
	827 - 977	68.2 ± 1.7	$10^{15.5 \pm 0.5}$	32
$1,3-(NO_2)_2C_2H_4$	420 - 480	68 ± 3	$10^{16.8 \pm 0.5}$	52
	827 - 977	70 ± 2.1	$10^{14.5 \pm 0.5}$	32
$1,4-(NO_2)_2C_6H_4$	420 - 470	68.6 ± 2.5	$10^{17.1 \pm 0.5}$	52
$1,3,5-(NO_2)_3C_6H_3$	380 - 470	67.3 ± 0.8	$10^{17.2 \pm 0.2}$	52

Table 7. Arrhenius Data for C-NO_2 Homolysis of Mononitrotoluene (NT) and Dinitrotoluene (DNT) Derivatives

Compound	T, °C	E_a, kcal/mol	A, sec^{-1}	Ref.
2-NT	797 - 907	61.47	$10^{14.81}$	33
	827 - 977	67.0 ± 2.2	$10^{16.4 \pm 0.6}$	32
3-NT	300 - 350	65	$10^{17.88}$	96
	400 - 470	68	$10^{16.9}$	52
4-NT	300 - 350	61.5	$10^{16.73}$	96
	400 - 470	65.9	$10^{16.7}$	52
	797 - 907	64.29	$10^{14.89}$	33
	827 - 977	68.2 ± 2.0	$10^{14.9 \pm 0.5}$	32
2,4-DNT	827 - 977	67.4 ± 1.7	$10^{15.3 \pm 0.4}$	32

anthranil, was found to be an important reaction channel in laser assisted homogeneous pyrolysis (Reference 32) and in shock tube pyrolysis (References 33,34). This reaction has been known throughout the 20th Century and is discussed in more detail in Section IV.1.a. The rate constant for equation (12) is $k = 1.2 \times 10^{10} \exp(-51520/RT)$ sec^{-1}. Tsang, et al. (Reference 34) also found a third reaction attributed to isomerization of the $C-NO_2$ bond, which is represented by equation (13) with k estimated to be

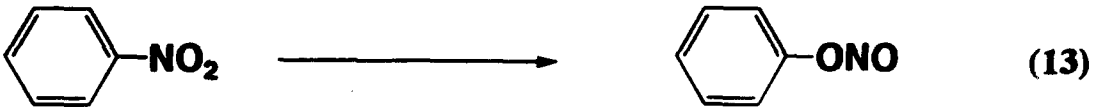

(13)

$10^{13} \exp(-55980/RT)$ sec^{-1}. However, a discrepancy exists concerning the relative importance of equations (11) and (12). Equation (12) was found to dominate in the studies of Tsang, et al. (References 33,34) while equation (11) dominated in the studies of McMillen, Golden, and co-workers (References 32,42). In both the laser pulse and the shock tube, the temperature of the reactant is stepped in several μsec to the 800 - 1000°C range. Ideally, the T-jump has a square waveform, but in reality the shock front can be inhomogeneous and the laser beam does not have a flat energy cross-section. The different conclusions about the relative importance of reaction channels (11) and (12) was proposed (References 33,34) to originate in the uncertainty of the reaction temperature. Although both studies (References 32,34) employed an internal standard to measure temperature, a 100°C higher temperature in the laser pyrolysis studies could account for the different results.

Figure 2 shows Arrhenius plots of equations (11), (12) and (13) using the rate constants of Tsang, et al. (References 33,34) for equations (12) and (13) and the 2-NT data for equation (11). Of the three reactions in the gas phase, equation (12) has the fastest rate up to 950°C. At this temperature equation (11) becomes the fastest reaction. A similar analysis of the relative rates of decomposition channels can be made of 1,3,5-trinitrobenzene versus 2 4,6-trinitroaniline. $C-NO_2$ homolysis of TNB equivalent to equation (11) has a rate constant (Reference 52) of $k = 10^{17.2} \exp(-67300/RT)$ sec^{-1}. 2,4,6-Trinitroaniline is known to decompose by two branches shown in equation (14) to the furazan and furoxan derivatives. These cyclized products are equivalent to equation (12) for nitrotoluene. Two gas phase rate constant measurements are available (References 53,84) for equation (14) giving $k = 10^{8.8} \exp(-38500/RT)$ sec^{-1} and $k = 10^{11} \exp(-41800/RT)$ sec^{-1}. Figure 3 shows a plot of these three rate constants. The cyclization reaction equation (14) is the favored process below 475°C or 625°C depending on which rate constant is chosen for 2,4,6-trinitroaniline. $C-NO_2$ homolysis is the favored process above these temperatures.

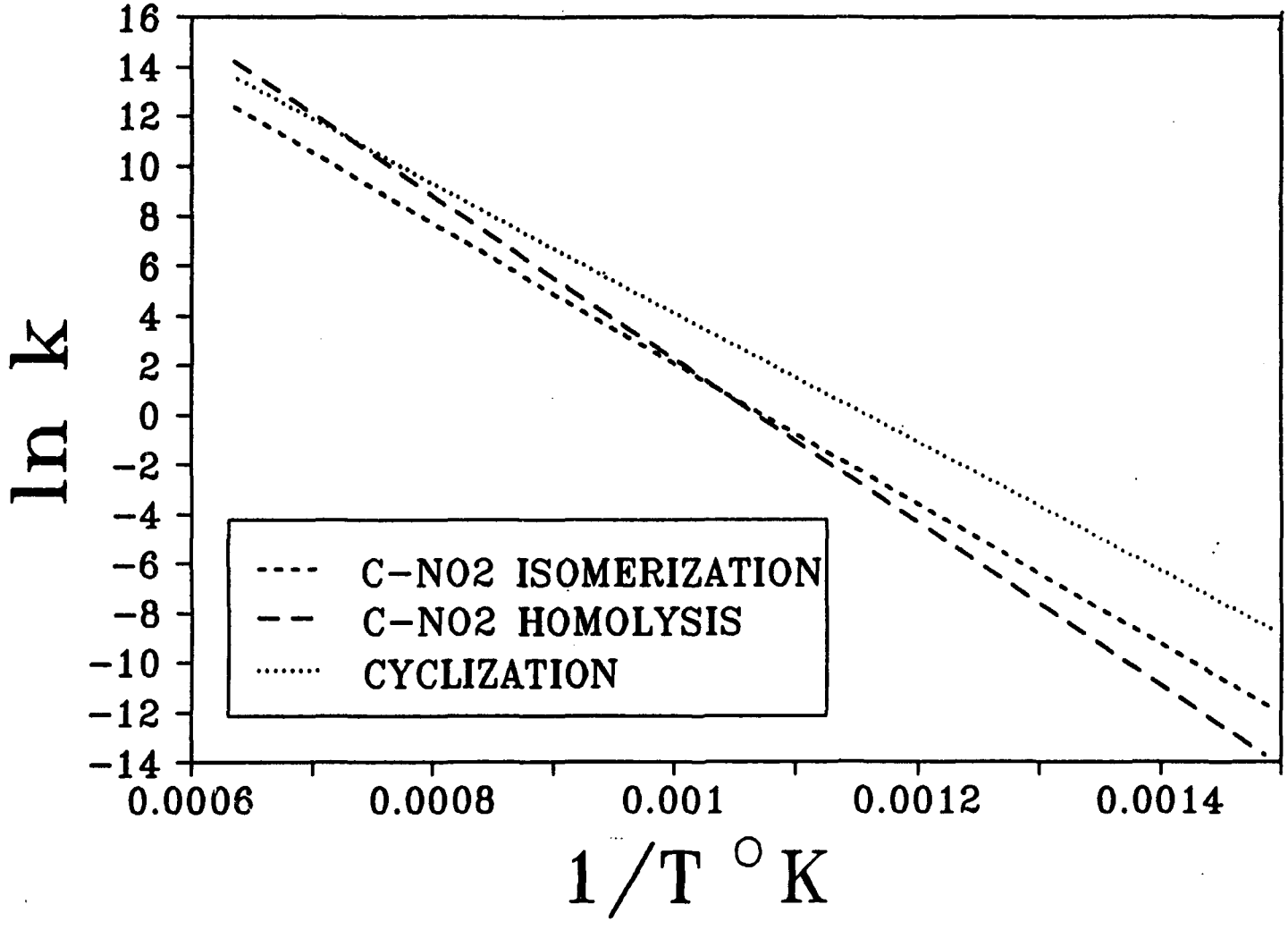

Figure 2. **Arrhenius Plots of the Rates of Decomposition of 2-Nitrotoluene by the Three Main Channels.**

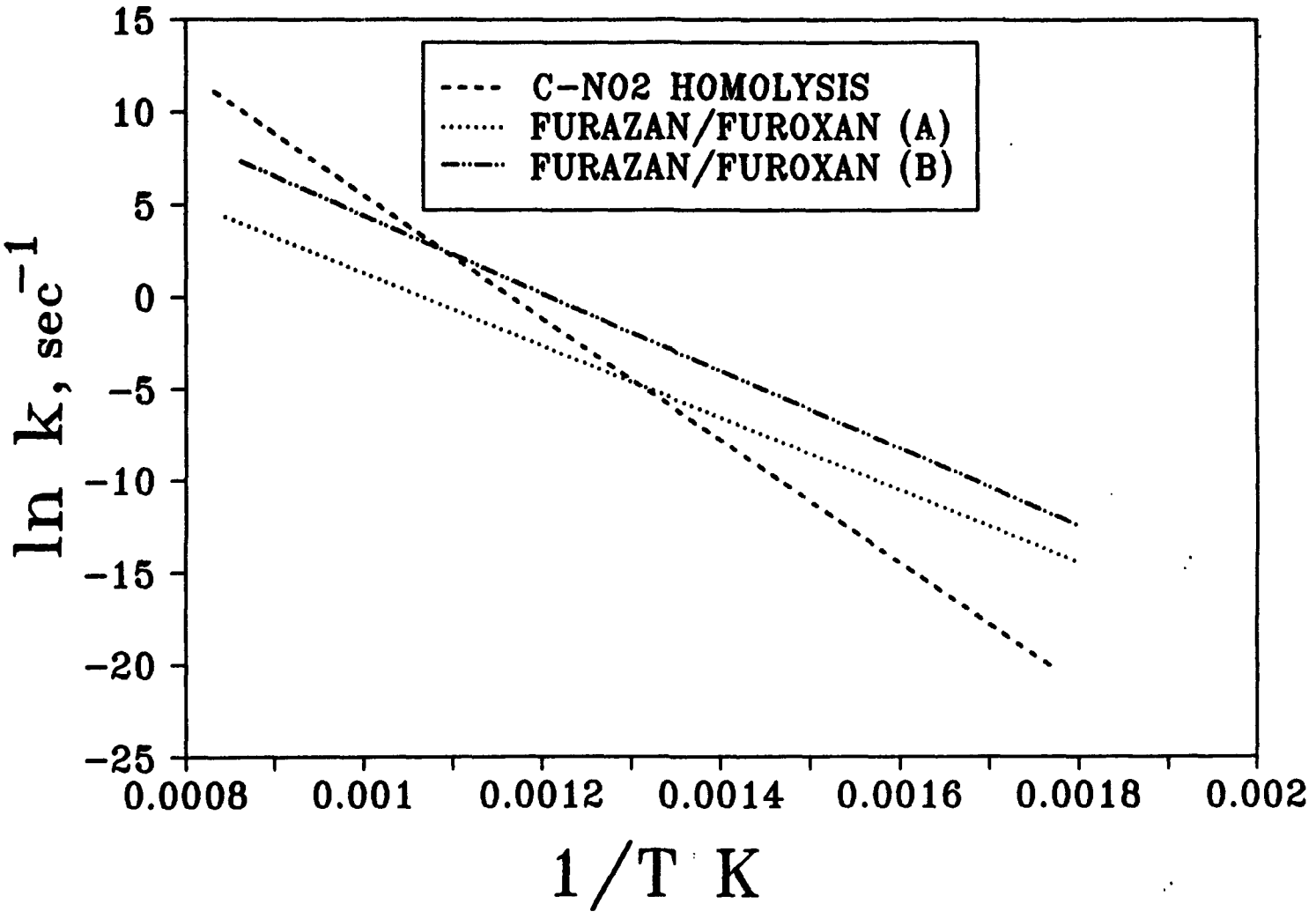

Figure 3. Arrhenius Plots of the Rates of Decomposition of MATB of in the Gas Phase by C-NO_2 Homolysis and Furazan/Furoxan Formations.

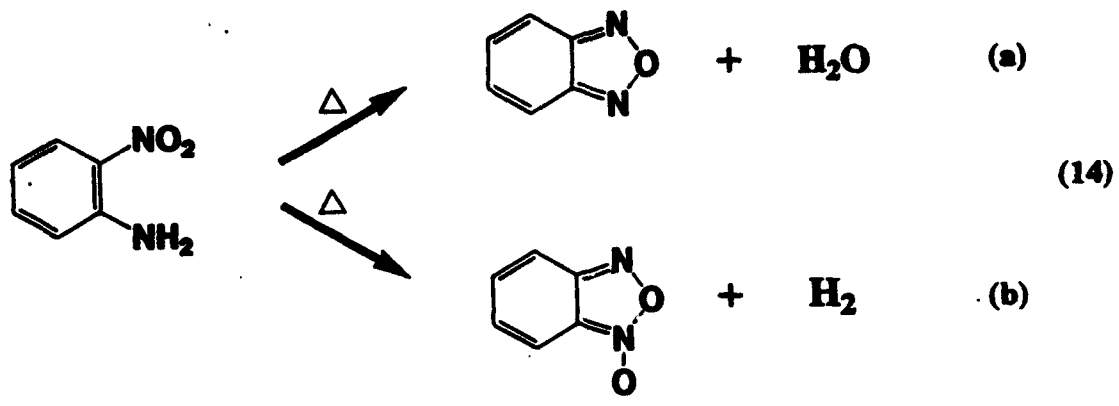

The conclusion reached from the appearance of Figures 2 and 3 is that C-NO_2 homolysis is the favored decomposition channel of nitroaromatic compounds in the gas phase when the temperature is high. The cyclization decomposition channels dominate at lower temperature.

All of the discussion above pertains to the gas phase pyrolysis mechanism. Reactions in the condensed phase can be strongly affected by near-neighbor interactions. For example, C-NO_2 homolysis in the condensed phase may be assisted by intermolecular H• atom transfer (Reference 48) to produce HONO rather than NO_2•. In this case, a concerted process involving both C-H and C-NO_2 homolysis might determine the rate constant. Moreover, during shock and impact initiation, the temperatures reached are relatively high. For instance, Wenograd (Reference 2) estimated that TNT and TNB reach 1000-1100°C during impact initiation. Consequently, C-NO_2 homolysis is likely to be competitive with other decomposition channels under shock and impact initiation. In fact, a number of studies conclude that shock and impact initiation of nitrobenzene derivatives correlate with attributes of the C-NO_2 bond. Owens (Reference 73) and Politzer and co-workers (References 74,75) correlated impact sensitivity with the electrostatic potential at the mid-point of the C-NO_2 bond. Delpuech and Cherville (References 117-119) correlated impact sensitivity with an index derived from the polarity of the C-NO_2 bond in the ground and excited states of nitroaromatic compounds.

Assertions that the rate of C-NO_2 homolysis is fundamentally important in the impact and shock sensitivity of nitroaromatic compounds (References 73,75) directly contradict conclusions drawn from other studies. In particular, Kamlet and Adolph (Reference 24) were able to separate the impact sensitivities of nitroaromatic compounds into two categories – those with α-CH bonds ortho to the -NO_2 group on the ring and those without α-CH bonds. These results are discussed in greater detail in Section IV.4.a. They imply that reactions of the α-CH bond as in equation (12) are important during the impact initiation process. In fact,

Dacons, et al. (Reference 20) proposed that bimolecular oxidative insertion of O into the CH bond was the initial and RDS. Bulusu and Autera (Reference 66) observed a small positive deuterium isotope in the shock sensitivity and detonation velocity when TNT was compared to TNT-α-d_3. Because a primary isotope effect is also observed in the low temperature decomposition of TNT (Reference 51) they concluded that the RDS of slow decomposition, shock initiation, and detonation are the same and involves C-H bond scission. The small size of the isotope effect implies, however, that significant dilution has taken place during shock initiation and detonation.

The direct conflict concerning whether C-NO_2 homolysis or α-CH bond scission is rate controlling in nitroaromatic compounds may simply stem from the temperature conditions of the experiment. As shown in Figure 2, the rates of C-NO_2 homolysis and the cyclization reaction equation (12) are competitive in the 850 - 1200°C range where shock and impact initiation takes place. This would imply that the chemical reactions responsible for shock and impact initiation are not necessarily the same as those of slow, controlled thermolysis. In fact, Storm, et al. (Reference 27) found TNT to be an outlying point in a plot of impact vs. shock sensitivity for 21 explosives.

In conclusion, C-NO_2 homolysis, whether unimolecular as in the gas phase or assisted by intermolecular interactions in the condensed phase, is the dominant early thermal decomposition reaction of nitroaromatic compounds at high temperature, probably above 900°C.

2. Nitro-Nitrite Isomerization

Evidence of the nitro-nitrite rearrangement on an aromatic backbone exists primary in the gas phase and in dilute solution. In the condensed phase of the bulk material, the evidence is more circumstantial. Unfortunately, no aryl nitrite compounds appear to have been isolated and characterized.

In the gas phase the clearest evidence of the nitrobenzene-to-nitritobenzene isomerization comes from the fact that the thermal decomposition of nitrobenzene is insensitive to the presence of excess NO_2 (Reference 32). An estimate (Reference 33) of the rate constant for this rearrangement produces the Arrhenius plot shown in Figure 2. While this estimate shows that isomerization is never the fastest reaction, a small change in the assumed A factor alters the importance of the isomerization process relative to the other reactions in Figure 2. The isomerization reaction also has a small or negative volume of activation, and, therefore, would be favored relative to unimolecular bond scission at high pressure (Reference 120).

In the condensed phase, isomerization would be expected to increase in importance relative to the gas phase because of the low volume of activation. Evidence of a reversible nitro-nitrite rearrangement involving a nitroaromatic compound exists in the ^{1}H and ^{13}C NMR spectra of 2,6-dichloro-4-methylphenol following nitration in chloroform (Reference 121). Nitration occurs at the 4-position which makes this carbon atom formally sp^3 hybridized. The nitro-nitrite rearrangement, therefore, does not actually occur on an aromatic carbon atom. Nitro-nitrite isomerization has long been known to take place on an aliphatic carbon atom (Reference 122).

A strong item of circumstantial evidence for the nitro-nitrite rearrangement of nitroaromatic compounds in the bulk state is the fact that $NO_2(g)$ is not observed or is, at most, a minor product of thermal decomposition below 500°C (Reference 123). Instead, a large quantity of NO is formed (References 48,49,123-125). These observations have been cited as evidence of the different contributions of equations (15) and (16) (Reference 125); (17) (References 32,33,49,120); and (18) (References 33,49,125,126).

(15)

(16)

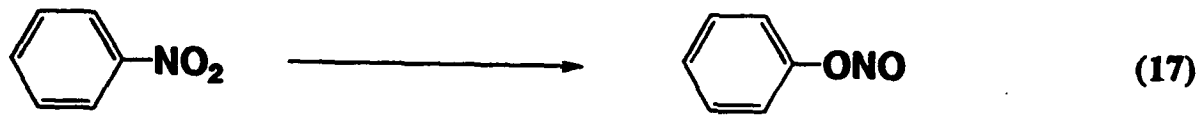

(17)

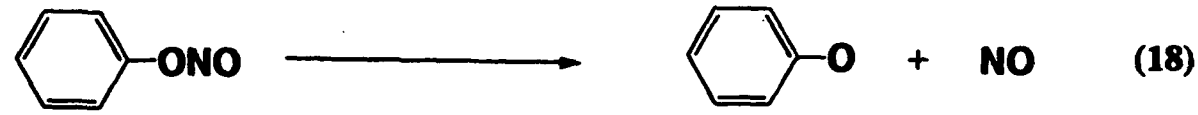

(18)

As with equation (15) in Section IV.1., equations (16)-(18) have been analyzed most extensively in the gas phase, but not in the condensed phase, where the details are more difficult to establish. Beynon, et al. (Reference 127) were among the first to contribute to this area. They observed that pyrolysis of nitrobenzene at 600°C produced NO and the phenoxy radical. Above 800°C, shock tube studies (Reference 33) indicated that equations

(17) and (18) occurred, while laser powered pyrolysis revealed (Reference 32) that the nitrite forms by equation (17), rather than equations (15) and (16). However, equation (15) is more than twice as prevalent as equation (17) above 800°C (Reference 33). The fact that these shock tube and laser pyrolysis studies were conducted at low pressure would disfavor the bimolecular equation (16). Equation (16) would be expected to be much more important in the condensed phase.

Values of E_a and the BDE for equation (15) are in the 65-72 kcal/mol range (Section IV.1.). Although the rate of isomerization by equation (17) has not been measured directly, it is likely to be slow based on the estimate of a relatively high E_a of 55.9 kcal/mol (Reference 33) and computational estimates (Reference 120). The BDE of equation (18) is approximately 23.7 kcal/mol (Reference 128). Taken together these results are consistent with equation (15) being the prevalent reaction at high temperature and low pressure (Reference 33).

Reactions of the type (15) - (18) also appear to occur when other substituents are present on the aromatic ring. Field and Meyerson (Reference 116) found ions in the mass spectrum consistent with equation (18) when 1,3- and 1,4-nitrotoluene and 1,3-dinitrobenzene decompose. The major pathway of decomposition of 3,4,5-trinitrotoluene in the EI/MS is loss of NO, which was proposed to result from equations (17) and (18) (Reference 39). Decanitrobiphenyl was speculated to decompose in solution through the isomerization steps, equation (17) (Reference 129). MNDO and MINDO/3 computations (Reference 130) on a model compound of TNT, 1-nitropropene, reveal that the transition state equivalent to equation (17) is favorable and is consistent with the formation of radicals by equation (18).

Considering the evidence available, concrete proof does not exist for nitro-nitrite isomerization of nitroaromatic compounds during thermal decomposition. However, circumstantial evidence is abundant. The isomerization equation (17) could occur directly in the condensed phase, or at higher temperatures it could occur by equations (15) and (16). A variation of equation (16), for which there is abundant evidence (References 121,122,131), involves converting an sp^2 carbon to an sp^3 carbon and adding NO_2 at the sp^3 carbon atom. The copious amount of NO(g) formed upon thermolysis of nitroaromatic compounds is further evidence of equation (18). However, it is doubtful that all of the NO(g) generated by nitroaromatic compounds comes from equation (18). Other sources of NO(g) need to be considered. In addition to equation (18), NO(g) can be formed by thermal decomposition of HONO, which forms when $\bullet NO_2$ and H$\bullet$ adventitiously encounter one another. Most nitroaromatic compounds are abundant sources of $\bullet$H (Reference 61). Equation (19) occurs readily at the temperature which nitrobenzene compounds thermally decompose. This route to NO(g) is indicated to be unimportant during pyrolysis of nitrobenzene in one study,

$$2HONO \rightarrow NO + NO_2 + H_2O \qquad (19)$$

(Reference 49) but contributing in another (Reference 125). Equation (19) has been mentioned frequently in the thermal decomposition mechanisms of substituted nitroaromatics (References 33,36,48,130,132). A third source of NO(g) is thermal decomposition of nitrosoaromatic compounds that form in the decomposition scheme of nitroaromatic derivatives (Section IV.3).

3. Formation of Nitrosoaromatic Intermediates

Kinetics measurements of the formation and thermal decomposition of nitrosoaromatic compounds from nitroaromatic compounds are not available. However, from a thermochemical point of view, the C-N BDE of nitrosobenzene is 50.8±1 kcal/mol compared to nitrobenzene at 71.3±1 kcal/mol (Reference 133). On this basis, formation and reaction of nitrosoaromatic compounds is probably a lower temperature process than $C-NO_2$ homolysis. Any temperature at which $C-NO_2$ homolysis is facile exceeds the temperature required to cleave the C-NO bond.

As is the case for other reactions of the $-NO_2$ substituent described in Sections IV.1. and 2., the clearest evidence of formation of the nitroso substituent from the nitro group exists in the gas phase. Equations (20) - (23) give several possible routes to the nitroso group.

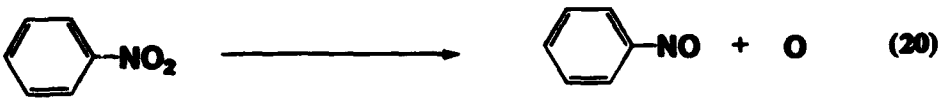

(20)

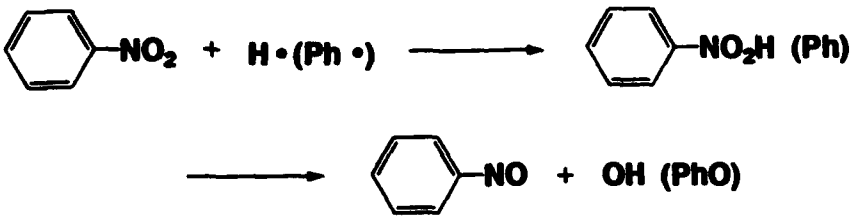

(21)

(22)

(23)

Equation (20) has been proposed on the basis of pyrolysis of nitrobenzene in benzene solution at 275°C where, after chromatography, nitrosobenzene is the dominant nitrogen-containing product (Reference 49). In the EI/MS (Reference 39) and MS/MS-CID (Reference 134) of TNT, an ion with m/e = 211 corresponding to the loss of O is important.

Equation (21), in which an oxygen atom is abstracted by reaction with a radical, would be expected with a radical-producing substituent ortho to the $-NO_2$ group. Since it can be a bimolecular reaction, equation (21) is potentially important in the condensed phase. Equation (21) has been proposed to occur for nitrobenzene in benzene solution (Reference 49) and in the gas phase of TNT by EI/MS (Reference 39), and MS/MS-CID (Reference 134) where loss of OH produces the dominant ion.

The fact that NO forms in high concentration when many bulk nitroaromatic compounds are pyrolyzed (References 48,49,123-125) makes equation (22) a probable source of nitrosoaromatic compounds by recombination in the condensed phase. Equation (23) has been analyzed computationally as a potential step in the decomposition of TNT (Reference 135). MINDO calculations suggest that equation (23) is favored over H transfer from $-CH_3$ to $-NO_2$ to form the aci-isomer (Reference 135). The same conclusion was reached from MNDO and MINDO/3 calculations of 1-nitropropene (Reference 130) a model compound for TNT. Oxidative insertion of O into the CH bond has been speculated upon as the RDS in the decomposition of TNT (Reference 20).

The chemistry of nitrosoaromatic derivatives must be considered in the lower temperature decomposition schemes of nitroaromatic explosives, but probably not in shock initiation processes. Evidence for this comes from XPS studies of Owens and Sharma (Reference 136) who found evidence of the nitroso group in thermally decomposed TNT, but not in shocked TNT. Indeed, Adams, et al. (Reference 137) isolated a toluene-soluble nitroso-containing compound proposed to be 2-nitroso-4,6-dinitrobenzyl alcohol from the thermal decomposition products of TNT. Thermal decomposition of TNT alone and in the presence of hexamethylbenzene produces a nitroxide radical that corresponds to condensation with loss of OH, equation (24) (Reference 138). This radical is closely related to the nitroso compounds discussed above. Likewise, nitrosoaromatics can couple to form azoxy and

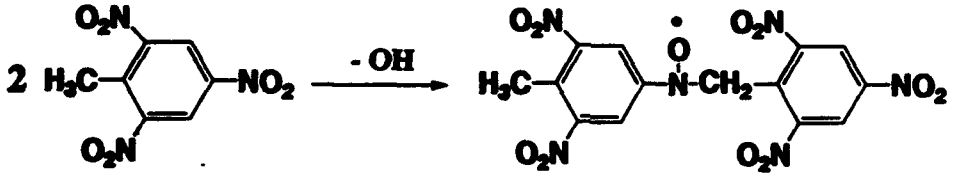

(24)

azo compounds which have been isolated from the residue of TNT formed during 16 hrs at 200°C (Reference 20). Coupling of nitrosoaromatics to form azo and azoxy compounds is proposed in other studies (Reference 139). Equation (25) is representative.

Decomposition of nitrosoaromatic compounds is a source of NO upon thermolysis. Both nitrosobenzene (Reference 139) and the nitroso products of TNT (Reference 134) produce NO by MS/MS-CID.

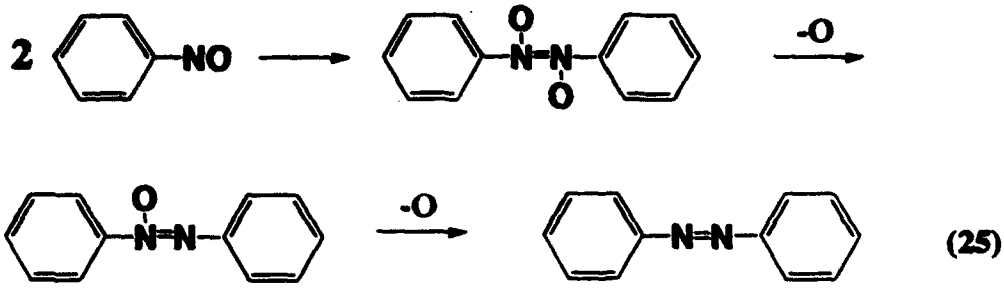

(25)

4. Reactions of the $-NO_2$ Group with an ortho Substituent

Numerous studies indicate that most polyatomic substituents positioned ortho to the $-NO_2$ group on the aromatic ring enhance the reactivity compared to meta and para positioning. Synthesis chemists knew this fact in the 19th Century. Reactions of substituents with an ortho $-NO_2$ group are now a widely used synthetic route to many heterobicyclic molecules (References 140-142). Mechanisms of these reactions have been discussed in the broad sense (References 140,143). Reactivity differences in relation to explosive properties began to be discussed in the early 20th Century (References 83,144). For example, 2,4,6-TNT self-ignites at about 210°C, whereas 1,3,5-TNB is stable at 300°C indicating that $-CH_3$ somehow activates the molecule.

Clear illustrations of the generality of the "ortho effect" arise when classes of substituted nitrobenzene compounds are compared. The relative rates of thermal decomposition of 2-nitrotoluene, 3-nitrotoluene, and 4-nitrotoluene in the vapor phase at 200°C are 400:0.8:2.0 (Reference 96). The EI/MS and MS/MS-CID of these molecules differ significantly. 2-NT loses OH while 3-NT and 4-NT lose O, NO, and NO_2 (References 36,126). $-CH_3 \cdots ON-$ Intermolecular interaction clearly destabilizes the molecule.

Kinetic data for the gas phase decomposition of a series of ortho-X-nitrobenzene derivatives (Reference 102) in Table 8 are further evidence of the generality of the ortho effect. In all three compounds the primary deuterium isotope effect indicates that the H atom is transferred in the transition state of the reaction. E_a for the 2-NT in Table 8 is 10 - 20 kcal/mol lower than those in Table 7 where the $C-NO_2$ homolysis occurs. All three compounds in Table 8 primarily fragment by loss of OH in the EI/MS and MS/MS-CID modes (References 36,126).

The reactions between $-NO_2$ and ortho related substituents profoundly affect the thermal decomposition chemistry and explosive properties of polynitroaromatic explosives. Individual substituents are now considered by category.

a. α-CH Bonds

The number of clear indications are overwhelming that an α-CH bond ortho to $-NO_2$ on an aromatic ring activates the thermal decomposition process (References 5,20,21,24,33,34,39,51,53,86, 96,126,132,134,140,145-147). That an alkyl group plays a fundamental role in thermal decomposition is not at all surprising when these compounds are viewed as a subclass of hydrocarbon chemistry. The RDS in the oxidation of hydrocarbons in the liquid phase involves C-H scission (Reference 148). The C-H bond of an alkyl group is more reactive than a C-H bond of an aryl group (Reference 148). However, for destabilization of the nitrobenzene fragment, it is not simply the presence of an ortho alkyl group that counts. The presence of an α-CH bond in the ortho alkyl group is the most significant factor. Evidence for this is the fact that at 200 - 260°C in the melt phase, 2,4,6-TNB substituted by $-CH_3$, $-CH_2CH_3$, and $-CH(CH_3)_2$ decompose at about the same rate, whereas $-C(CH_3)_3$ substitution produces a 30 - 50 times slower rate (Reference 86). Following α-CH abstraction the reaction sequence for this series of compounds is very different (Reference 37).

Chemical details about how a nitroaromatic compound becomes activated by ortho $-CH_3$ substitution came to light nearly a century ago when 2-NT was found to condense to anthranil, equation (12), upon heating (References 149-151). In particular, 2-NT heated in aqueous or alcoholic base rearranged to anthranilic acid (References 149-151) which is the hydrolysis product of anthranil. Likewise, Fields and Meyerson (Reference 116) recovered methylanthranilate when 2-NT in CH_3OH was heated to 600°C in a Vycor tube for 11 sec. The mechanism of this reaction has been discussed (Reference 65). Because these reactions occur in the condensed phase, the role played by bimolecular processes and wall effects is unknown. These perturbations are eliminated by the use of a single pulse shock tube (References 33,34). The kinetics and products of unimolecular thermal decomposition of 2-NT reveal that equation (12) is the dominant reaction pathway at least below about 900°C (References 33,34). Previous kinetic studies of 2-NT using the rate of gas evolution (References 96,102) and these shock tube data are given in Table 9. The Arrhenius factors are smaller than those for $C-NO_2$ homolysis (Table 7). The relatively low A factor suggests a tight transition state that is expected of a cyclic activated complex collapsing to a closed ring (References 34,84). Indeed, $\Delta S^{\ddagger}$ is -15 cal/deg for 2-NT compared to 20 and 14.5 cal/deg for 3-NT and 4-NT (Reference 96). As described in Section IV.1, 3-NT and 4-NT thermally decompose by $C-NO_2$ homolysis which produces a positive $\Delta S^{\ddagger}$. The clear experimental evidence

Table 8. Gas Phase Kinetic Data (Reference 102) for Nitrobenzene Derivatives having ortho-X Substitution

X	T, °C	k_s/k_0	E_a, kcal/mol
CH_3	350 - 420	1.54	49.5
NH_2	400 - 470	1.48	57.5
OH	390 - 460	1.75	52.4

Table 9. Arrhenius Data for Condensation of 2-Nitrotoluene to Anthranil (equation 12)

T, °C	E_a, kcal/mol	A, sec^{-1}	Ref.
300 - 350	42.5	$10^{10.22}$	96
400 - 450	49.5 ± 1.3	$10^{12.4 \pm 0.4}$	102
797 - 907	51.520	$10^{13.08}$	33

that 2-NT condenses to anthranil upon heating is supported by therelative energies determined by ab initio SCF-MO methods (Reference 152). The bicyclic tautomer intermediate and the anthranil product of equation (26) form exothermically and thus are thermodynamically

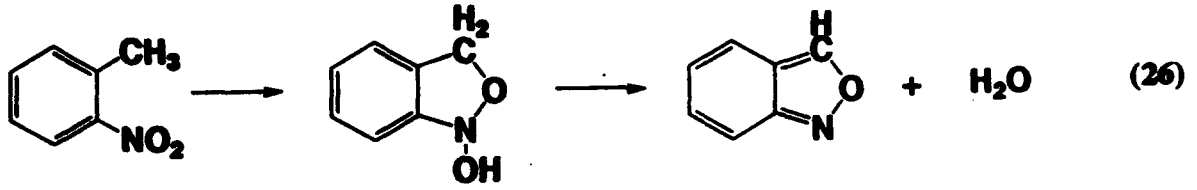

(26)

favored relative to 2-NT. The first step of equation (26) is suggested by UV photolysis of 2-NT which produces a short-lived

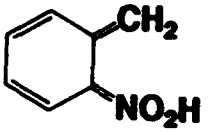

(I)

aci tautomer of 2-NT (I), (References 153-156). (I) is the precursor of the intermediate species in equation (26). SCF-MO calculations on 2-NT at the STO-3G level indicate that the barrier to H transfer when forming (I) is 54 kcal/mol (Reference 157), which is 4-13 kcal/mol larger than the global induction phase activation energy of 2-NT (Table 5). An earlier MNDO calculation on TNT concluded (Reference 135) that intramolecular H transfer to form (I) was less likely than O insertion into the CH bond by equation (23). However, the SCF-MO model is more dependable for assessing the relative energy of these processes. Elsewhere the MNDO model of 1-nitropropene indicated that H transfer from $-CH_3$ to $-NO_2$ is energetically favorable (Reference 130). This result is consistent with the SCF-MO results.

The experimental and computational results for 2-NT are useful guides to the possible behavior of TNT. However, 2-NT is only a model of an explosive and has been studied primarily in the gas phase. From the point of view of an explosive, the behavior of the bulk material in the condensed phase must be understood. Consequently, the unimolecular reaction conditions of the gas phase need to be modified to account for bimolecular reactions and catalysis that are important in the condensed phase. Condensed phase decomposition is further complicated by the fact that H atoms are such important participants in the decomposition of TNT (References 61,158). The rate of H transfer is fast, being less than 3.1 μsec in solution (Reference 156). Consequently, many H atom transfer steps can occur in a very short time at temperatures below 300°C where most decomposition studies of polynitroaromatic

explosives are conducted. Moreover, O transfer occurs under certain conditions in the condensed phase (Reference 159).

TNT melts at 81°C so that studies of condensed phase decomposition almost always refer to the molten state. Several studies report separation and identification of products in an attempt to determine how the methyl group activates thermal decomposition. Many products are possible because all of the oxidized forms of $-CH_3$ and reduced forms of $-NO_2$ are present and each displays its own intermolecular and intramolecular chemistry. Consequently, anthranil, alcohol, aldehyde, carboxylic acid, nitroso, oxime, nitrile, nitrone, nitroxide, azo, and azoxy groups form (References 20,21,137,139,160-162). Disruption of the aromatic ring also occurs leading to gas products including NO, CO, CO_2, N_2 and H_2O (References 87,137). An insoluble high molecular weight "explosive coke" having the elemental composition of $C_6H_3N_2O_{3.75}$ forms from TNT (Reference 137). All of these products result from "cooking" reactions and, as such, can not be attributed with confidence to the initiation or explosion chemistry of TNT. However, several useful results emerge from this work and are discussed below.

Rogers (Reference 21) used thin-layer chromatography to separate the products formed by programmed heating of TNT at 300 °C. 1,3,5-TNB, 2,4-dinitroanthranil, 2,4,6-trinitrobenzyl alcohol, and 2,4,6-trinitrobenzoic acid were isolated from a large quantity of unreacted TNT. He proposed that oxidation of $-CH_3$ to $-CH_2OH$ is the first step. Dacons, et al. (Reference 20) heated TNT for 16 hrs at 200°C in a loosely capped vial. About 25 benzene-soluble compounds were extracted from the dark brown residue. An insoluble residue included the "explosive coke" reported by Adams, et al. (Reference 137). Unreacted TNT constituted 75 - 90% of the material. The same benzene-soluble products found by Rogers (Reference 21) (except for TNB) were obtained, but, in addition, 2,4,6-trinitrobenzaldehyde and dimeric reduction products suspected of containing azo and azoxy linkages (II) were found. None of the products amounted to more than 1% of

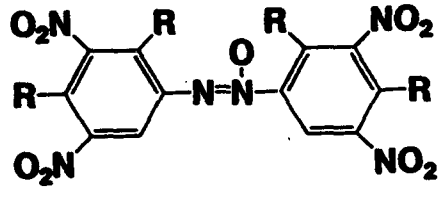

(II)

the original quantity of TNT. Neither Rogers (Reference 21) nor Dacons, et al. (Reference 20) analyzed the gases formed, but Rogers noted that only a few percent of the weight is lost. Consequently, most of the decomposition reactions produced products with low volatility. It is not surprising that the

products in these two studies differ somewhat because of the different reaction temperature. While Dacons, et al. (Reference 20) stress the importance of these differences, Rauch, et al. (References 163-165) repeated this work by using TNT heated at 275°C, which is intermediate between the temperatures used by Rogers (Reference 21) and Dacons, et al. (Reference 20). Products common to both studies were isolated indicating that the main factor in the product differences was simply the reaction temperature. After merging the results of these cooking degradation studies, the presence of successive oxidation products of the $-CH_3$ group, equation (27), is conspicuous. All of these products also appear in the synthesis of TNT.

Many of the products discussed above are formed from TNT because of the relatively low decomposition temperature and the long reaction time. It is unlikely that they all are present or contribute significantly during rapid decomposition where the reaction times are shorter and the temperature is higher. As has already been emphasized, high temperature favors higher E_a and more endothermic processes. Therefore, experiments designed to

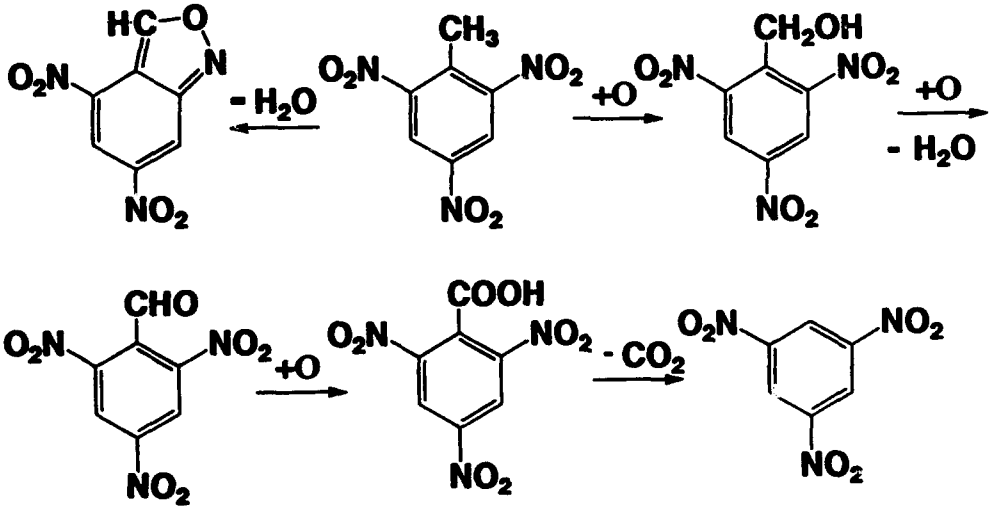

(27)

specify individual steps or to control the conditions more precisely require interpretative care if the goal is to define the decomposition mechanism of TNT. For example, a low E_a process is revealed by ESR spectroscopy during UV photolysis of TNB in toluene at 200 K. The primary radical is (III) which converts with time or on heating to two conformers of (IV) (Reference 166). Caution must be exercised when using these results to understand TNT decomposition because these are low E_a processes. Moreover, Davies, et al. (Reference 167) found that the radical formed by photolyzing TNT in diethylether is not the same as those formed by heating TNT. On the other hand, there is absolutely no doubt about the ease by which an H atom can migrate from the $-CH_3$ group of TNT. In solution, UV photolysis gives evidence of H atom

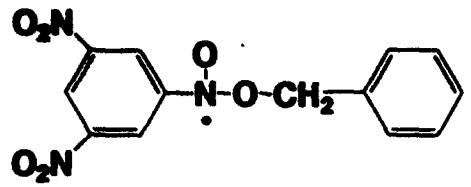

(III)

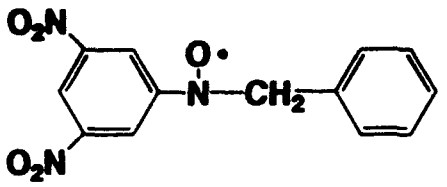

(IV)

transfer to give (I') (References 153-156), which is in equilibrium with the trinitrobenzyl anion (V) (equation 28) (References 145,156). Lewis bases, such as OCH_3^- and $OC_2H_5^-$,

(28)

(I') (V)

abstract H^+ from the $-CH_3$ group of TNT (References 158,168) to produce (V). (V) is highly reactive and under appropriate conditions is able to couple to produce HNS (Reference 169). In the gas phase, the dominant fragmentation step of TNT and 1,3,5-trinitroxylene is loss of OH (References 39,126,132,134,170). For this to occur H atom transfer to $-NO_2$ followed by $-N(O)-OH$ homolysis must be the dominant initial decomposition step of the isolated molecule. In fact, all TNT isomers, except for 3,4,5-TNT, fragment by loss of OH (Reference 146).

Solid evidence of C-H bond scission from the $-CH_3$ group of neat TNT is the primary deuterium isotope effect observed by DSC during the induction phase (Figure 1) of TNT and TNT-α-d_3 (Reference 51). A primary isotope effect indicates that C-H bond scission occurs in the RDS. Shackelford, et al. (Reference 51) proposed that a single unidentified catalyst promotes the reaction rate in the induction phase. They were apparently unaware of the earlier report of Maksimov, et al. (Reference 59) who suggested that 2,4-DNAn or 2,4,6-trinitrobenzaldehyde (equation (27)) was the catalyst. Maksimov, et al., found that a 9:1 TNT:2,4-DNAn mixture reproduced the acceleratory decomposition characteristics of TNT (Reference 59). 2,4,6-Trinitrobenzaldehyde was shown previously to catalyze the decomposition of TNT (Reference 20). In reality it is very difficult to specify the catalysts of decomposition of TNT with certainty. Robertson found that all 25 compounds that he added to TNT were catalysts (Reference 44). Molecules that are able to produce H• catalyze the decomposition (Reference 51). Unfortunately, ample concentrations of such species (10^{-4} M) appear at relatively low temperature when neat TNT is heated (Reference 61).

Whether it is intra- or intermolecular H• transfer that produces the aci tautomer of TNT (I') and starts the decomposition chain is more of academic mechanistic interest than practical importance. However, some studies emphasize intra- or intermolecular H- transfer (Reference 48) to the exclusion of the other. Considering all of the literature together, there is little doubt that when both are possible, both will contribute. In solution and in the gas phase at low pressure, unimolecular H• transfer dominates (References 32,34,36,37,96,102,116,155,156). If the pressure is raised in the vapor phase, the decomposition of TNT shifts from unimolecular at lower pressure to bimolecular at higher pressure (Reference 53). In the face of this result it is interesting that the decomposition rate of molten TNT is independent of pressure up to 50 kbar (Reference 171). This has been attributed to the fact that the volume of activation of 2,4-DNA is similar to that of TNT (Reference 172). On the other hand, it could mean that intermolecular association and H• transfer dominate at all pressures studied.

Evidence of significant intermolecular association of polynitrobenzene molecules in the condensed phase that would facilitate intermolecular H• transfer appears in many forms. The crystal structure of TNT (References 173,174) reveals that intramolecular and intermolecular H• transfer may be equally probable in the condensed phase. The intermolecular -CH•••ON- distances (2.39 - 2.62Å) are very similar to the intramolecular distances (2.38 - 2.70Å). Structural details of the solid phase do not necessarily carry over to other phases, but the vibrational spectra of TNT in the solid, liquid, and vapor state are similar (References 174-177). This suggests that the intermolecular -CH•••ON- distances in the solid are similar to those in the melt where decomposition occurs. The large amount of intermolecular association in the melt is responsible for the unusually high Trouton's ratio of $\Delta H_{vap}/T_b$ = 23 - 33 cal/deg•mol (Reference 48) for polynitrobenzene compounds compared to about 22 cal/deg•mol for weakly associating molecules. Aggregates of nitrobenzene molecules exist even at 350°C, (Reference 178). The A factors for thermal decomposition of many polynitroaromatic compounds (Reference 48) are in the range of 10^5 -10^{10} sec^{-1} which is smaller than the lower limit of unimolecular reactions of about 10^{12} sec^{-1}. The negative $\Delta S^{\ddagger}$ for some of these reactions is suggestive of an ordered transition state (Reference 34). An energetically stable transition state forms by intermolecular H• transfer from $-CH_3$ to $-NO_2$ according to MNDO and MINDO/3 MO calculations on 1-nitropropene (Reference 130). Finally, the mere fact that the rate of thermal decomposition of TNT is about ten times faster in the melt than in the vapor phase (Reference 48) is reasonable evidence of the importance of intermolecular H• transfer in the condensed phase. However, this latter observation could also be attributed to catalysis by the decomposition products.

C-H bond scission from the $-CH_3$ group of TNT appears to play a practical role in the sensitivity and explosive properties of polynitroaromatic explosives in the bulk state. The explosive properties of interest include the sensitivity to impact and shock initiation. As discussed in Section II.1, impact sensitivity is determined by the drop weight impact test and is governed to a large extent by thermal decomposition processes (References 1,2). Thermal decomposition is influenced by the structure and composition of the molecule. In accordance with this notion, log H_{50} for polynitroaromatic compounds is found to correlate with the oxidant balance (Reference 24), the reducing and oxidizing valencies of the composing elements (Reference 179), the molecular electronegativity (Reference 180), and the polarity of the $C-NO_2$ bond in the ground and excited states (Reference 117). Particularly interesting results are those of Kamlet and Adolph (Reference 24) and Bliss, et al. (Reference 181) who found a statistically significant separation of log H_{50} vs. OB_{100} for nitroaromatic explosives into two families. With several exceptions the distinguishing feature is the presence or absence of an α-CH bond ortho to $-NO_2$. Compounds with α-CH bonds were more sensitive to impact. Bliss, et al. (Reference 181) noted that this separation may merely be the result of dilution of OB_{100} by the CH_3 group. Bulusu and Autera (Reference 66) noted a small deuterium isotope effect in the shock sensitivity (1.09 - 1.14) and detonation velocity (1.04 - 1.06) when TNT was compared to TNT-α-d_3. This observation suggests that α-CH bond scission might have some role in shock initiated chemistry and in steady detonation. Consistent with this is the fact that the shifts of the N(1s) and O(1s) XPS peaks in shocked TNT have been interpreted as showing migration of H toward O (Reference 136).

All of the observations in the foregoing paragraph are phenomenological in that they suggest a role for the α-CH bond in the explosive properties, but do not give a mechanism. In some cases different processes produce the same effect. The primary kinetic isotopic effect ($k_H/k_D = 1.66 \pm 0.2$) found for the decomposition of TNT over minutes at 263°C is likely to result from the formation of 2,4-DNA or a related compound (Reference 51). The small values for the deuterium isotope effect observed for shock initiation and the detonation velocity (Reference 66) could result from dilution of the C-H homolysis isotope effect by $C-NO_2$ homolysis. Shock initiation and the velocity of detonation are dominated by reactions in the submicrosecond and the higher temperature regime. In this regime an isotope effect can also arise from the transport rate differences of H and D (1:1.4). Therefore, the small isotope effects observed may be caused by transport rate differences mixed with C-H homolysis chemistry and diluted by $C-NO_2$ homolysis. Furthermore, polynitroaromatic compounds containing α-CH bonds are not distinguishable from other compounds when the detonation pressure and E_a of slow thermal decomposition are correlated (Reference 7). In fact, Kamlet and

Hurwitz (Reference 182) do not believe that reaction kinetics even influences the velocity of detonation.

The overall description of the decomposition process of neat TNT in relation to the explosive characteristics requires both kinetic and mechanistic footing. The following view of TNT rests on firm ground based on the foregoing discussion:

(a) The dominant initiating processes of TNT are: $-CH_3$ oxidation producing 2,4-dinitroanthranil, 2,4,6-trinitrobenzaldehyde, etc.; $C-NO_2$ homolysis; and catalyst-dominated chemistry. Validation of this statement emerges from consideration of the kinetics and the mechanistic discussions in this section. The global reaction rates for the induction, acceleratory, and decay phases of TNT below 400°C were given in Table 5, and for nitrobenzene and nitrotoluene derivatives in Tables 6, 8 and 9. With these data the reaction time at a given temperature can be assessed for these main classes of reactions. E_a values in Table 5 for the induction phase of TNT are 41 - 51 kcal/mol, whereas for anthranil formation from 2-NT in Table 9, E_a is the range of 42.5 - 51.5 kcal/mol. This overlap is reasonably good evidence that the rate of the induction phase reactions of bulk TNT below 400°C is dominated by the formation of 2,4-DNA and compounds closely related to it. Moreover, there is virtually undisputable augmenting mechanistic evidence discussed above that both intra- and intermolecular H• transfer from $-CH_3$ to $-NO_2$ initiate thermal decomposition of TNT below 400°C. To represent the rate of this induction phase process in bulk TNT, the E_a and A values of Cook and Abegg (Reference 79) are useful because they are about the average of the data available (Table 5).

As discussed in Section IV.1., $C-NO_2$ homolysis is the dominant initial reaction of nitrobenzene compounds above about 900°C. To assess this reaction in TNT, the rate data for 1,3,5-TNB in Table 6 are valuable. Finally, for the acceleratory phase, the global rate data reflect the effects of catalysis on the numerous reactions that take place in this stage. The dominant reactions are unknown, but catalysis is an important factor in the rate. The rate data of Robertson (Reference 44) in Table 5 are useful for representing this phase. These three reactions lead to conclusion (b).

(b) The proper description of the dominant initiation reaction of bulk TNT depends on the temperature and reaction time. This statement follows from consideration of the relative importance of the three classes of reactions highlighted in (a) in terms of the time required to complete the reaction at a given temperature. This can be assessed by equation (29). Figure 4 is a plot of the

$$T_{rxn} = \frac{E_a}{R(\ln A + \ln \Delta t)} \qquad (29)$$

results. Note that the rate of the bulk phase induction reaction corresponding to the formation of 2,4-DNAn and the oxidation of $-CH_3$ matches the rate of $C-NO_2$ homolysis at about 770°C. Above 770°C, $C-NO_2$ homolysis is the faster reaction, while below 770°C, the $-CH_3$ oxidation reaction is faster. The reaction time at this crossover temperature is about 1 msec. Consequently, the impact sensitivity which results in heating for about 250 μsec might be expected to be influenced by reactions of the $-CH_3$ group, as Kamlet and Adolph (Reference 24) and Bliss, et al. (Reference 181) found. However, for shock sensitivity, in which the full energy input occurs in about 1 μsec or less and $T \geq 1000°C$, $C-NO_2$ homolysis contributes more than the $-CH_3$ group oxidation. It is, therefore, understandable that the deuterium isotope effect (Reference 66) is diluted, because $C-NO_2$ homolysis has become very important. The fact that the impact sensitivity, H_{50}, is more influenced by $-CH_3$ group oxidation, while the shock sensitivity, P_{90}, is more influenced by $C-NO_2$ homolysis, is the probable reason why TNT is an outlying point on a plot of H_{50} vs. P_{90} for a series of explosives (Reference 27).

(c) Times-to-explosion of TNT longer than 0.1 sec are controlled by catalytic reactions of the acceleratory phase. Shorter thermal explosion times are more controlled by $C-NO_2$ homolysis and $-CH_3$ oxidation. Experimental times-to-explosion measured in different ways over eight decades of time are given for TNT in Figure 4. Notice that between 1 and 60000 sec the time-to-explosion is not modeled by the induction phase kinetics of Table 1, as might be expected, but rather by the acceleratory phase kinetics which reflects catalysis. At shorter reaction times (10^{-2} - 10^{-3} sec) the times-to-explosion depart from the acceleratory phase kinetics. This could simply be the result of experimental inadequacies, such as the inability to achieve efficient heat transfer, that place the measured temperature higher than the true sample temperature. Acknowledging the experimental shortcomings, the times-to-explosion in Figure 4 at short times depart toward the induction phase rate and the $C-NO_2$ homolysis rate and away from the catalytically dominated acceleratory phase rate. Hence, at short reaction times primary reaction steps increasingly determine the time-to-explosion. However, at longer reaction times, catalysis and secondary reactions dominate the time-to-explosion. It is no surprise, therefore, that E_a values from times-to-explosion measurements have never been correlatable with the molecular structure and elementary reaction kinetics of polynitroaromatic compounds.

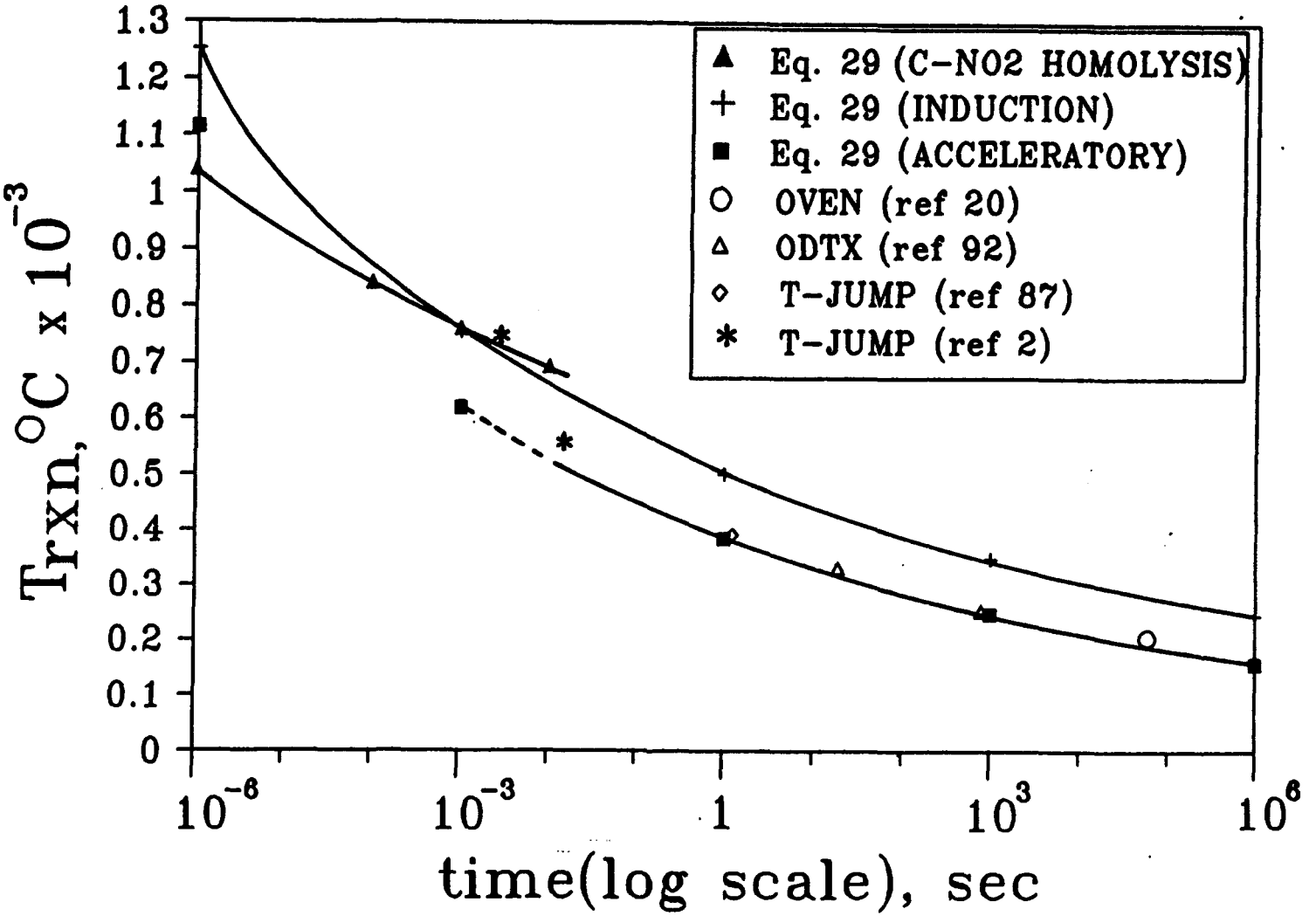

Figure 4. **Times-to-Explosion for TNT Modelled with Rate Constants of Three Processes: C-NO_2 Homolysis, -CH_3 Oxidation (Induction Phase), and Catalysis by Decomposition Products (Acceleratory Phase).**

b. α-NH Bonds

The difficulty of correlating the explosive characteristics of o-aminonitrobenzene compounds with their molecular and crystal features was described in Section II.4. The amino group stabilizes the nitroaromatic molecule toward shock sensitivity (Reference 67) and impact sensitivity (Reference 24,181), but hexanitrobiphenyl explosives are exceptions in that the impact sensitivity is actually increased by the presence of $-NH_2$ (Reference 183). In these latter compounds, steric demands may weaken several of the C-NO_2 bonds. In reality, many variables change when $-NH_2$ groups are added to the trinitrobenzene backbone making it unlikely that a single parameter holds the key to the dramatic changes in the chemical and physical properties through the series TNB, MATB, DATB, TATB. The differences are partly due to the crystal structure and partly due to the molecular and electronic structure. The important features of the crystal structure are considered first.

Structurally, TNB, MATB, DATB and TATB are very different. The intermolecular bond distances were given in Table 3. TNB contains both planar and non-planar benzene rings with $-NO_2$ groups twisted and bent out the plane and O atoms with large thermal parameters (Reference 68). The $-NO_2$ groups of MATB are non-coplanar with the benzene ring (Reference 69). The dihedral angles are 22.5°, 4.0° and 8.5°. Curiously, the most rotated $-NO_2$ group is 2-NO_2 which might have been expected to be coplanar because of intramolecular hydrogen bonding. Instead, intermolecular hydrogen bonds force this $-NO_2$ group out of the plane. From the point of view of the structure alone DATB (Reference 70) and TATB (Reference 71) are relatively similar. Both molecules are planar with chain-like intermolecular hydrogen bonding in DATB and layer-like bonding in TATB.

Electronically, the presence of the $-NH_2$ and $-NO_2$ substituents on an aromatic ring produces intricate competitive effects. The $-NH_2$ group is inductively withdrawing but resonance donating of electron density, whereas the $-NO_2$ group is both resonance and inductively withdrawing. Therefore, it is difficult to predict the reactivity of the ring when both groups are present. Politzer, et al. (Reference 184) and Rogers, et al. (Reference 67) addressed this problem computationally. The addition of an $-NH_2$ group in the ortho position of nitrobenzene stabilizes the ring because of resonance. Accordingly, the C-NO_2 bonds become progressively shorter as the number of $-NH_2$ groups increases (Table 3). SCF-3-21G MO calculations (Reference 185) reveal no energy minimum for the aci tautomer (VI) compared to o-

(VI)

nitroaniline. However, a significant body of experimental data is at odds with these computational findings. First, Matveev, et al. (Reference 102) observed a primary deuterium isotope effect (Table 8) in the gas phase when o-nitroaniline and o-nitroaniline-d_2 thermally decompose. This indicates that N-H bond scission, possibly of the type shown in (VI), occurs in the RDS. E_a for the decomposition step is relatively large (57.5 kcal/mol) which necessitates a relatively high temperature for the reaction to occur at a rapid rate. This temperature is still below that of other plausible reaction routes, such as C-NO_2 homolysis for which the E_a values are 65 - 70 kcal/mol (Tables 6 and 7). Second, the principal mass spectral fragmentation step of ortho-aminonitrobenzene compounds is loss of OH (References 36,126). This fact strongly suggests that H transfer as in (VI) is facile. Third, ESR spectra of irradiated TATB produces long-lived radicals consistent with protonated TATB (VII), which is proposed to result

(VII)

from intermolecular H• transfer (References 186,187). In view of positive evidence for species or processes involving or formally resembling (VI) in either the transition state or as the stable form, the negative computational evidence (Reference 185), evokes skepticism. More consistent with experiment is the computational finding that conversion of 2-nitroaniline to benzofurazan by equation (14a) is nearly thermally neutral (Reference 152). There is substantial experimental evidence discussed below for these conversions when -NH_2 and -NO_2 groups are ortho related.

Equation (14a) has been known for at least 80 years and is especially prevalent in an oxidizing environment (References 188,189). These reactions are standards in organic synthesis (References 141,190). In addition to the primary deuterium isotope effect when 2-nitroaniline decomposes (Reference 102), Rogers, et al. (Reference 191) found a primarily isotope effect (k_H/k_D = 1.5) when TATB thermally decomposes at 297 - 382°C. These findings support equation (14) as the lower temperature decomposition channel. The unimolecular decomposition of MATB is a straightforward extension of the behavior of 2-nitroaniline in that it loses OH by MS/MS-CID (Reference 126). However, in addition to the potential for cyclization reactions, equation (14), MATB also loses NO from the radical cation produced by CID (Reference 126). The mechanism is proposed to be equation (30), whose product is resonance stabilized. Furazan and furoxan formation occurs with TATB that has been thermally decomposed and

subcritically shocked or impacted (References 162,192-194). At least three different furazans were extracted by TLC and analyzed

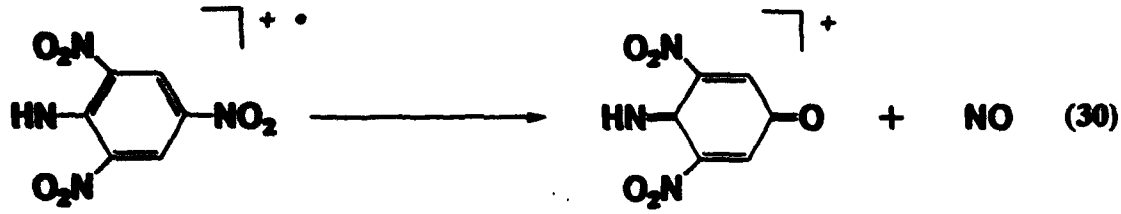

by CI-MS when TATB was thermally decomposed (Reference 192). Curve resolution of the XPS lineshapes of TATB subjected to shock and impact are consistent with formation of about 6% furazan and 6% furoxan derivatives (Reference 193). On the other hand, there is no IR evidence of the furazan ring in thermally decomposed TATB (Reference 195).

Kinetics information on MATB, DATB, and TATB in the solid, liquid and gas phase is compiled in Table 10. Data for several alkylamine derivatives of 2,4,6-trinitrobenzene are not shown but are available (Reference 54). The tendency for these compounds to react by equation (14) is the most logical explanation for the much smaller values of E_a and A compared to TNB (Table 6). Unfortunately, further analysis is necessarily qualitative because of scatter in the data and the fact that the measurements were made by different methods (DTA, DSC, manometry, electron beam heating traces, and effusion cell mass spectrometry). In the liquid and solid phase, matrix effects and catalysis by the decomposition products influence the Arrhenius constants (Section II.3.). There is a rough pattern of increasing E_a and A from MATB to TATB, which is consistent with the decrease in impact sensitivity along this series (Table 1). However, the Arrhenius factors of TNB are clearly out of line because the initiation process ($C-NO_2$ homolysis) is different from equation (14). To analyze the relative roles of $C-NO_2$ homolysis and furazan/furoxan cyclization in the aminonitrobenzene series, the gas phase data for MATB in Table 10 are perhaps least encumbered by matrix effects and catalysis. These rate data are compared in Figure 3 to that of TNB in Table 6 (Reference 198). The temperature at which $C-NO_2$ homolysis equals cyclization is 475°C or 625°C depending on the MATB rate chosen. Of course, these are crossover temperatures for the gas phase. Their relevance to the condensed phase is uncertain. If trusted, these temperatures are easily achieved in the condensed phase during shock and impact where Wenograd (Reference 2) estimated that TNB reaches 1060°C in about 250 μsec. Estimates of the crossover temperatures using the other data in Table 10 for MATB, DATB and TATB produce unreasonably large temperatures or impossible negative temperatures. Consequently, it is uncertain at which temperature $C-NO_2$ homolysis becomes competitive with cyclization in these compounds. However, Owens, et al. (References 73,74) and Murray, et al. (Reference 75) proposed that characteristics of the $C-NO_2$ bond are the main

Table 10. Arrhenius Data for Thermal Decomposition of Amino-2,4,6-Trinitrobenzene Compounds

Compound	Phase	T, °C	E_a, kcal/mol	A, sec^{-1}	Ref.
MATB	gas	301 - 343	38.5	$10^{8.8}$	53
	gas	240 - 280	41.8	10^{11}	84
	liquid	240 - 280	32	$10^{7.2}$	84
	liquid	249 - 259	48	-	54
DATB	liquid	320 - 323	46.3	$10^{15.07}$	12
	liquid	-	50	10^{15}	58
	solid	220 - 270	47	$10^{13.2}$	58
TATB	gas/solid	250 - 300	43	-	196
	solid	297 - 382	59.1	$10^{18.57}$	191
	solid	331 - 332	59.9	$10^{19.5}$	12
	solid	345 - 375	62±4	10^{19}	197

or rate controlling factor in the shock and impact sensitivity. This is the only initiation reaction that TNB, MATB, DATB, and TATB could have in common to account for the smoothly increasing trend of impact sensitivity (Table 1). The observation of furazan and furoxan compounds in heated, impacted and shocked samples of TATB (References 162,192-194) is understandable from the fact that the temperature during heat-up and cool-down emphasizes the lower E_a cyclization channel. The shocked and impacted samples did not explode and, therefore, did not reach the temperature range where $C-NO_2$ homolysis could dominate. Essentially the same spectral features subsequently interpreted as furazan and furoxan formation (References 162,192-194) were once interpreted as evidence of $C-NO_2$ homolysis (References 119,200).

$C-NO_2$ homolysis lacks appeal as the source of the decrease in shock and impact sensitivity as $-NH_2$ groups are added. This is because the $C-NO_2$ BDE is not especially sensitive to the other substituents on the ring (References 32,52). Thus, while $C-NO_2$ homolysis is the only common chemical initiation process possible TNB, MATB, DATB, and TATB, the increase in the amount of inter- and intramolecular hydrogen bonding along this series is a structural variable that may influence the shock sensitivity. These interactions have been proposed by Rogers, et al. (Reference 67) to absorb shock energy and prevent it from being localized in the molecule. This effect is difficult to judge kinetically, but it could be accommodated in theories of how mechanical energy converts into chemical processes (References 14-19). Raman spectroscopy during dynamic shock loading also suggests that the N-H•••O bond becomes compressed (Reference 35). A qualitative indication of the increase in the cohesive force in the lattice as $-NH_2$ groups are added is the increase in melting points (Table 2).

Taken together, the cyclization reactions (equation 14) of aminonitrobenzene explosives dominate the initial thermal reactions in the lower temperature range. These reactions could be important in sensitizing a "rough handled" explosive (Reference 78). At high temperatures characteristic of shock and impact initiation, $C-NO_2$ homolysis appears to play a large and perhaps even dominant role in the initiation chemistry. However, the decreased shock and impact sensitivity as $-NH_2$ groups are added to the ring seems to be best accounted for by shock-absorbing hydrogen bonding in the crystal lattice.

TATB is the most important explosive of this category and, as such, deserves further comment. TATB is infamous for its high thermal stability (>300°C), low impact sensitivity, and low solubility. The $C-NH_2$ bonds are unusually short (1.319(7) Å), while the C-C bonds are unusually long (1.444(7) Å) compared to C-C of benzene (1.40 Å) (Reference 71). A typical C-C single bond distance is about 1.47 Å. The π^* MO's of the ring are partially occupied (Reference 67). Strong intramolecular NH•••O hydrogen bonding leads to a planar molecule while moderate intermolecular

hydrogen bonding causes stacking of the molecules in graphite-like layers (References 71,201).

Given the unusual materials properties of TATB and the significant amount of intermolecular association, complexity in the decomposition behavior of TATB comes as no surprise. Unlike most nitroaromatic explosives, TATB decomposes from the solid phase unless it is heated rapidly (Reference 197). A melting point of about 450°C has been mentioned (Reference 197) although Meyer (Reference 13) gives 350°C. Discoloration rather than melting is visually observed when TATB is heated at 2000°C/sec to 500°C on a Pt filament (Reference 22). Catalano, et al. (References 45,195,202) made numerous observations and measurements on the slow thermal decomposition of TATB. Reactions resulting in a residue and gas formation occur simultaneously with sublimation in the 305 - 357°C range (Reference 45). By DSC, the process is exothermic despite the fact that ΔH_{vap} is endothermic by 40 kcal/mol (References 203,204). Perhaps five processes occur at 342 - 357°C necessitating the use of multiple rate expressions (Reference 45). The initial stage is autocatalytic with E_a = 50 - 60 kcal/mol and appears to consist of at least two consecutive reactions. The global reaction order is 0.5. The overall E_a resembles the values given in Table 10. The remaining stages of decomposition have E_a values in the range of 50 - 80 kcal/mol (Reference 3).

MS and IR analyses of the gaseous products from confined and unconfined TATB suggest (Reference 202) that the removal of intercalated CO_2, acetone, H_2O and N_2 occurs initially. 1 - 2% of the space between the layers is occupied by these trapped molecules. It is conceivable that the small amount of H_2 also observed comes from furazan formation, equation (14a), while some of the H_2O may result from furoxan formation, equation (14b). As the reaction rate accelerates into an explosion CO_2, H_2O and N_2 increase in concentration and are joined by HCN, CO and NO. Other gaseous products detected in small amounts included N_2O, NO_2, CH_4 and C_2N_2. A solid residue containing C, H, N, and O remained. The gas products from rapid thermolysis of TATB are available in other studies (Reference 198) and are discussed in Section VI. Furazans and furoxans are detected in some thermal decomposition studies of TATB (References 162,192-194) but not others, (Reference 195). These compounds are not likely to have a high steady-state concentration because they are less thermally stable than TATB. The gas products of decomposition of furoxans closely resemble those of TATB (Reference 205). It should be noted that a completely different view of thermal decomposition of TATB has been presented from MS studies by Farber and Srivastava (Reference 196). The EI mass spectrum of the products following use of an effusion cell and Langmuir evaporation at 200 - 300°C showed sublimation followed by splitting of TATB into two fragments of m/e = 114 and 144. These two masses are consistent with fission of the molecule along the dashed line of (VIII). Species having

other m/e values are detected as well that would result from various entities cleaved directly from TATB. These results are unique and perhaps reflect the conditions of the experiment more

(VIII)

than the relevance to the behavior of TATB as a bulk explosive. For instance, they contradict the primary deuterium isotope effect found during decomposition of bulk TATB (Reference 191). The value of E_a = 43 kcal/mol in Table 10 from MS studies of TATB (Reference 196) was determined from the rate of growth of m/e = 114. This value of E_a is disquietingly similar to ΔH_{vap} of TATB of 40 kcal/mol. Moreover, Langmuir evaporation and effusion cell results for another molecule, HMX, sharply differ from those of another MS technique, simultaneous thermogravimetry-modulated beam mass spectrometry (Reference 38).

c. α-OH Bonds

The -OH group plays a major role in the thermal stability of nitroaromatic compounds, but the effect has to do with the tendency of -OH to become a quinoid group, rather than with cyclization. The -OH group is a resonance electron donor as is the $-NH_2$ group. However, the -OH substituent shortens the C-NO_2 bond and lengthens the N-O bond less than does $-NH_2$ (References 185,206). Since $-NH_2$ stabilizes the nitrobenzene backbone toward initiation by impact (Table 1), it might be expected that -OH also stabilizes the molecule compared to TNB. The opposite is found in practice because -OH derivatives are more impact sensitive than TNB (Reference 24). This has recently been explained by the fact that the aci-nitro structure (X) is computed to have an energy minimum, but at only 1.54 kcal/mol above (IX) (Reference 185). Upon shock or impact stimulus, vibrational excitation could force

(IX) (X)

a significant fraction of the molecule into the more reactive form (X). This computational finding (Reference 185) is consistent with a century of observations in organic chemistry. Quinones are

isolated upon thermal decomposition of p-nitrophenols, equation (31) (References 207,208). The quinoid form (X) has long been suspected to be the source of bright color when picric acid (PA) is dissolved in basic solution. For this reason, nitrophenol compounds are useful as acid-base indicators.

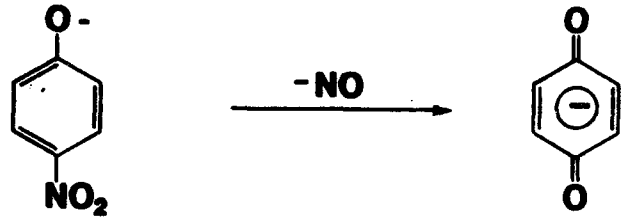

(31)

PA is a historically important explosive, but is hazardous because of its high sensitivity to shock. The acidity of PA (k_a = 1.6 x 10^{-1} M) is also detracting because it corrodes metal and attacks many organic materials with which PA might be mixed. Despite these problems, PA was used extensively as an explosive up to World War II.

Compared to the $-CH_3$ and $-NH_2$ groups relatively little work has been conducted on the details of thermal decomposition of hydroxy-substituted nitrobenzene compounds (Reference 209). The behavior of PA is reminiscent of TNT and other nitroaromatics in that melting followed by decomposition occurs. The process is first-order autocatalytic after the initial induction period (Reference 209). Like TNT, the rate of decomposition in the gas phase is slower than in the liquid state suggesting that catalysis and intermolecular interactions are important. Arrhenius data are sparse, but are shown in Table 11. The large variation in values makes conclusions difficult to draw. However, the TTX value (Reference 94) probably can be discarded because of the difficulty of obtaining efficient heat transfer.

The initial reaction step of PA at the temperatures in Table 11 appears to involve the quinoid structure (X) on the basis of ESR and MS studies (References 126,132,170,211). Radicals (XI) and (XII) that are readily formed from the equivalent of (X) were suggested to explain the ESR spectra of thermally decomposing PA

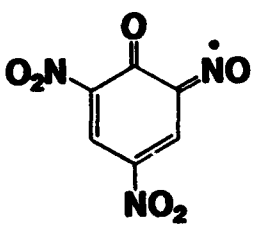

(XI)

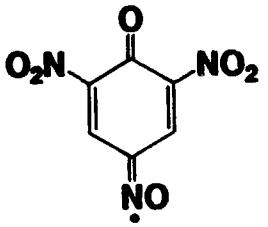

(XII)

Table 11. Arrhenius Data for Hydroxy-substituted Trinitrobenzene Compounds

Compound	T, °C	E_a, kcal/mol	A, sec^{-1}	Method	Ref.
PA	183 - 270	38.6	$10^{11.7}$	EG	210
	233 - 244	51.9	-	DTA	56
	267 - 350	27.4	-	TTX	94
1,3-$(OH)_2$-2-4,6-TNB	180 - 200	34.6	$10^{11.2}$	EG	210
1,3,5-$(OH)_3$-2,4,6-TNB	145 - 165	54.3	10^{22}	EG	50

(Reference 211). A thermal decomposition reaction that appears to be unique to PA (and MATB) is inferred from the ions in CI-MS (Reference 170) and MS/MS-CID (References 126,132). This is loss of NO as the dominant decomposition pathway. In a manner similar to equation (31), resonance stabilization through the quinoid structure according to equation (32) was proposed to be the main reason for the facileness of this process. When all data are taken together, a clear understanding of the decomposition

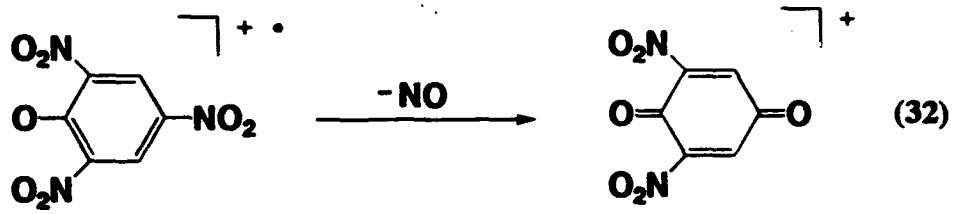

(32)

mechanism of PA does not exist. The mobility of the H atom bound to -OH almost certainly plays a major role in thermal decomposition mechanism at lower temperatures. Unlike when $-CH_3$ and $-NH_2$ groups are ortho to $-NO_2$, cyclization does not occur. It is logical to extrapolate from the more extensive data available on $-CH_3$ and $-NH_2$ substituted trinitrobenzene compounds that C-NO_2 homolysis is also a major, if not the dominating, early reaction during impact and shock initiation of PA.

d. $-N_3$ ortho to $-NO_2$

The azide group cyclizes an ortho $-NO_2$ group in a manner resembling the behavior when $-CH_3$ and $-NH_2$ groups are ortho to $-NO_2$. Upon heating above 70°C 2-nitrophenylazide eliminates N_2 and forms benzofuroxan according to equation (33). This reaction has been used for years as a facile synthetic route to substituted benzofuroxans (References 141,190,212). In the EI mass spectrum

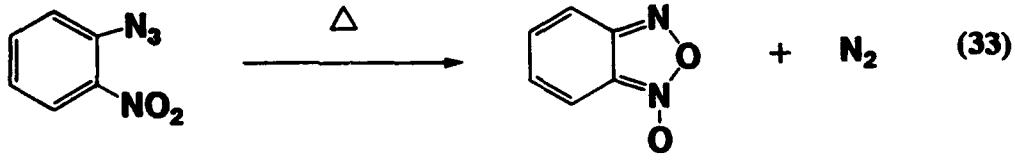

(33)

of 2-nitrophenylazide, an m/e = 136 fragment is observed corresponding to benzofuroxan (Reference 64). Equation (33) contrasts with the behavior of meta and para isomers where the rate of thermolysis is 10^4 times slower at 100°C owing to a different decomposition mechanism, equation (34) (References 106,213).

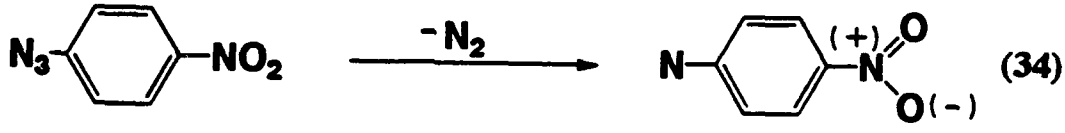

(34)

The Arrhenius data compiled in Table 12 reflect the significantly different rates of equations (33) and (34). When ortho related $-N_3$ and $-NO_2$ groups are present on the ring, the decomposition rate is insensitive to the presence of other $-N_3$ or $-NO_2$ groups, because equation (33) dominates the process (Reference 106). On the other hand, equation (33) is accelerated by the presence of electron-withdrawing groups para to $-NO_2$ (Reference 215).

Whether equation (33) or (34) dominates has a pronounced effect on the burn rate of these compounds. Despite the higher E_a of equation (34), the burn rates of 3- and 4-nitrophenylazide are 1.4 - 1.7 times higher than 2-nitrophenylazide (Reference 106). This is because the nitrene product of equation (34) decomposes much more exothermically than the furoxan product of equation (33). Release of a large amount of heat early in the decomposition reaction scheme near the burning surface produces a high burn rate for the material (References 216,217).

The initial decomposition chemistry when an azide group is present on a nitroaromatic backbone appears to be straightforward based on current knowledge of these compounds. However, the explosive characteristics of these compounds are essentially unknown.

e. Other ortho Substituents

Cyclization of an $-NO_2$ group with an ortho substituent is so widely occurring that a few additional studies are worthy of mention to dispel any lingering thought that the results in Sections IV.4.a, b, and d are unique.

As noted in Section IV.4.a, α-CH abstraction from a $-CR_2'R''$ group ($R' = R'' = H$; $R' = H$, $R'' = CH_3$; $R' = CH_3$, $R'' = H$) is a general reaction in the presence of an ortho $-NO_2$ group. However, further reaction of the molecule following this initial C-H abstraction step proceeds by different routes (Reference 37). For instance, the formation of anthranil by equation (26) occurs for the $-CH_3$ group. On the other hand, 2-nitroethylbenzene yields

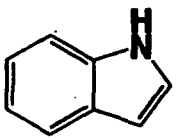

(XIII)

indole (XIII) through a series of H rearrangements (Reference 37). When $R' = H$ and $R'' = N(CH_3)_2$ equation (35) occurs in the sample on sitting at room temperature for several days (Reference 218).

Table 12. Arrhenius Data for Thermal Decomposition of Nitrophenylazide Compounds

Compound	E_a, kcal/mol	A, sec^{-1}	Ref.
2-Nitrophenylazide	26.1	$10^{12.3}$	214
4-Nitrophenylazide	40.6	$10^{16.8}$	213
1,3,5-Triazido-2,4,6 -trinitrobenzene	26.0	$10^{12.1}$	106

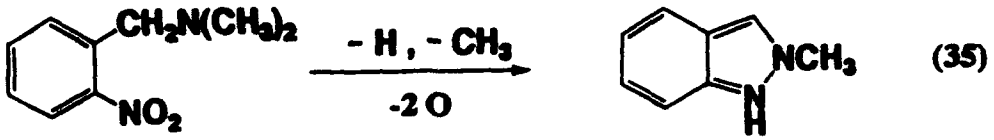

(35)

Unimolecular decomposition of 2-nitroanisole has been proposed to occur via H migration and ring closure, equation (36) (Reference 144). This species then collapses to benzoxazole (Reference 37).

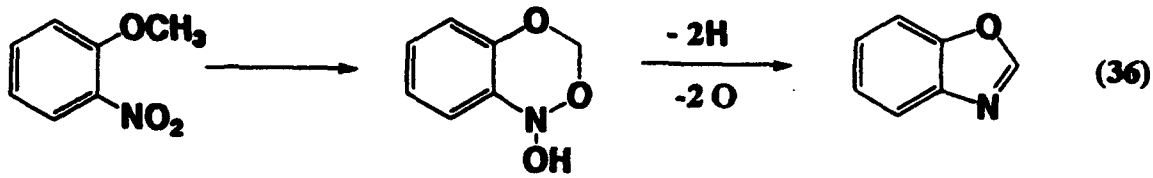

(36)

Such a rearrangement is consistent with the formation of a substituted benzoxazole when a longer alkoxy chain is present, equation (37) (Reference 219). Likewise, 2-nitro(methylamino)

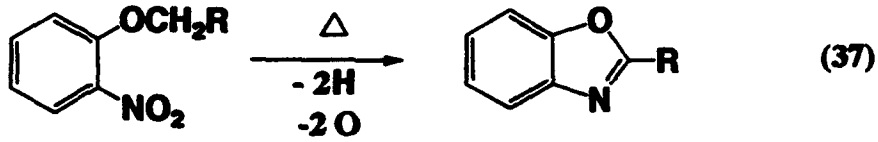

(37)

benzene was observed to form benzimidazole at a relatively relatively low temperature by equation (38) (Reference 37). Benzofurazan is isolated from methyl-N-(2-nitroaryl)carbamate

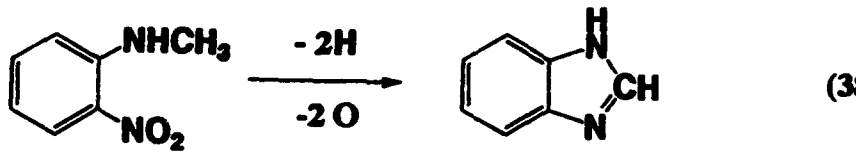

(38)

according to equation (39) (References 220,221).

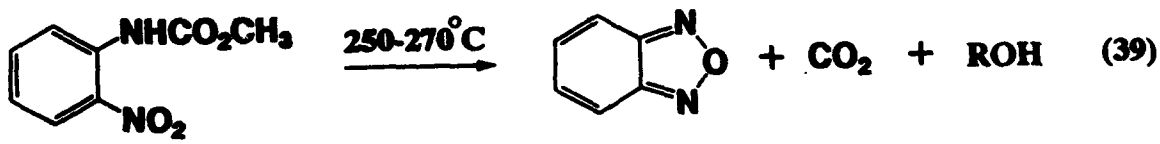

(39)

The hydrazine derivative of nitrobenzene also decomposes at a relatively low temperature liberating water and forming

benzotriazole, equation (40) (Reference 123). Even 1,2-dinitrobenzene loses O_2 upon heating giving small amounts

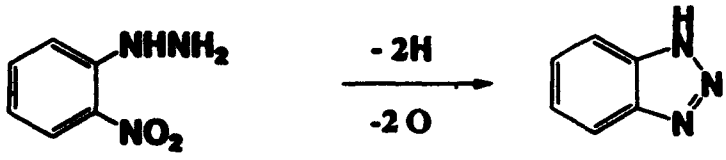

(40)

of benzofurazan and benzofuroxan (References 102,110) by equation (41).

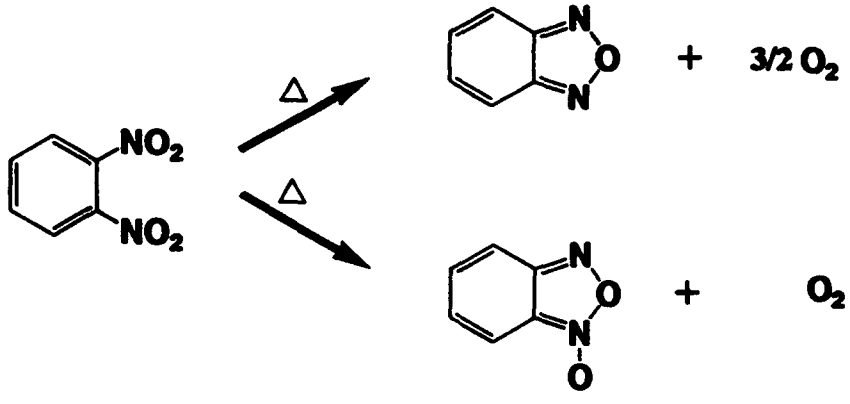

(41)

SECTION V

EFFECT OF SUBSTITUENTS ON THE KINETICS OF THERMOLYSIS

Throughout Section IV, the positioning of a reactive substituent ortho to the $-NO_2$ group stands out as a very important factor in the low E_a thermal decomposition pathways of nitroaromatic compounds. In this section a broader view is taken of the effect of various substituents on the decomposition rate.

Hammett championed the notion that rate constants of various reactions are related to the structure and composition of the parent aromatic molecule (References 222,223). More specifically, the electron density of the aromatic ring influences its reactivity and the reactivity of the attached substituents. Linear free energy relationships for the substituents were determined that are frequently referred to as Hammett or Taft constants (References 224-226).

An outstandingly prominent feature of polynitroaromatic compounds is that thermal decomposition data generally do not correlate with Taft or Hammett constants. The absence of correlation is independent of the phase of decomposition in that neither the gas phase nor the condensed phase kinetic data correlate (Reference 52). Several possible reasons for non-correlation are possible. Hammett constants depend on the solvent and the temperature of measurement. First, the temperature at which polynitroaromatic compounds decompose is usually very different from the temperature at which the Hammett constants are determined. Second, the molecular environment during thermal decomposition is different from that in which the Hammett constants are determined. Third, the foregoing sections illustrate that catalysis and bimolecular processes frequently dominate during thermal decomposition of nitroaromatic compounds. Fourth, the rates of thermal decomposition of nitroaromatic compounds may not depend very much on the resonance and inductive electronic effects of the substituents. For example, E_a for thermal decomposition of nitrobenzene compared to a variety of 1,3- and 1,4-substituted nitrobenzene compounds differs by only ±2 kcal/mol and the A values differ by only a factor of five (Reference 52).

Despite the absence of correlations with Hammett constants, the substituents on the ring still exert a profound effect on the explosive properties and the kinetics of decomposition. The most ambitious attempt to discover structure/reactivity/detonation relationships has been the work of Zeman, et al. (References 5-8, 54). That a relation might even exist could be traced to comments of Cook, et al. (References 3,4) who proposed that the early decomposition kinetics affect the detonation velocity of an explosive. Zeman, et al., based their conclusions on values E_a before the onset of autocatalysis; T_D, the temperature immediately

after the onset of the exotherm; P, the C-J pressure; D, the detonation velocity; and Q, the heat of explosion. Equation (42) was used. The values of the constants a and b depend on the

$$\log(E/T_D) = \frac{b(P,\ D^2,\ Q) + a}{\rho} \qquad (42)$$

variable P, D^2 or Q chosen. By using data for 74 compounds, 41 of which are nitroaromatic compounds without other energetic substituents, Zeman found groupings of 3 - 5 compounds that gave reasonably linear solutions for equation (42). One group contained 10 compounds. On this basis, structure and electronic relationships were proposed to exist between the early kinetics of slow thermal decomposition and detonation (References 6,7). Few of these groupings, however, are chemically satisfying. For example, the largest group containing 10 compounds contains both sensitizing (-OH) and desensitizing ($-NH_2$) substituents (Reference 7). Another contains both $-CH_3$ and -Cl substituents (Reference 5) which do not decompose by the same mechanism. In fact, Rogers, et al. (Reference 191) would dispute the foundation of Zeman's assumed connection, at least for TATB. Zeman (Reference 5) also related the equilibrium constant for the activated complex, $K^{\ddagger}$, to D on a log-log plot and found selected groupings of compounds in the 74 compound data base. A caveat is that a log-log plot tends to be relatively insensitive to curvature. Moreover, some of the correlations are rather loose, which partly reflects the difficulty of obtaining accurate experimental data. Zeman's DTA data are sensitive to the sample weight (References 55,56,97-101).

Considering all of the literature, the decomposition and explosive properties of nitroaromatic compounds are clearly sensitive to the substituents. However, most relationships defy simple chemical interpretation. The trends in the liquid phase and the gas phase are usually different because of the role of catalysis, bimolecular processes, and the environment. Nevertheless, a few correlations merit further mention.

According to the Hammett and Taft constants, the $-NO_2$ substituent is one of the strongest electron withdrawing groups available. Accordingly, the ionization potential of the π-HOMO of the benzene ring increases as the number of $-NO_2$ groups is increased (Reference 227). Perhaps for this reason, the decomposition rate is faster as the number of $-NO_2$ groups on the ring is increased (Reference 55). The relative rate constants at 330°C in the gas phase (Reference 53) for $C_6H_5NO_2$: $1,3-(NO_2)_2C_6H_4$: $1,3,5-(NO_2)_3C_6H_3$ are 1:20:34. This is also the trend in the burn rate of these compounds at a given pressure and value of the pressure exponent (References 106,228). The position of the $-NO_2$ groups relative to one another on the ring affects the reaction rate at 330°C. This is evident for 1,2,3-TNB, 1,2,4-TNB, and 1,3,5-TNB which have relative rates of 1:0.175:0.03 (Reference 53). This trend suggests that within a given stoichiometry the

thermal stability is improved by making the molecule more symmetrical (Reference 229). Bliss, et al. (Reference 181) explained this same pattern in the sensitivity to impact in terms of the greater ease of nitro-nitrite isomerization when $-NO_2$ groups are ortho related.

As substituents other than $-NO_2$ are added to the ring, resonance and inductive effects shift the π-MO's relative to one another in complex ways. The resulting effect on the rates of thermal decomposition frequently makes random chemical sense. For example, -OH is thermally destabilizing. The addition of -OH increases the decomposition rate in the order (Reference 229) 2,4,6-trinitroresorsinol > 2,4,6-trinitrophenol > 1,3,5-TNB. This additivity effect is satisfying. On the other hand, the trend for multiple $-CH_3$ groups in the liquid phase is not additive. One $-CH_3$ group destabilizes the molecule while two and three $-CH_3$ groups stabilize it relative to TNB; e.g. the trend in thermal stability is TNT < TNB < 2,4,6-trinitroxylene < 2,4,6-trinitromesitylene (Reference 229). Other evidence exists that the effect of the $-CH_3$ group on a nitroaromatic backbone is complicated. For example, in the gas phase, the 2-NT is less thermally stable than nitrobenzene because of anthranil formation (Reference 33) (Section IV.4.a), while 1,4-NT is more stable because of the lower A factor of decomposition (Reference 32). A -Cl substituent destabilizes 2,4,6-trinitrochlorobenzene as revealed by the increase of 1.75 in the gas phase reaction rate compared to 1,3,5-TNB (Reference 53). When a second or third -Cl group is added to the TNB backbone, there is no further effect on the rate of decomposition (Reference 53). Substituents with built-in reactivity (Reference 230) can override all of the conventional notions about thermal stability of the nitroaromatic ring. Furthermore, except for the "ortho effects" discussed in Section IV, the MS cracking patterns of substituted trinitrobenzene compounds follow few systematic patterns (References 126,170).

SECTION VI

LATER STAGE REACTIONS

All of the forementioned thermolysis reactions of polynitrobenzene explosives have occurred among the substituents while leaving the aromatic backbone intact. These substituent homolysis and cyclization reactions are obviously early reactions of nitroaromatic explosives, and can be thought of as initiation steps in which little energy is generated. The next stage of thermal decomposition involves propagation reactions. These reactions involve exothermic oxidation and reduction that lead to lower molecular weight and thermodynamically stable gaseous products. While much is known about the related kinetics and thermochemistry of hydrocarbon/air flames (References 231-233) and nitrogen chemistry in combustion (Reference 234), the processes by which large, bulk phase energetic molecules thermolyze to form the reactants for the high temperature flame is a challenging area of research (References 41,107,217). Specifically, by what intervening steps does 2,4-DNAn or the dinitrotoluene radical proceed to CO, NO, CO_2, HCN, N_2 and H_2O?

At least in the gas phase according to MS/MS/CID (Reference 134) ring dissociation does not occur until most of the attached substituents have been removed. On the other hand, dissociation of NO_2 from the ring leaves the ring with excess internal energy to drive further reactions (Reference 111). In the simplest situation, the EI mass spectrum gives a scheme for further unimolecular reactions of the aromatic ring in the collisionless gas phase. 2-Nitrotoluene is believed to react further according to equation (43) based on ^2H and ^{13}C labelling (Reference 36).

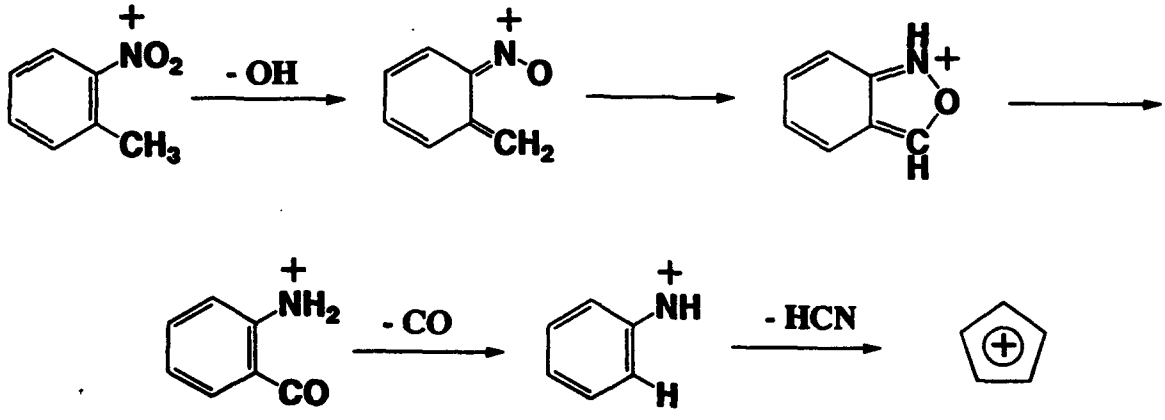

Consistent with this scheme is the fact that anthranil (equation 12) decomposes by rupture of the NO bond with a rate constant (Reference 34) of $k = 3.7 \times 10^{15} \exp(-51084/T)\ sec^{-1}$. The large A factor is in line with high entropy of the transition state. The

proposed pathway for anthranil degradation is equation (44) (Reference 34).

The relevance of the findings described above to the bulk state of an explosive is dubious because of the important role played by bimolecular processes. In fact, attack on the ring is quite plausible because the aromaticity of the benzene ring is

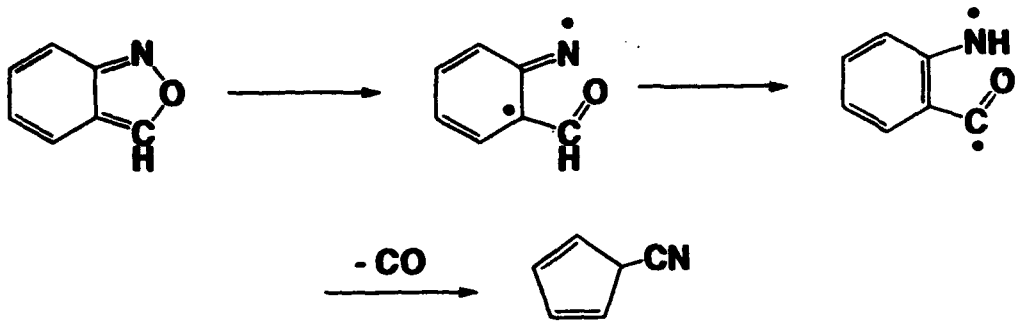

(44)

reduced by ring closure to anthranil (equation 12), or furazan/furoxan species (equation 14). This makes the ring more susceptible to reactions that ultimately lead to C-C bond cleavage. For example, trinitroaromatics are notoriously susceptable to nucleophilic addition (References 235-237) which also reduces the aromaticity. While $NO_2(g)$ is not liberated to any great extent from decomposition of trinitroaromatic explosives at temperatures below about 700°C, NO_2 or NO from thermal decomposition in the bulk phase may be attacking the aromatic ring producing CO and CO_2. Maksimov (Reference 63) examined the decomposition of TNB vapor and noticed first a rise and then a drop in the NO concentration, which was attributed to the reaction of a nitrosoaromatic compound, RNO, with NO according to equation (45). The NO consumption occurs as CO_2 is formed, perhaps owing to the reaction of the nitrate radical with ·R (Reference 63).

$$RNO + 2NO \longrightarrow R\cdot + N_2 + NO_3\cdot \qquad (45)$$

The energy released by the propagations reactions of polynitroaromatic explosives is sometime reflected in the relative concentrations of the gaseous products that are liberated after the exotherm. For example, Table 13 gives the IR active products for TNB, MATB, DATB and TATB (Reference 198). Endothermic products NO, HCN and N_2O form when $-NH_2$ groups are present on the ring. HNCO also increases as the NH_2 content increases. Even though the C/O ratio in this series of parent compounds remains fixed, the CO_2/CO ratio increases as the NH_2 content increases. The energy distribution among the gaseous products reflects the fact that the heat of explosion of TNB is higher than those of the aminonitrobenzene explosives (Table 1). The high heat of explosion of TNB results from the dominance of products with negative ΔH_f° (CO, CO_2, HNCO) and the absence of products with positive ΔH_f° (NO, HCN, N_2O). For MATB, DATB and TATB the amount

of energy from the exothermic products (CO, CO_2) is lower than for TNB and is further aggravated by the formation of endothermic products (NO, HCN, N_2O). In sum, the energy output of TNB results from a different set of propagation reactions than occurs for MATB, DATB and TATB.

Table 13. Quantified Gas Products from Heating at 2000°C/sec to 520°C under 10-40 atm Ar

	Percentage					
Compound	CO_2	CO	NO	HCN	N_2O	HNCO
TNB	6	94	-	-	-	-
MATB	17	38	28	13	-	3
DATB	20	31	21	18	2	8
TATB	27	20	26	13	3	11

SECTION VII

CONCLUSIONS

Consideration of the literature and the addition of new data from this program has clarified a number of issues about nitroaromatic explosives. The main points are highlighted here.

A relatively fruitless approach to understanding the shock and impact sensitivity of nitroaromatic explosives is the comparison of these properties to the parent ground state molecular and electronic structure. The parameters that control shock and impact sensitivity in this type of compound only partially depend on the molecular and electronic structure of the compound. Physical properties, such as the void volume and density, are very important. The essential point of this report is that the rates of chemical reactions are equally important.

The analysis presented in this report makes it completely understandable why the time-to-explosion does not correlate with the molecular and electronic characteristics, such as are reflected in the Hammett or Taft linear free energy relationships. The time-to-explosion at times longer than about 0.1 sec is controlled by catalysis of the decomposition products of the parent molecule and not the parent molecule per se.

In general, the thermal decomposition of nitroaromatic explosives begins with one or more endothermic initiation steps. These steps include C-NO_2 homolysis, isomerization of the nitro group to the nitrite linkage, and reactions of the non-energetic substituent on the ring. The relative importance of these initiation steps depends on the temperature and pressure reached during the stimulus step. Shock initiation predominantly produces C-NO_2 homolysis in TNT and the aminonitrobenzene series. Impact initiation results in competitive contributions of C-NO_2 homolysis and reactions involving the nonenergetic substituent, especially in the case of TNT. In sum, decomposition at lower temperature favors reactions of the non-energetic substituent, whereas higher temperature favors direct bond homolysis.

Following the initiation reaction steps mentioned above, a different gas/solid product mixture will exist depending on the temperature. The propagation steps that follow will, therefore, differ and, in turn, cause the explosive characteristics to differ from compound to compound. For example, as the number of -NH_2 groups increases in the aminonitrobenzene series, the quantity of products with positive heats of formation increases relative to the products with negative heats of formation. This difference causes a decrease in the heat of explosion as -NH_2 groups are added to the ring.

It would appear that the rational design of a nitroaromatic explosive can not be restricted to considerations of the ground state molecular and electron structure of the target molecule. Instead, the initiation and propagation reactions need to be the focal issue.

REFERENCES

1. Robertson, A. J. B.; Yoffe, A. D. Nature, **1948**, 161, 806.

2. Wenograd, J. Trans. Farad. Soc., **1961**, 57, 1612.

3. Cook, M. A.; Horsley, G. S.; Partridge, W. S.; Ursenbach, W. O. J. Chem. Phys. **1956**, 24, 60.

4. Cook. M. A.; Mayfield, E. B.; Partridge, W. S. J. Chem. Phys. **1975**, 59, 675.

5. Zeman, S. Thermochim. Acta **1981**, 49, 219.

6. Zeman, S.; Dimun, M.; Truchlik, S. Thermochim. Acta **1984**, 78, 181.

7. Zeman, S. Thermochim. Acta **1980**, 41, 199.

8. Zeman, S. Thermochim. Acta **1979**, 31, 269.

9. Frank-Kamenetskii, D. A. Acta Physicochem. USSR **1939**, 10, 365.

10. Chambré, P. L. J. Chim. Phys. **1952**, 20, 1795.

11. Zinn, J.; Mader, C. L. J. Appl. Phys. **1960**, 31, 323.

12. Rogers, R. N. Thermochim. Acta **1975**, 11, 131.

13. Meyer, R. Explosives, Third Edition, VCH Publishers, New York, NY 1987.

14. Walker, F. E.; Wasley, R. J. Prop. Explos. **1976**, 1, 73.

15. Coffey, C. S.; Toton, E. T. J. Chem. Phys. **1982**, 76, 949.

16. Trevino, S. F.; Tsai, D. H. J. Chem. Phys. **1984**, 81, 348.

17. Zerilli, F. J.; Toton, E. T. Phys. Rev. B **1984**, 29, 5891.

18. Walker, F. E. J. Appl. Phys. **1988**, 63, 5548.

19. Dlott, D. D.; Fayer, M. D. J. Chem. Phys. **1990**, 92, 3798.

20. Dacons, J. C.; Adolph, H. G.; Kamlet, M. J. J. Phys. Chem. **1970**, 74, 3035.

21. Rogers, R. N. Anal. Chem. **1967**, 39, 730.

22. Brill, T. B.; Brush, P. J.; James, K. J.; Shepherd, J. E.; Pfeiffer, K. J. Appl. Spectrosc. **1992**, 46, 900.

23. Brill, T. B.; Shepherd, J. E. Tenth Symp. (Int.) Detonation, Office of Naval Research, Arlington, VA, 1993.

24. Kamlet, M. J.; Adolph, H. G. Prop. Explos. 1979, 4, 30.

25. Brill, T. B.; Brush, P. J. Phil. Trans. Roy. Soc. (Lond.) A 1992, 339, 377.

26. Kanel, G. I. Fiz. Goreniya Vzryva 1978, 14, 113.

27. Storm, C. B.; Stine, J. R.; Kramer, J. F. in Chemistry and Physics of Energetic Materials, S. Bulusu, Ed. Kluwer Academic Publ., Dordrecht, The Netherlands, p. 605.

28. Dremin, A. N. Phil. Trans. Roy. Soc. (Lond.) A 1992, 339, 355.

29. Engelke, R. P.; Sheffield, S. A. Encyclopedia of Applied Physics, Vol. VI, G. L. Trigg, Ed., VCH Publishers, New York, NY, 1993.

30. Urizar, M. J.; Peterson, S. W.; Smith, L. C. LA-7193-MS, Los Alamos Scientific Laboratory, Los Alamos, NM, April, 1978.

31. Hosoya, F.; Shiino, K.; Itabashi, K. Prop. Explos. Pyrotech. 1991, 16, 119.

32. Gonzalez, A. C.; Larson, C. W.; McMillen, D. F.; Golden, D. M. J. Phys. Chem. 1985, 89, 4809.

33. Tsang, W.; Robaugh, D.; Mallard, W. G. J. Phys. Chem. 1986, 90, 5968.

34. He, Y. Z.; Cui, J. P.; Mallard, W. G.; Tsang, W. J. Am. Chem. Soc. 1988, 110, 3754.

35. Trott, W. M.; Renlund, A. M. J. Phys. Chem. 1988, 92, 5921.

36. Meyerson, S.; Puskas, I.; Fields, E. K. J. Am. Chem. Soc. 1966, 88, 4974.

37. Fields, E. K.; Meyerson, S. Adv. Free Rad. Chem. 1965, 5, 101.

38. Behrens, R., Jr. J. Phys. Chem. 1990, 94, 6706.

39. Bulusu, S.; Axenrod, T. Org. Mass Spectrom. 1979, 14, 585.

40. Yinon, J. in Chemistry and Physics of Energetic Materials S. Bulusu, Ed., Kluwer Academic Publ's., Dordrecht, The Netherlands, 1990, p. 685.

41. Brill, T. B. Prog. Energy Comb. Sci. 1992, 18, 91.

42. Lewis, K. E.; McMillen, D. F.; Golden, D. M. J. Phys. Chem. 1980, 84, 226.

43. Emanuel, N. V. The Oxidation of Hydrocarbons in the Liquid Phase MacMillan, New York, New York, 1958.

44. Robertson, A. J. B. Trans. Farad. Soc. 1948, 48, 977.

45. Catalano, E.; Crawford, P. C. Thermochim. Acta. 1983, 61, 23.

46. Maksimov, Yu. Ya; Dubovitskii, V. F. Dokl. Akad. Nauk SSR 1966, 170, 371.

47. Maksimov, Yu. Ya; Glushetskaya, L. S.; Sorochkin, S. B. Tr. Mosk. Khim. Technol. Inst. im. D. I. Mendeleeva 1979, 104, 22.

48. Maksimov, Yu. Ya. Russ. J. Phys. Chem. 1971, 45, 441.

49. Hand, C. W.; Merritt, C., Jr.; DiPietro, C. J. Org. Chem. 1977, 42, 841.

50. Maksimov, Yu. Ya.; Kogut, E. N. Izv. Vyssh. Uchebn. Zaved. Khim. Khim. Technol. 1977, 20, 349.

51. Shackelford, S. A.; Beckmann, J. W.; Wilkes, J. S. J. Org. Chem. 1977, 42, 4201.

52. Matveev, V. G.; Dubikhin, V. V.; Nazin, G. M. Izv. Akad. Nauk SSR, Ser. Khim. 1978, 675.

53. Maksimov, Yu. Ya, Russ. J. Phys. Chem. 1972, 46, 990.

54. Zeman, S. Thermochim. Acta 1980, 39, 117.

55. Zeman, S. J. Therm. Anal. 1979, 17, 19.

56. Zeman, S. J. Therm. Anal. 1980, 19, 99.

57. Roginskii, S. Physik. Z. Sowjetunion 1932, 1, 640.

58. Maksimov, Yu. Ya. Russ. J. Phys. Chem. 1967, 41, 635.

59. Maksimov, Yu. Ya.; Sapranovich, V. F.; Polyakova, N. V. Tr. Mosk. Khim. Technol. Inst. im. D. I. Mendeleeva 1974, 83, 51.

60. Smith, L. C. Explosivstoffe 1969, 17, 252.

61. Janzen, E. G. J. Am. Chem. Soc. 1965, 87, 3532.

62. Bernecker, R. R.; Smith, L. C. J. Phys. Chem. 1967, 71, 2381.

63. Maksimov, Yu. Ya.; Egorcheva, G. I. Kinetics and Catalysis 1971, 12, 734.

64. Abramovitch, R. A.; Kyba, E. P.; Schriven, E. F. J. Org. Chem. 1971, 36, 3796.

65. Willadsen, P.; Zerner, B.; MacDonald, C. G. J. Org. Chem. 1973, 38, 3411.

66. Bulusu, S.; Autera, J. R. J. Energet. Mat. 1983, 1, 133.

67. Rogers, J. W., Jr.; Peebles, H. C.; Rye, R. R.; Houston, J. E.; Binkley, J. S. J. Chem. Phys. 1984, 80, 4513.

68. Choi, C. S.; Abel, J. E. Acta Cryst. 1972, B28, 193.

69. Holden, J. R.; Dickenson, C.; Bock, C. M. J. Phys. Chem. 1972, 76, 3597.

70. Holden, J. R. Acta Cryst. 1967, 22, 545.

71. Cady, H. H.; Larson, A. C. Acta Cryst. 1965, 18, 485.

72. Odiot, S. in Chemistry and Physics of Energetic Materials, S. Bulusu, Ed. Kluwer Acad. Publ., Dordrecht, The Netherlands, 1990, p. 79.

73. Owens, F. J. J. Mol. Struct. 1985, 121, 213.

74. Owens, F. J.; Jayasuriya, K.; Abrahmsen, K.; Politzer, P., Chem. Phys. Lett. 1985, 116, 434.

75. Murray, J. S.; Lane, P.; Politzer, P.; Bolduc, P. R. Chem. Phys. Lett. 1990, 168, 135.

76. Sharma, J.; Beard, B. C.; Chaykovsky, M. J. Phys. Chem. 1991, 95, 1209.

77. Liteanu, C.; Rica, I. Statistical Theory and Methodology of Trace Analysis, Ellis Horwood Publ., Chichester, U.K., 1980, p. 45.

78. Sharma, J.; Beard, B. C. in Chemistry and Physics of Energetic Materials, S. Bulusu, Ed. Kluwer Academic Publ., Dordrecht, The Netherlands, 1990, p. 569.

79. Cook, M. A.; Abegg, M. T. Ind. Eng. Chem. 1956, 48, 1090.

80. Guidry, R. M.; Davis, L. P. Thermochim. Acta 1979, 32, 1.

81. Zinn, J.; Rogers, R. N. J. Phys. Chem. 1962, 66, 2646.

82. Beckmann, J. W.; Wilkes, J. S.; McGuire, R. R. Thermochim. Acta 1977, 19, 111.

83. Robertson, R. J. Chem. Soc. 1921, 119, 1.

84. Maksimov, Yu. Ya.; Kogut, E. N. Russ. J. Phys. Chem. 1978, 52, 805.

85. Urbanskii, T.; Rychter, S. Compt. rend. 1939, 208, 900.

86. Maksimov, Yu. Ya.; Pavlik, L. T. Russ. J. Phys. Chem. 1975, 49, 360.

87. Brill, T. B.; James, K. J. J. Phys. Chem. submitted (TNT).

88. Beck, W. H. Combust. Flame 1987, 70, 171.

89. Chen, J. K.; Brill, T. B. Combust. Flame 1991, 87, 217.

90. Maksimov, Yu. Ya. Russ. J. Phys. Chem. 1968, 42, 1550.

91. Edwards, G. Trans. Farad. Soc. 1950, 46, 423.

92. McGuire, R. R.; Tarver, C. M. Seventh Symp. (Int.) Deton., Office of Naval Research, Arlington, VA, 1981, p. 56.

93. Freeman, E. S.; Gordon, S. J. Phys. Chem. 1956, 60, 867.

94. Henkin, H.; McGill, R. Ind. Eng. Chem. 1952, 44, 1391.

95. Brill, T. B.; Brush, P. J. Ninth Symp. (Int.) Deton. Office of Naval Research, Arlington, VA, 1988, p. 228.

96. Maksimov, Yu. Ya. Russ. J. Phys. Chem. 1969, 43, 396.

97. Zeman, S. J. Thermal Anal. 1980, 19, 207.

98. Zeman, S.; Zemanova, E. J. Thermal Anal. 1980, 19, 417.

99. Zeman, S.; Zemanova, E. J. Thermal Anal. 1981, 20, 87.

100. Zeman, S.; Zemanova, E. J. Thermal Anal. 1981, 20, 331.

101. Zeman, S.; J. J. Thermal Anal. 1981, 21, 9.

102. Matveev, V. G.; Dubikhin, V. V.; Nazin, G. M. Izv. Akad. Nauk SSSR, Ser. Khim. 1978, 474.

103. Maksimov, Yu. Ya.; Sorochkin, S. B. Tr. Mosk. Khim. Technol. Inst. im. D. I. Mendeleeva 1980, 112, 36.

104. Maksimov, Yu. Ya.; Kogut, E. N. Tr. Mosk. Khim. Technol. Inst. im. D. I. Mendeleeva 1979, 104, 30.

105. Maksimov, Yu. Ya.; Kuchina, T. A.; Kogut, E. N. Tr. Mosk. Khim. Technol. Inst. im. D. I. Mendeleeva 1979, 104, 28.

106. Fogelzang, A. E.; Egorshev, V. Yu.; Sinditsky, V. P.; Dutov, M. D. Combust. Flame 1991, 87, 123.

107. Brill, T. B. in Chemistry and Physics of Energetic Materials S. Bulusu, Ed. Kluwer Academic Publ., Dordrecht, The Netherlands, 1990, p. 277.

108. Melius, C. F. in Chemistry and Physics of Energetic Materials, S. Bulusu, Ed. Kluwer Academic Publ., Dordrecht, The Netherlands, 1990, p. 21.

109. McCarthy, E.; O'Brien, K. J. Org. Chem. 1980, 45, 2086.

110. Fields, E. K.; Meyerson, S. J. Org. Chem. 1972, 37, 3861.

111. Meyerson, S.; Vander Haar, R. W.; Fields, E. K. J. Org. Chem. 1972, 37, 4114.

112. Maksimov, Yu. Ya.; Sorochkin, S. B.; Titov, S. V. Tr. Mosk. Khim. Technol. Inst. im. D. I. Mendeleeva 1980, 112, 26.

113. Smith, R. E. Trans. Farad. Soc. 1940, 36, 985.

114. Maksimov, Yu. Ya. Symposium on Theory of Explosives Oborongiz, Moscow, 1963, p. 338.

115. Evans, M. G.; Polanyi, M. Trans. Farad. Soc. 1938, 34, 11.

116. Fields, E. K.; Meyerson, S. J. Org. Chem. 1968, 33, 4487.

116a. Itoh, M.; Okamoto, Y.; Akutsu, Y.; Tamura, M.; Yoshida, T.; Andolh, T.; Morisaki, S. Kogyo Kayaku 1990, 51, 76.

117. Delpuech, A.; Cherville, J. Prop. Explos. 1978, 3, 169.

118. Delpuech, A.; Cherville, J. Prop. Explos. 1979, 4, 61.

119. Delpuech, A.; Cherville, J. Prop. Explos. 1979, 4, 121.

120. Dewar, M. J. S.; Ritchie, J. P.; Alster, J. J. Org. Chem. 1985, 50, 1031.

121. Amin, M. R.; Dekker, L.; Hibbert, D. B.; Ridd, J. H.; Sandall, J. P. B. J. C. S. Chem. Comm. 1986, 9, 658.

122. Gray, P.; Rathbone, P.; Williams, A. J. Chem. Soc. 1960, 3932.

123. Brill, T. B.; James, K. J. to be published (substituent effects).

124. Koroban, V. A.; Maksimov, Yu. Ya. Kinet. Katal. 1990, 31, 775.

125. Fields, E. K.; Meyerson, S. J. Am. Chem. Soc. 1967, 89, 3224.

126. Yinon, J. Org. Mass Spectrom. 1987, 22, 501.

127. Beynon, J. H.; Saunders, R. A.; Williams, A. E. Ind. Chim. Belge 1964, 29, 311.

128. Egger, K. W.; Cooks, A. T. Helv. Chim. Acta 1973, 56, 1516.

129. Nielson, A. T.; Norris, W. P.; Atkins, R. L.; Vuono, W. R. J. Org. Chem. 1983, 48, 1056.

130. Turner, A. G.; Davis, L. P. J. Am. Chem. Soc. 1984, 106, 5447.

131. Morrison, H. A. in The Photochemistry of Nitro and Nitroso Groups Part I, H. Feuer, Ed., Interscience, New York, 1969, p. 158.

132. McLuckey, S. A.; Glish, G. L.; Carter, J. A. J. Forensic Sci. 1985, 30, 773.

133. McMillen, D. F.; Golden, D. M. Ann. Rev. Phys. Chem. 1982, 33, 493.

134. Carper, W. R.; Dorey, R. C.; Tomer, K. B.; Crow, F. W. Org. Mass. Spectrom. 1984, 19, 623.

135. Guidry, R. M.; Davis, L. P. Modelling and Simulation 1978, 9, 331.

136. Owens, F. J.; Sharma, J. J. Appl. Phys. 1980, 51, 1494.

137. Adams, G. K.; Rowland, P. R.; Wiseman, L. A. Ministry of Supply Report A. C. 3982 Great Britain, 1943.

138. McKinney, T. M.; Warren, L. F.; Goldberg, I. B.; Swanson, J. T. J. Phys. Chem. 1986, 90, 1008.

139. Feinstein, A. J.; Fields, E. K. J. Org. Chem. 1971, 36, 3878.

140. Preston, P. N.; Tennant, C. R. Chem. Rev. 1972, 72, 627.

141. Chaykovsky, M.; Adolph, H. G. J. Energet. Mat. 1990, 8, 392.

142. Chaykovsky, M.; Adolph, H. G. J. Heterocyclic Chem. 1991, 28, 1491.

143. Tomer, K. B.; Gebreyesus, T.; Djerassi, C. Org. Mass. Spectrom. 1973, 7, 383.

144. Farmer, R. C. J. Chem. Soc. 1920, 117, 1432.

145. Burlinson, N. E.; Sitzman, M. E.; Kaplan, L. A.; Kayser, E. J. Org. Chem. 1979, 44, 3695.

146. Jenkins, T. F.; Murrmann, R. P.; Leggett, D. C. J. Chem. Eng. Data 1973, 18, 438.

147. Swanson, J. T.; Davis, L. P.; Dorey, R. C.; Carper, W. R. Mag. Reson. Chem. 1986, 24, 762.

148. Emanuel, N. V.; Denison, E. T.; Malzus, Z. K. Liquid Phase Oxidation of Hydrocarbons Plenum Publ. Co., New York, 1967.

149. Preuss, L.; Binz, A. Angew. Chem. 1900, 16, 385.

150. Lob, W. Z. Electrochem. 1902, 8, 715.

151. Sacks, F.; Hilbert, S. Ber. 1904, 3425.

152. Murray, J. S.; Lane, P.; Politzer, P.; Bolduc, P. R.; McKenney, Jr., R. L. J. Mol. Struct. 1990, 209, 349.

153. Wettermark, G. J. Phys. Chem. 1962, 66, 2560.

154. Wettermark, G.; Ricci, R. J. Chem. Phys. 1963, 39, 1218.

155. Morrison, H.; Migdalof, B. H. J. Org. Chem. 1965, 30, 3996.

156. Suryanarayanan, K.; Capellos, C. Int. J. Chem. Kin. 1974, 6, 89.

157. Cox, J. R.; Hillier, I. H. Chem. Phys. 1988, 124, 39.

158. Buncel, E.; Norris, A. R.; Russell, K. E.; Tucker, R. J. Am. Chem. Soc. 1972, 94, 1646.

159. Fields, E. K.; Meyerson, S. Tetrahedron Letters 1968, 10, 1201.

160. Patterson, J. M.; Shiue, C. Y.; Smith, Jr., W. T. J. Org. Chem. 1973, 38, 2447.

161. Sharma, J.; Forbes, J. W.; Coffey, C. S.; Liddard, J. P. in Shock Waves in Condensed Matter S. C. Schmidt; N. Holmes, Eds. Elsevier Scientific Publs., Amsterdam, 1987, p. 565.

162. Sharma, J.; Beard, B. C. in Chemistry and Physics of Energetic Materials S. Bulusu, Ed., Kluwer Academic Publs., Dordrecht, The Netherlands, 1990, p. 587.

163. Rauch, F. C.; Wainwright, R. B. Picatinny Arsenal Report A.D. No. 850928, 1969.

164. Rauch, F. C.; Colman, W. P. Picatinny Arsenal Report A. D. No. 869226, 1970.

165. Colman, W. P.; Rauch, F. C. Picatinny Arsenal Report A. D. No. 881190, 1971.

166. Menapace, J. A.; Marlin, J. E. J. Phys. Chem. 1990, 94, 1906.

167. Davis, L. P.; Wilkes, J. S.; Pugh, H. L.; Dorey, R. C. J. Phys. Chem. 1981, 85, 3505.

168. Fyfe, C. A.; Malkiewich, C. D.; Damji, S. W. H.; Norris, A. R. J. Am. Chem. Soc. 1976, 98, 6983.

169. Shipp, K. G.; Kaplan, L. A. J. Org. Chem. 1966, 31, 857.

170. Zitrin, S.; Yinon, J. Org. Mass Spectrom. 1976, 11, 388.

171. Lee, E. L.; Sanborn, R. H.; Stromberg, H. D. Fifth Symp. (Int.) Detonation, Jacobs, S. J., Ed. Office of Naval Research, Washington, DC, 1970, p. 331.

172. Engelke, R. P.; Earl, W. L.; Rohlfing, C. M. Int. J. Chem. Kin. 1986, 18, 1205.

173. Carper, W. R.; Davis, L. P.; Extine, M. W. J. Phys. Chem. 1982, 86, 459.

174. Nash, C. P.; Nelson, T. E.; Stewart, J. J. P.; Carper, W. R. Spectrochim. Acta 1989, 45A, 585.

175. Stewart, J. J. P.; Bosco, S. R.; Carper, W. R. Spectrochim. Acta 1986, 42A, 13.

176. Carper, W. R.; Bosco, S. R.; Stewart, J. J. P. Spectrochim. Acta 1986, 42A, 461.

177. Carper, W. R.; Stewart, J. J. P. Spectrochim. Acta 1987, 43A, 1249.

178. Leichenko, A. A.; Maksimov, Yu. Ya. Russ. J. Phys. Chem. 1973, 47, 712.

179. Sundararajan, R.; Jain, S. R. Ind. J. Technol. 1983, 21, 474.

180. Mullay, J. Prop. Explos. Pyrotech. 1987, 12, 60.

181. Bliss, D. E.; Christian, S. L.; Wilson, W. S. J. Energet. Mat. 1991, 9, 319.

182. Kamlet, M.; Hurwitz, H. J. Chem. Phys. 1968, 48, 3685.

183. Bell, A. J.; Eadie, E.; Read, R. W.; Skelton, B. W.; White, A. H. Aust. J. Chem. 1987, 40, 175.

184. Politzer, P.; Abrahmsen, L.; Sjoberg, P. J. Am. Chem. Soc. 1984, 106, 855.

185. Politzer, P.; Seminario, J. M.; Bolduc, P. R. Chem. Phys. Lett. 1989, 158, 463.

186. Britt, A. D.; Moniz, W. B.; Chingas, G. C.; Moore, D. W.; Heller, C. A.; Lo, C. L. Prop. Explos. 1981, 6, 94.

187. Miles, M. H.; Gustaveson, D.; Devries, K. L. J. Mat. Sci. 1983, 18, 3243.

188. Green, A. G.; Rowe, F. M. J. Chem. Soc. 1912, 101, 2443.

189. Green, A. G.; Rowe, F. M. J. Chem. Soc. 1912, 101, 2452.

190. Khmelnitsky, L. I.; Novikov, S. S.; Godovikova, T. I. Chemistry of Furoxans, Nauka, Moscow, 1981.

191. Rogers, R. N.; Janney, J. L.; Ebinger, M. H. Thermochim. Acta 1982, 59, 287.

192. Sharma, J.; Hoffsommer, J. C.; Glover, D. J.; Coffey, C. S.; Santiago, F.; Stolovy, A.; Yasuda, S. in Shock Waves in Condensed Matter, Asay, J. R.; Graham, R. A.; Straub, G. K. Eds., Elsevier Scientific Publishers, Amsterdam, 1983, 543.

193. Sharma, J.; Forbes, J. W.; Coffey, C. S.; Liddiard, T. P. J. Phys. Chem. 1987, 91, 5139.

194. Sharma, J.; Beard, B. C.; Forbes, J.; Coffey, C. S.; Boyle, V. M. Ninth Symp. (Int.) Deton. Vol, II, Office of Naval Research, Arlington, VA, 1989, 897.

195. Catalano, E.; Rolon, C. E. Thermochim. Acta 1983, 61, 53.

196. Farber, M.; Srivastava, R. D. Combust. Flame 1981, 42, 165.

197. Stolovy, A; Jones, E. C., Jr.; Aviles, J. B., Jr.; Namenson, A. I.; Fraser, W. A. J. Chem. Phys. 1983, 78, 229.

198. Brill, T. B.; James, K. J. J. Phys. Chem. submitted [amino].

199. Sharma, J.; Owens, F. J. Chem. Phys. Lett. 1979, 61, 280.

200. Sharma, J.; Garrett, W. L.; Owens, F. J.; Vogel, V. L. J. Phys. Chem. 1982, 86, 1657.

201. Kolb, J. R.; Rizzo, H. F. Prop. Explos. 1979, 4, 10.

202. Catalano, E.; Rolon, C. E. Thermochim. Acta 1983, 61, 37.

203. Shaw, R. J. Phys. Chem. 1971, 75, 4047.

204. Rosen, J.; Dickerson, C. J. J. Chem. Eng. Data 1969, 14, 120.

205. Oyumi, Y.; Brill, T. B. Combust. Flame 1986, 65, 313.

206. Duesler, E. N.; Engelmann, J. H.; Curtin, D. Y.; Paul, I. C. Cryst. Struct. Comm. 1978, 7, 449.

207. Jones, E. C. S.; Kenner, J. J. Chem. Soc. 1931, 1842.

208. Kaplan, R. B.; Shechter, H. J. Am. Chem. Soc. 1961, 83, 3535.

209. Maksimov, Yu. Ya.; Sorochkin, S. B.; Zharkova, L. S. Tr. Mosk. Khim. Technol. Inst. im. D. I. Mendeleeva 1980, 112, 31.

210. Andreev, K. K. Termicheskoye Razlozhenyie i Gorenyie Vzryvchatykh Veschestv, Izdat. Nauka, Moscow, 1966.

211. Boguslavskaya, N. I.; Martyanova, G. F.; Yakimehenko, O. E.; Korsunskii, B. L.; Lebedev, Ya. S.; Dubovitskii, F. I. Dokl. Akad. Nauk SSSR 1975, 220, 617.

212. Abramovitch, R. A.; Davis, B. A. Chem. Rev. 1964, 64, 149.

213. Dyall, L. K.; Kemp, J. E. J. Chem. Soc. B 1968, 9, 978.

214. Patai, S.; Gotshal, Y. J. Chem. Soc. B 1966, 6, 489.

215. Anderson, E.; Birkhimer, E. H.; Bak, T. A. Acta Chem. Scand. 1960, 14, 1899.

216. Brill, T. B.; Brush, P. J.; Patil, D. G.; Chen, J. K. Twenty-Fourth Symp. (Int.) Combustion, The Combustion Institute, Pittsburgh, PA, 1992, in press.

217. Brill, T. B. Structure and Properties of Energetic Materials, Armstrong, R. W.; Gilman, J. G.; Liebenberg, D. A. Eds., Materials Research Society, Pittsburgh, PA, 1992, in press.

218. Patey, A. L.; Waldrom, N. M. Tet. Lett. 1970, 3375.

219. Higgenbottom, R.; Suschitzky, H. J. Chem. Soc. 1962, 2367.

220. Prokipcak, J. M.; Forte, P. A.; Lennox, D. D. Canad. J. Chem. 1969, 47, 2482.

221. Prokipcak, J. M.; Forte, P. A.; Lennox, D. D. Canad. J. Chem. 1970, 48, 3059.

222. Hammett, L. P. Chem. Rev. 1935, 17, 125.

223. Hammett, L. P. Physical Organic Chemistry, 2nd Edit. McGraw Hill, New York, 1970.

224. Ehrenson, S.; Brownlee, R. T. C.; Taft, R. W. Prog. Phys. Org. Chem. 1973, 10, 1.

225. Hansch, C.; Leo, A.; Unger, S. H.; Kim, K. H.; Nikaitani, D.; Lien, E. J. J. Med. Chem. 1973, 16, 1207.

226. Swain, C. G.; Lupton, E. C., Jr. J. Am. Chem. Soc. 1968, 90, 4328.

227. Rabalais, J. J. Chem. Phys. 1972, 57, 960.

228. The burn-rate of the material is proportional to pressure according to P^n, where n is called the pressure exponent.

229. Klimenko, G. K. Gorenie i Vzryu 1977, 585.

230. Storm, C. B.; Ryan, R. R.; Ritchie, J. P.; Hall, J. H.; Bachrach, S. M. J. Phys. Chem. 1989, 93, 1000.

231. Glarborg, P.; Miller, J. A.; Kee, R. J. Combust. Flame 1986, 65, 177.

232. Miller, J. A.; Branch, M. C.; McLean, W. J.; Chandler, D. W. Twentieth Symp. (Int.) Combust. The Combustion Institute, Pittsburgh, PA, 1984, p. 673.

233. Thorne, L. R.; Branch, M. C.; Chandler, D. W.; Kee, R. J.; Miller, J. A. Twenty-First Symp. (Int.) Combust. The Combustion Institute, Pittsburgh, PA, 1986, p. 965.

234. Miller, J. A.; Bowman, C. T. Prog. Energ. Combust. Sci. 1989, 15, 287.

235. Hall, T. N.; Poranski, C. F. in Chemistry of Nitro and Nitroso Groups, H. Feuer, Ed. John Wiley and Sons, New York, 1970, Chapt. 6.

236. Dewar, M. J. S. The Electronic Theory of Organic Chemistry, Oxford University Press, London, 1949, p. 77.

237. Terrier, F. Nucleophilic Aromatic Displacement, VCH Publishers, New York, 1991.

The Appendix

The appendix contains time-to-explosion data for a series of nitroaromatic compounds. The data were acquired by the use of T-jump/FTIR spectroscopy (Reference 22). About 200 μg of thinly spread sample was heated at 2000°C/sec under the pressure given in the caption. The time-to-exotherm was recorded along with the gaseous products, which were quantified by the well established procedure using the absolute intensities (Reference 41). Some of these data were used in the text of this report, but most are simply archived here because they are not discussed but are valid time-to-explosion data in the time range given. For reasons discussed in the text, the connection between the time-to-explosion and the parent molecular structure is vague. The time-to-explosion is predominantly controlled by the decomposition intermediates of these compounds which in turn catalyze the decomposition further.

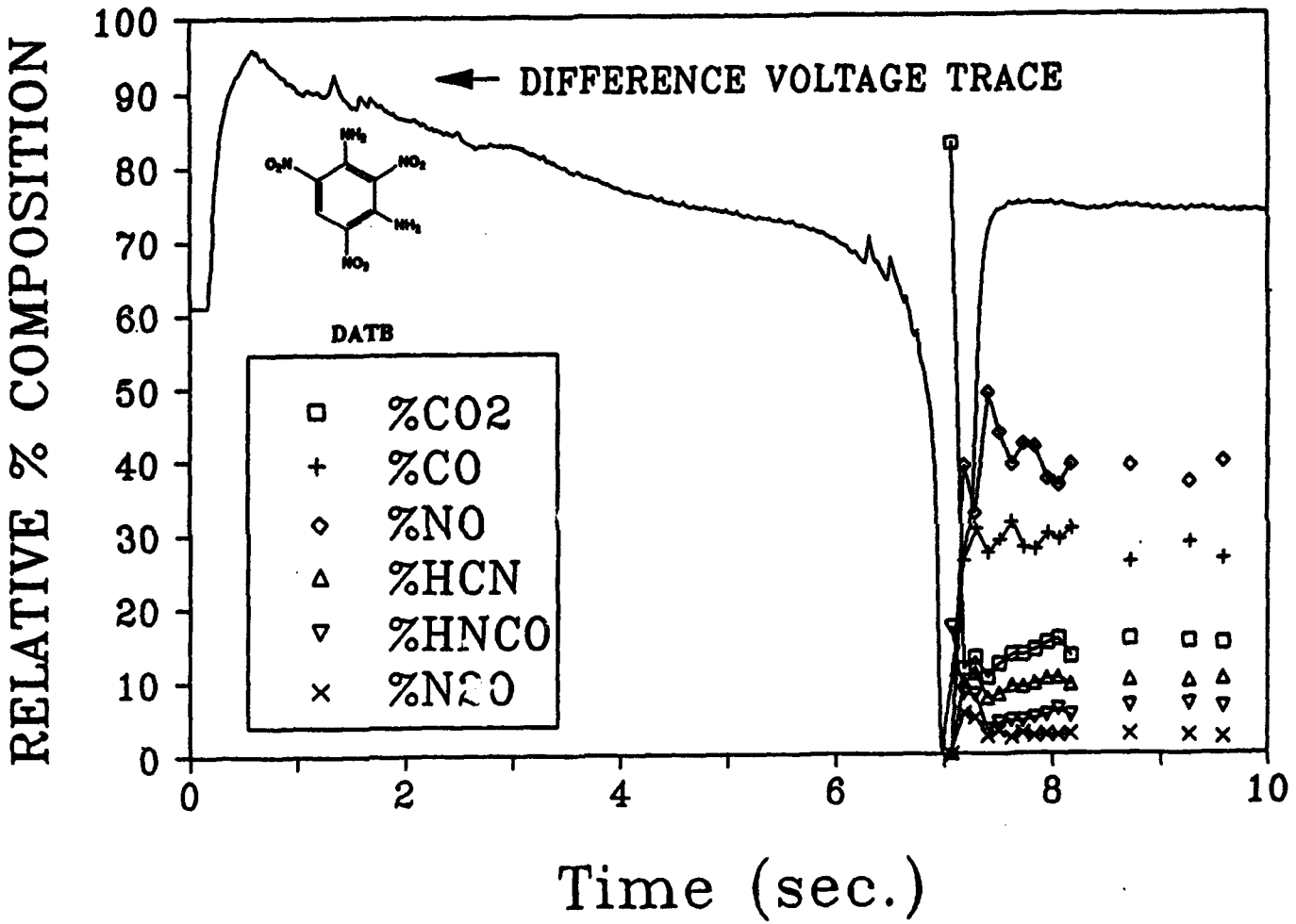

Figure 5. T-Jump/FTIR Data for 1,3-Diamino-2,4,6-trinitrobenzene at 339°C and 3.3 Atm Ar. Trace CO_2 Appears at 1.4 Seconds and Trace H_2O was Present.

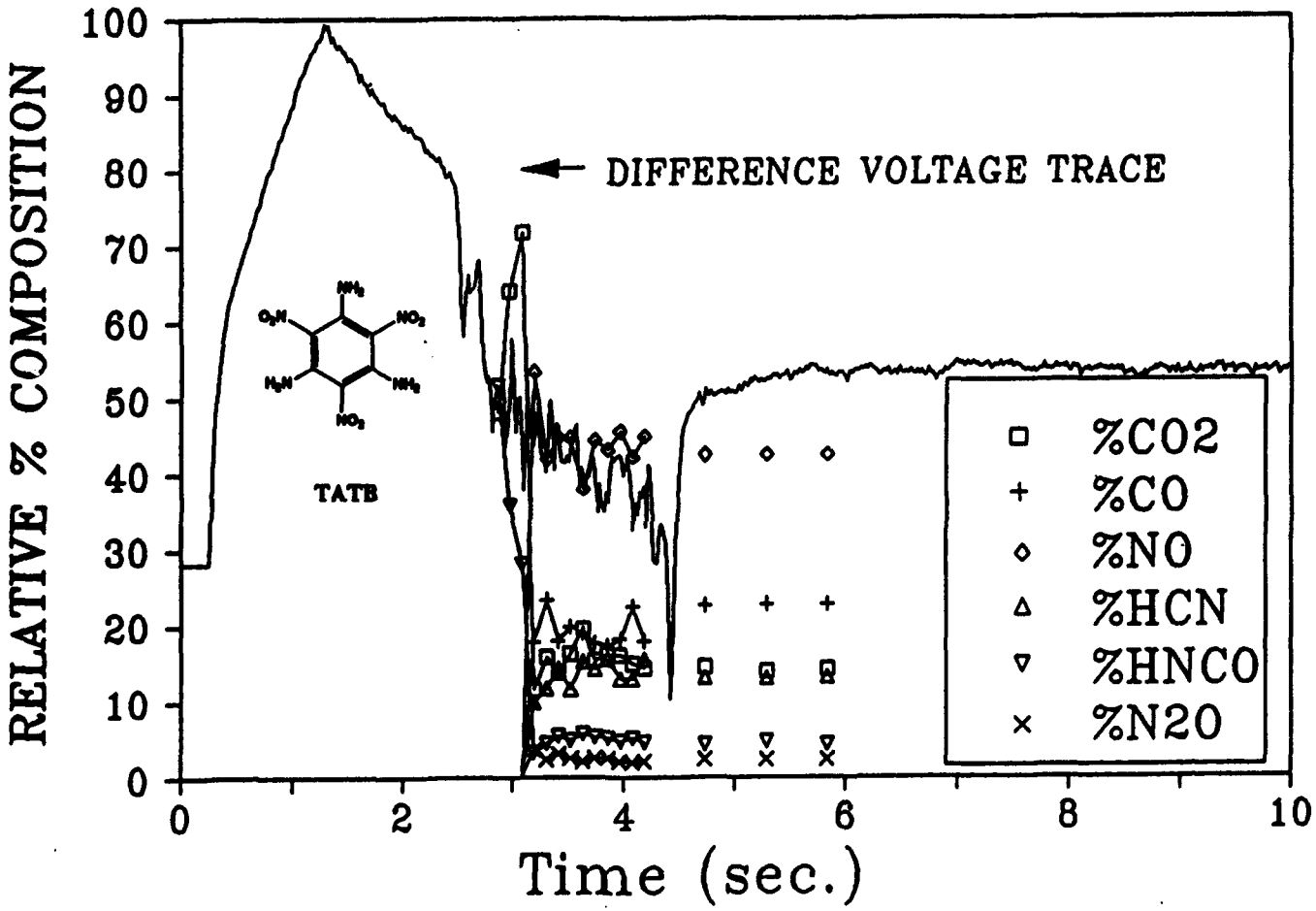

Figure 6. T-Jump/FTIR Data for 1,3,5-Triamino-2,4,6-trinitrobenzene at 422°C and 3.3 Atm Ar. Trace CO_2 appears at 2.6 Seconds and Trace H_2O was Present.

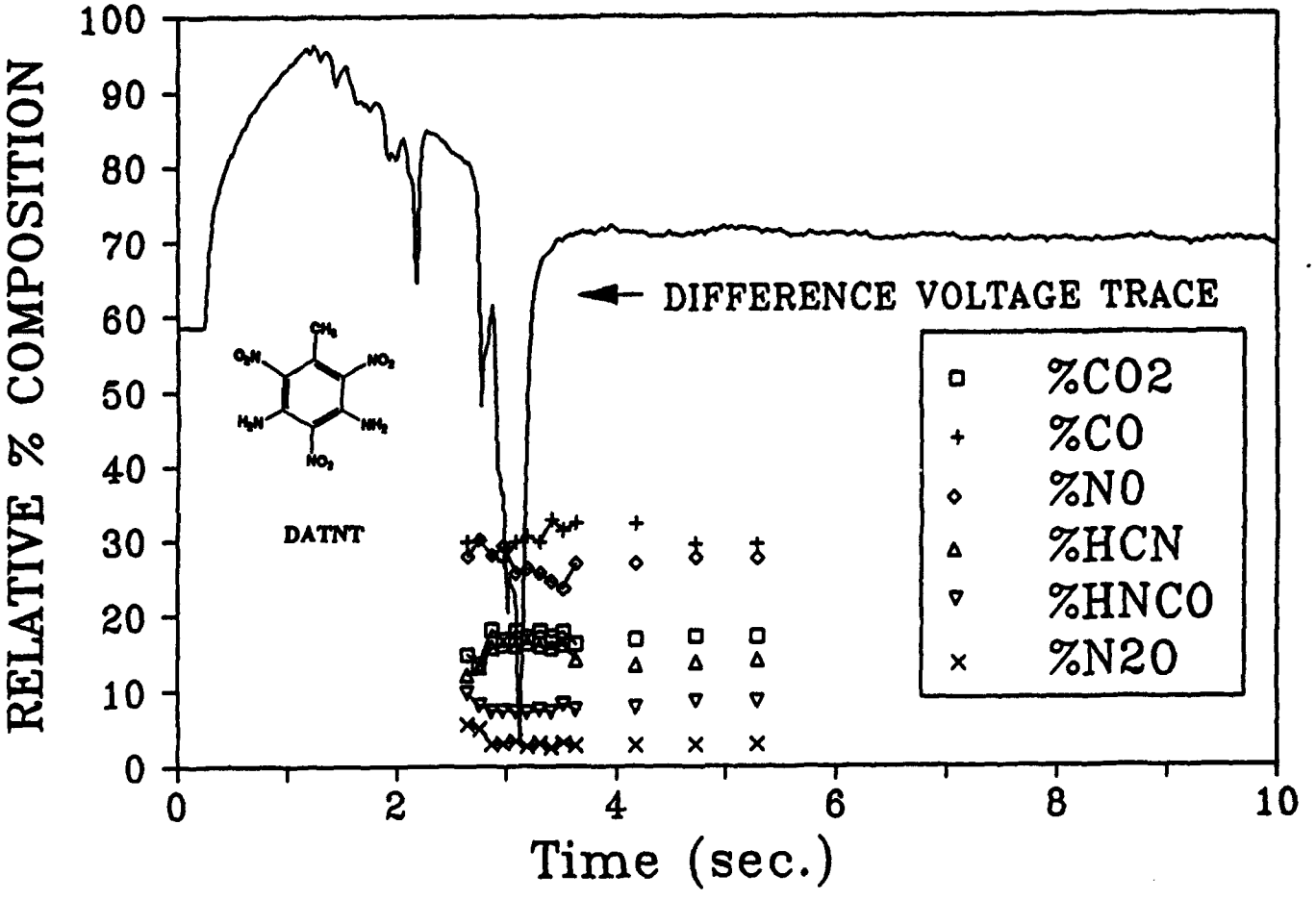

Figure 7. T-Jump/FTIR Data for 3,5-Diamino-2,4,6-trinitrotoluene at 471°C and 3.3 Atm Ar. Trace CO_2 appears at 0.6 Seconds and Trace H_2O was Present.

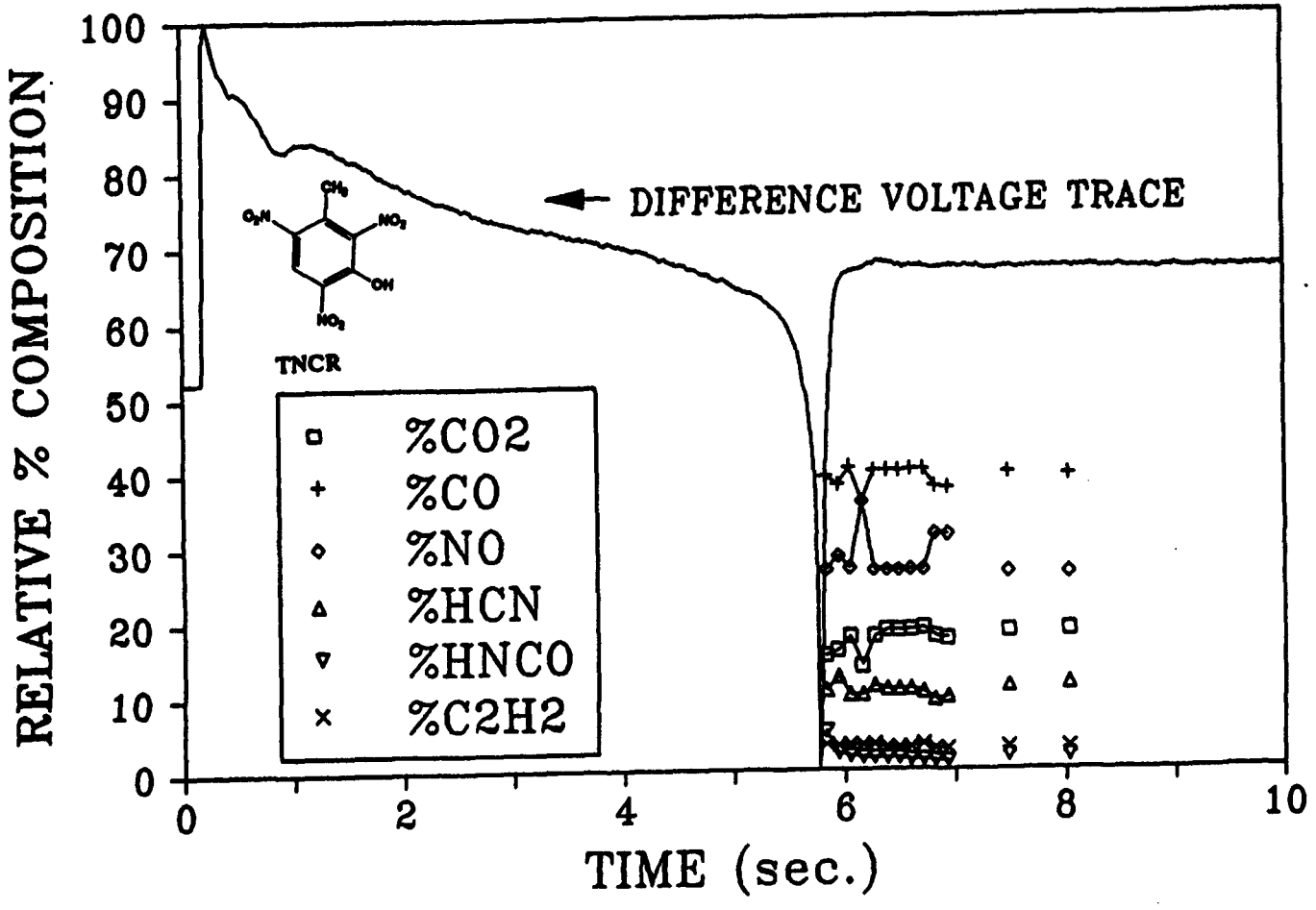

Figure 8. T-Jump/FTIR Data for 2,4,6-Trinitrocresol at 370°C and 3.3 Atm Ar. Trace CO_2 appears at 4.5 Seconds and Trace H_2O was Present.

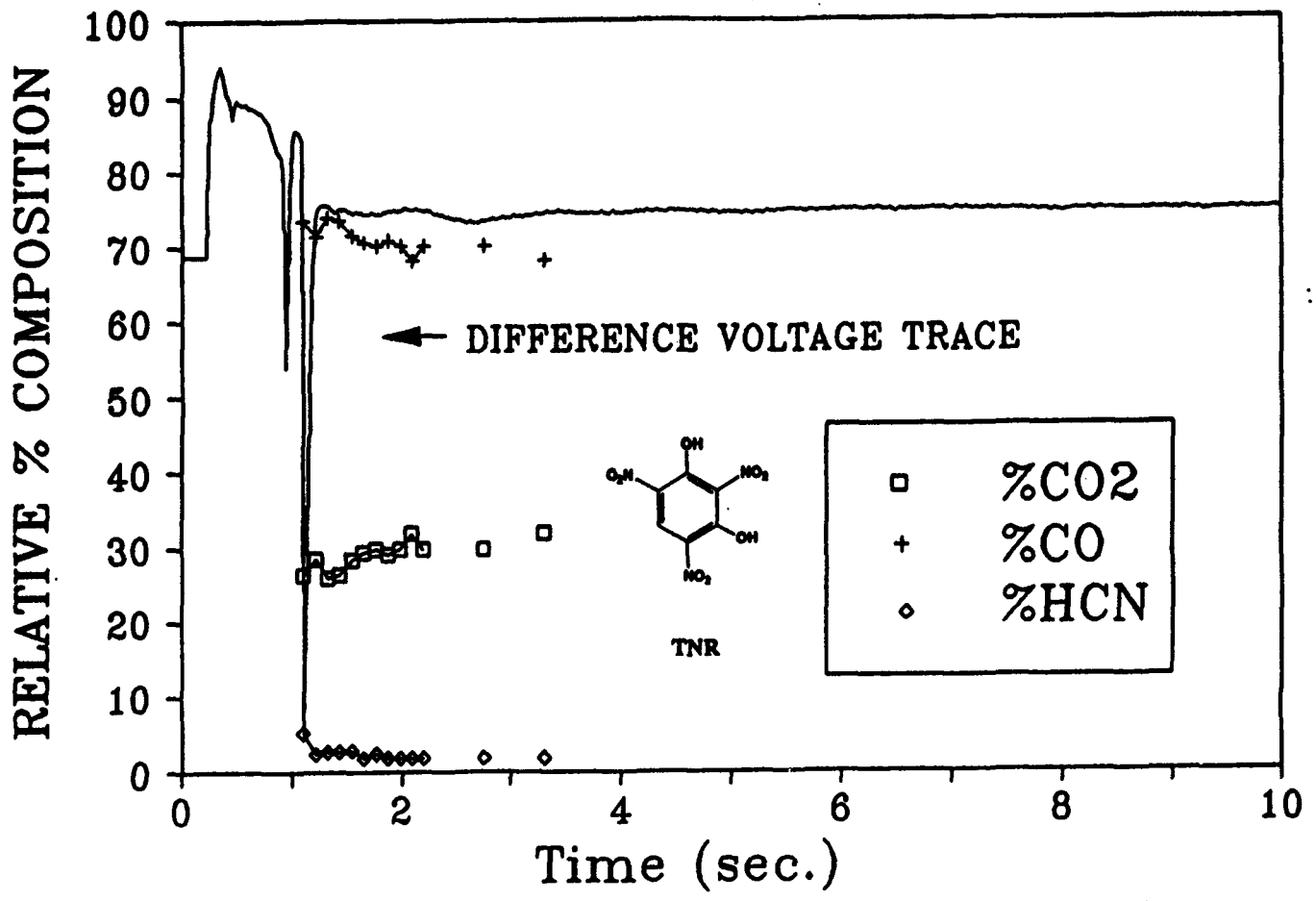

Figure 9. T-Jump/FTIR Data for 2,4,6-Trinitroresorcinol at 521°C and 3.3 Atm Ar. Trace H_2O was Present.

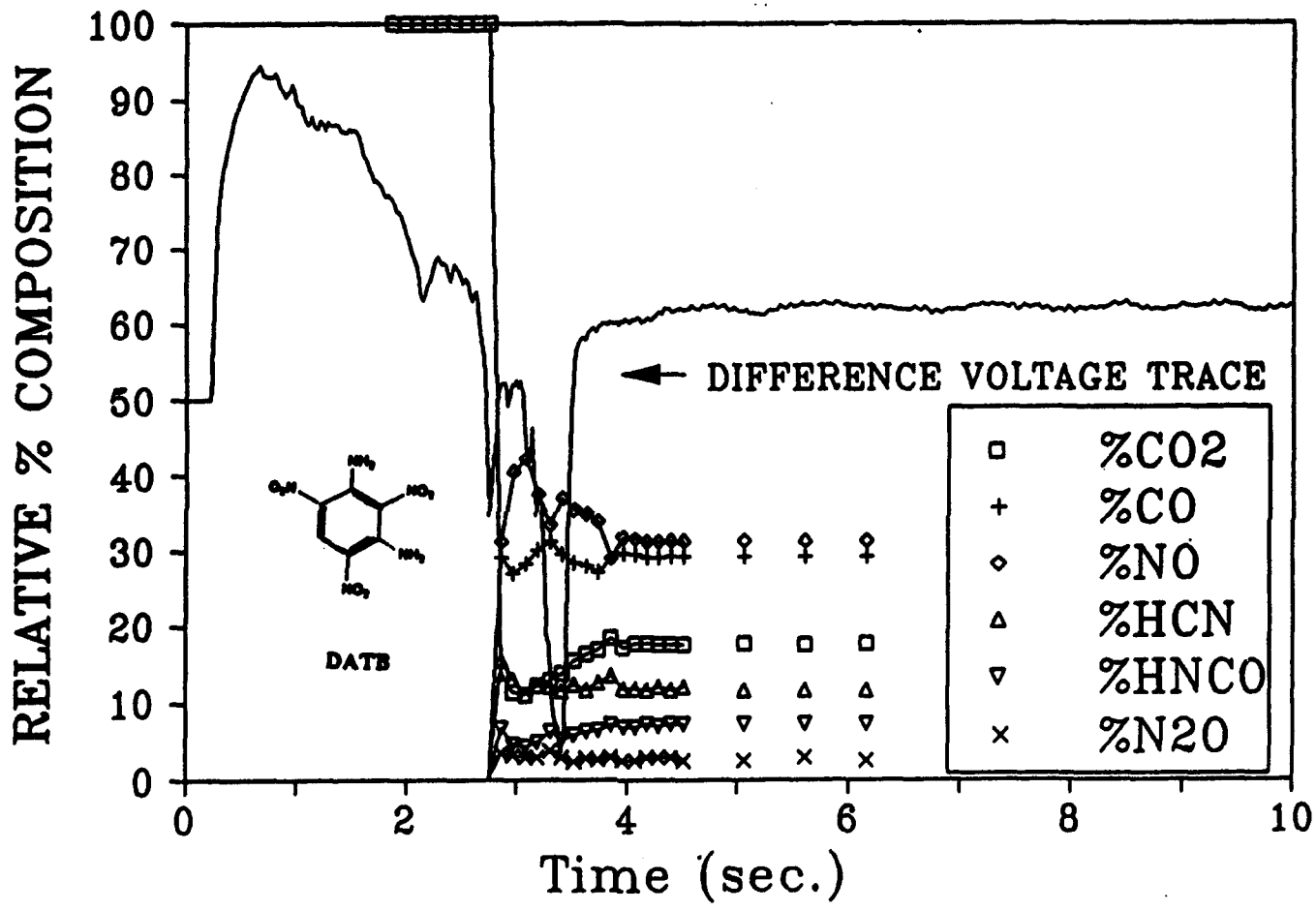

Figure 10. T-Jump/FTIR Data for 1,3-Diamino-2,4,6-trinitrobenzene at 469°C and 6.67 Atm Ar. Trace H_2O was Present.

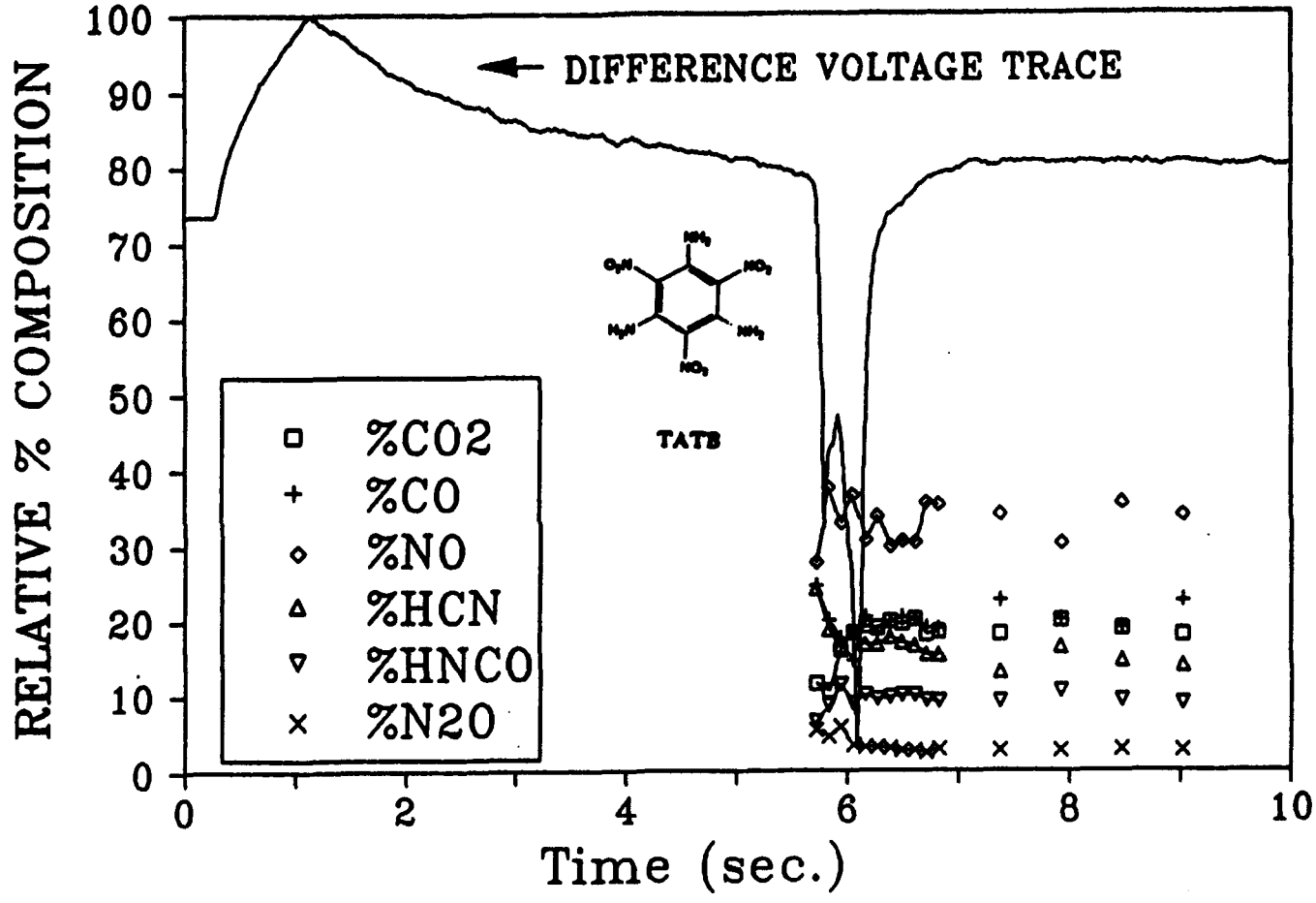

Figure 11. T-Jump/FTIR Data for 1,3,5-Triamino-2,4,6-trinitrobenzene at 390°C and 6.67 Atm Ar. Trace H_2O was Present.

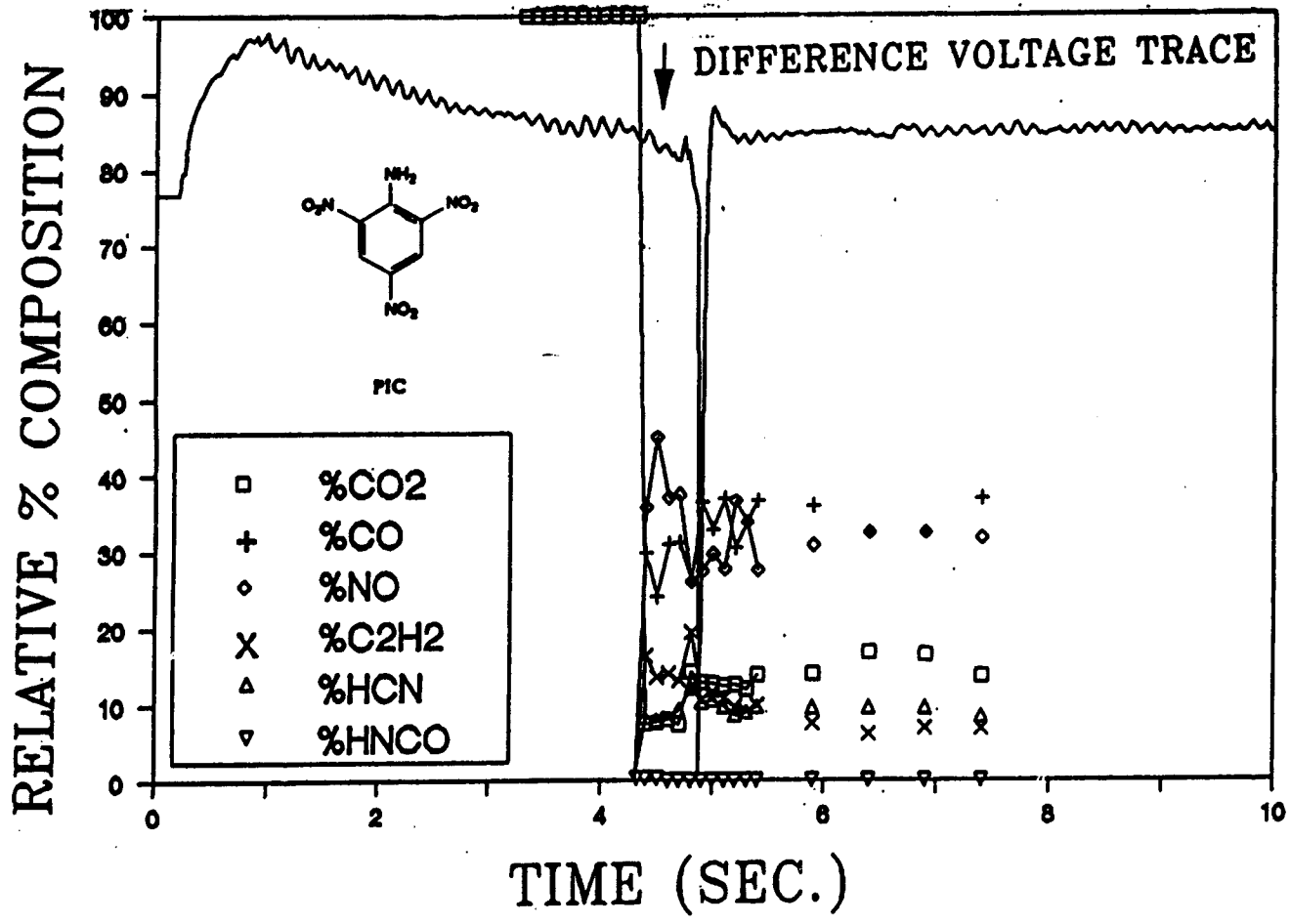

Figure 12. T-Jump/FTIR Data for 2,4,6-Trinitroaniline at 454°C and 10 Atm Ar. Trace H_2O was Present.

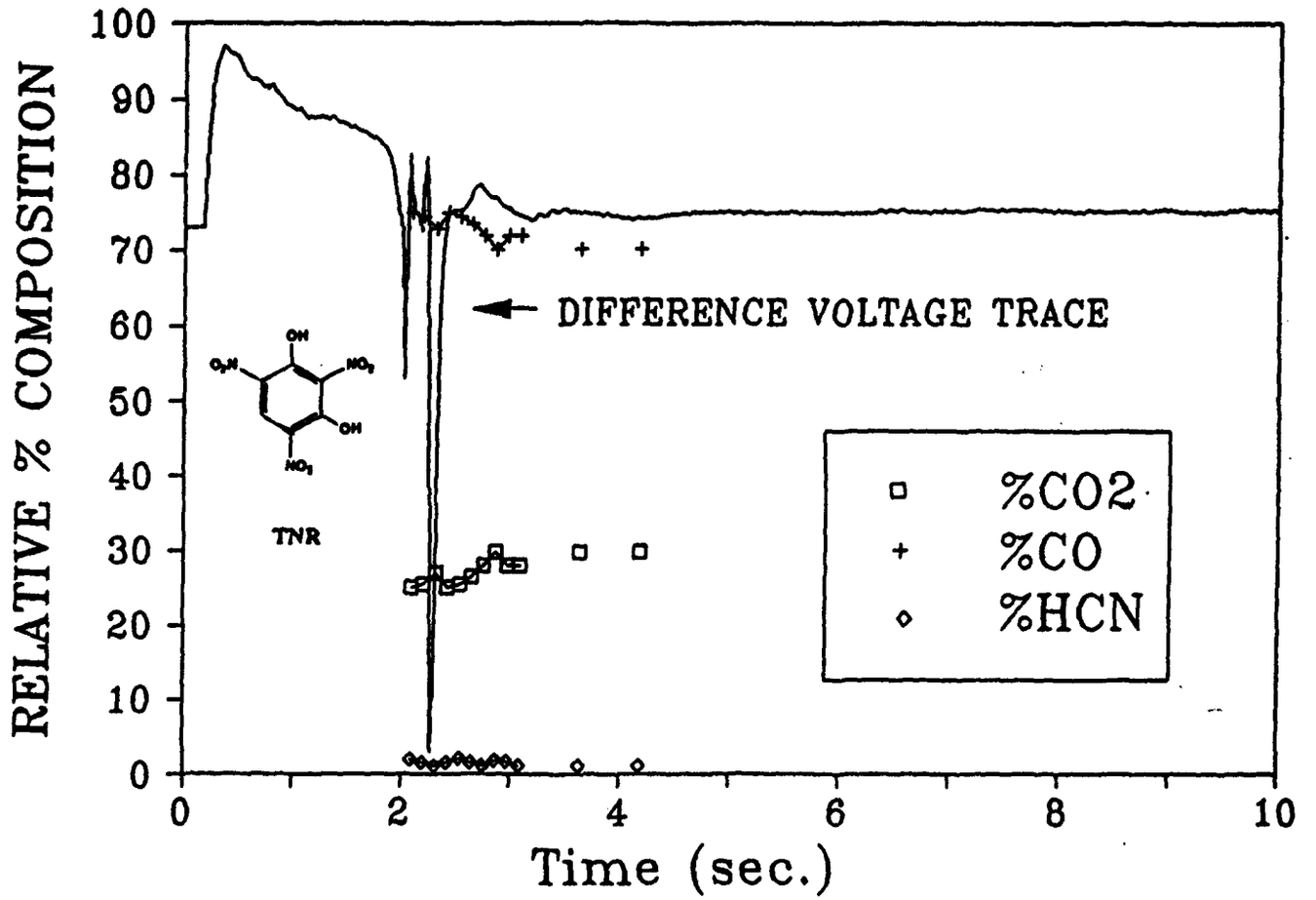

Figure 13. T-Jump/FTIR Data for 2,4,6-Trinitroresorcinol at 401°C and 10 Atm Ar. Trace H_2O was Present.

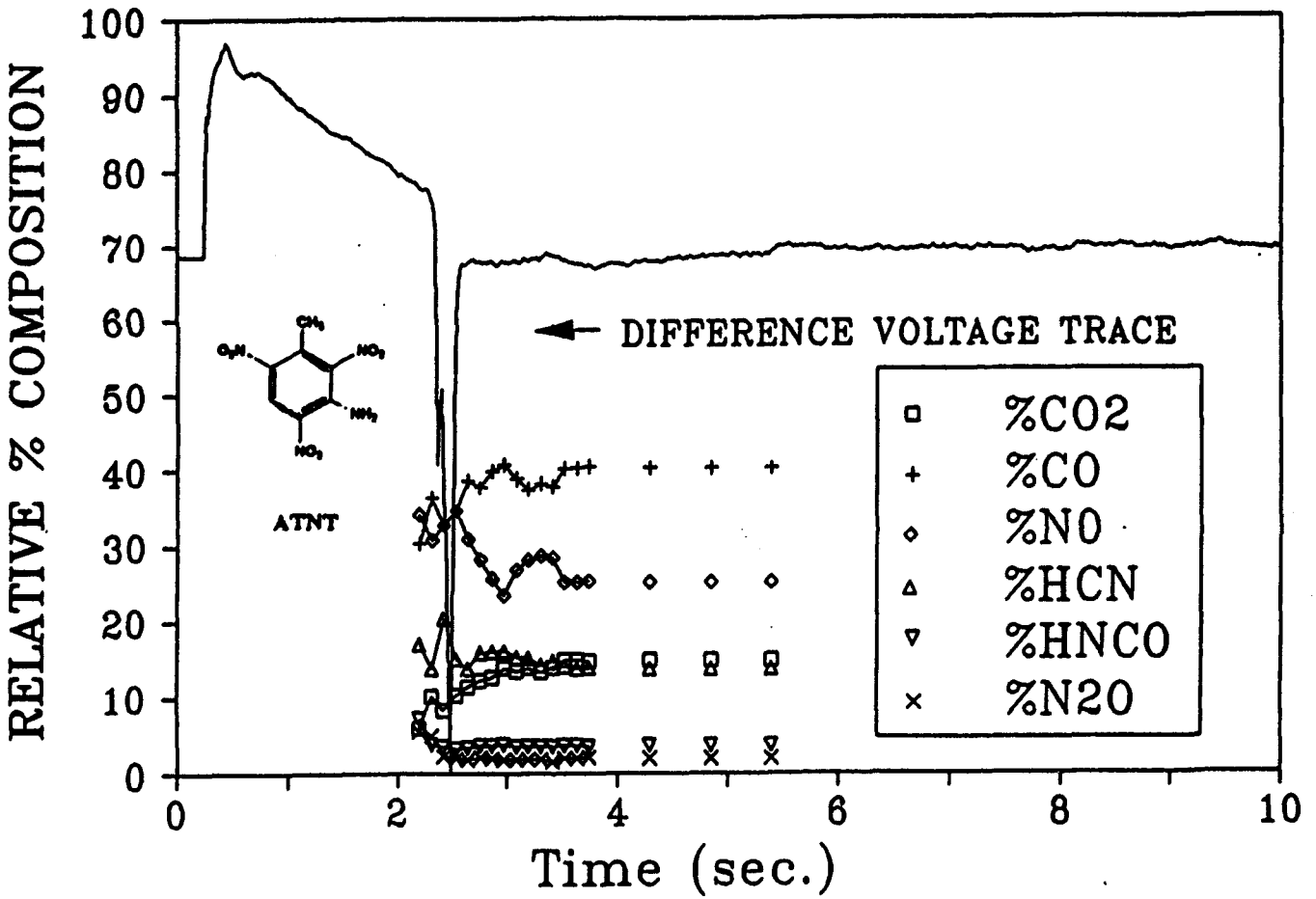

Figure 14. T-Jump/FTIR Data for 3-Amino-2,4,6-trinitrotoluene at 513°C and 10 Atm Ar. Trace H_2O was Present.

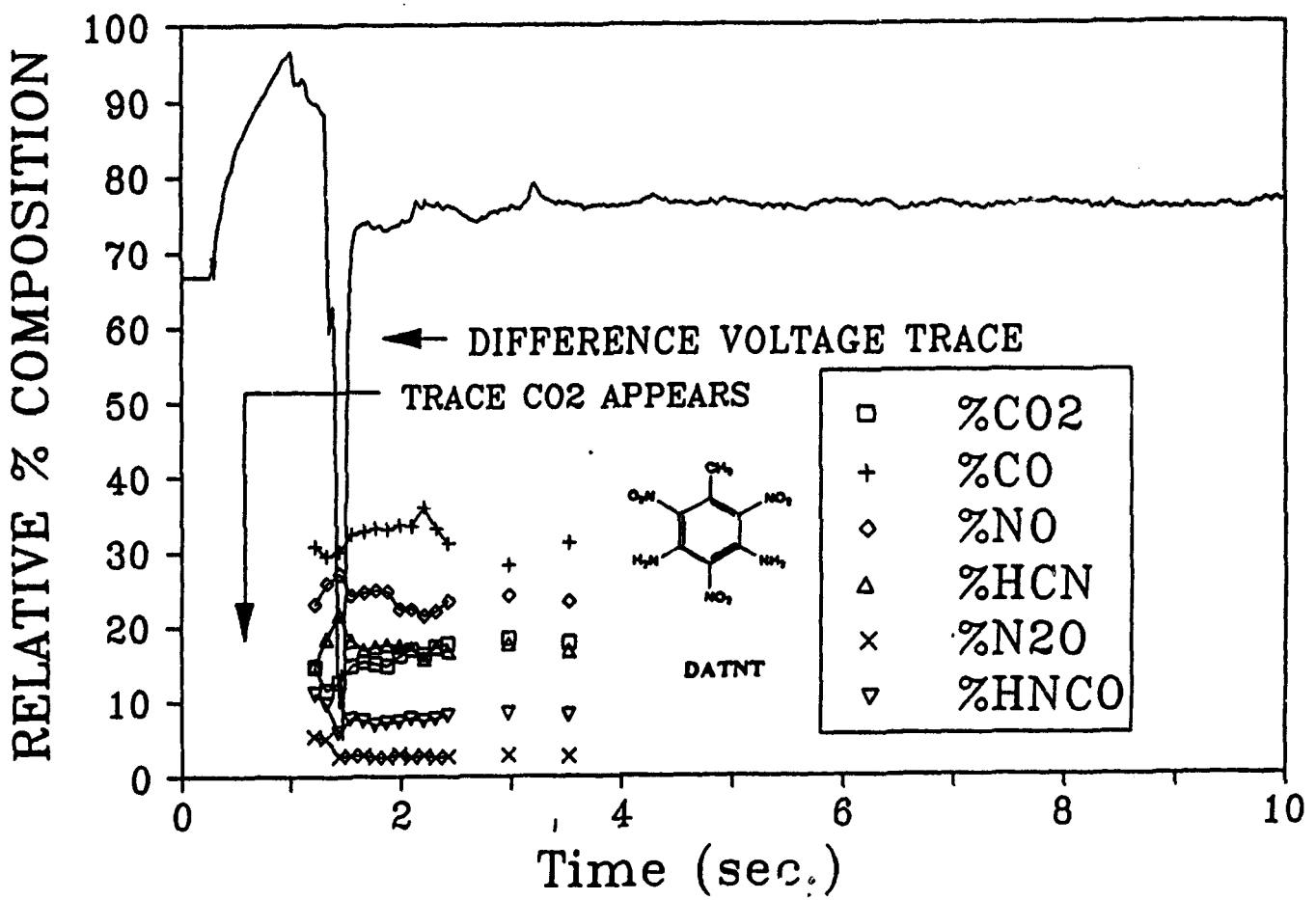

Figure 15. T-Jump/FTIR Data for 3,5-Diamino-2,4,6-trinitrotoluene at 548°C and 10 Atm Ar. Trace H_2O was Present.

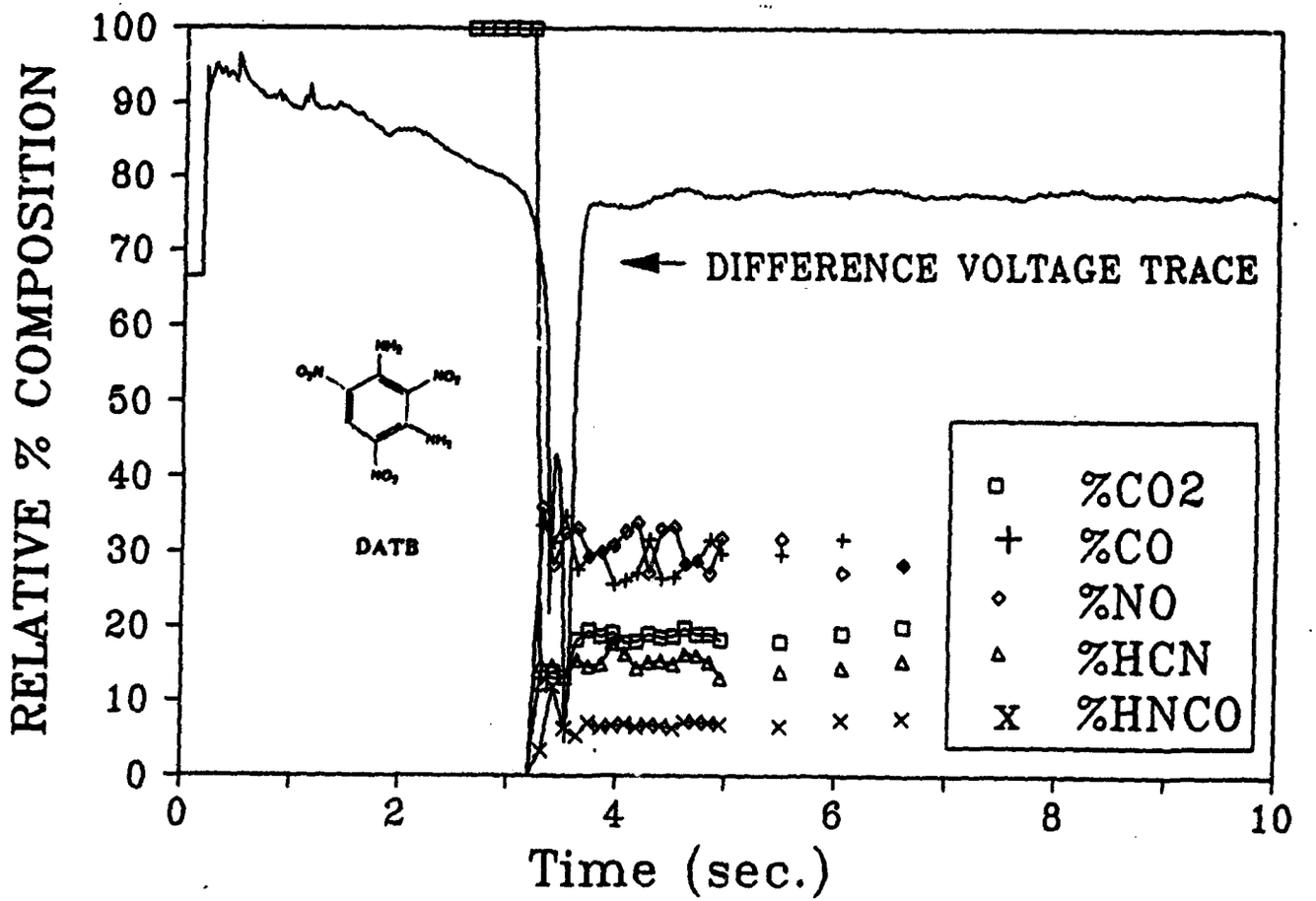

Figure 16. T-Jump/FTIR Data for 1,3-Diamino-2,4,6-trinitrobenzene at 405°C and 10 Atm Ar. Trace H_2O was Present.

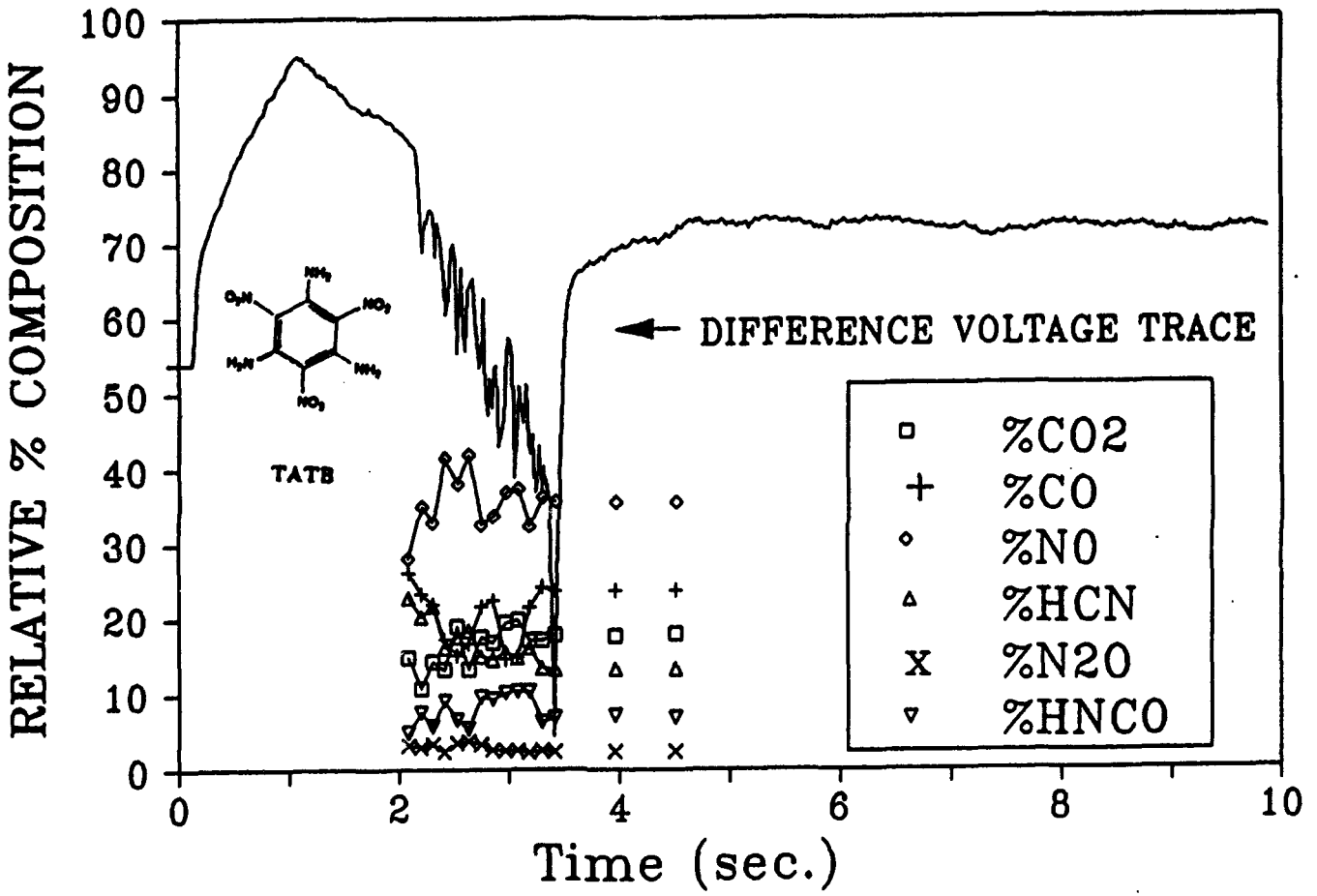

Figure 17. T-Jump/FTIR Data for 1,3,5-Triamino-2,4,6-trinitrobenzene at 452°C and 10 Atm Ar. Trace H_2O was Present.

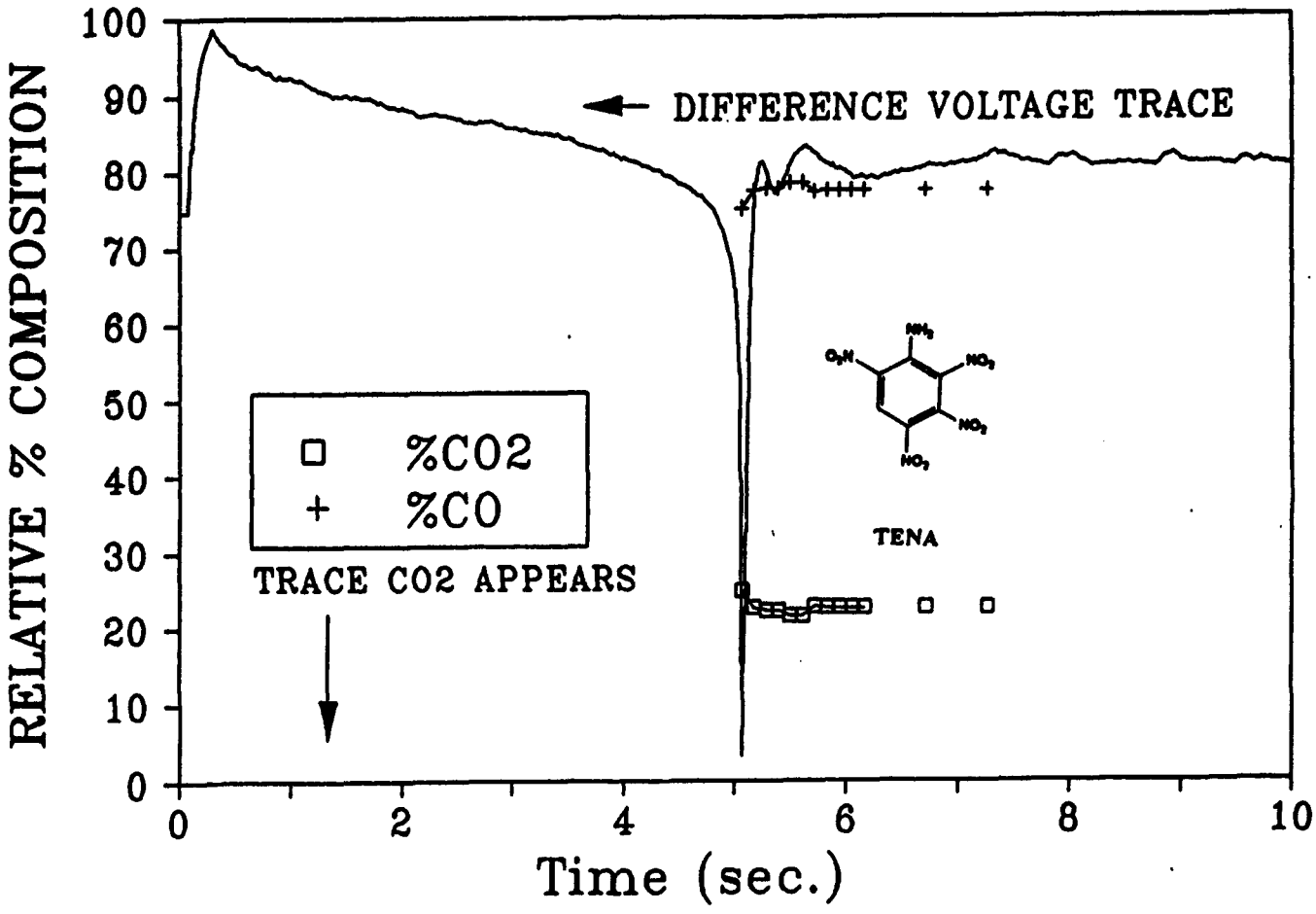

Figure 18. T-Jump/FTIR Data for 2,3,4,6-Tetranitroaniline at 308°C and 10 Atm Ar.

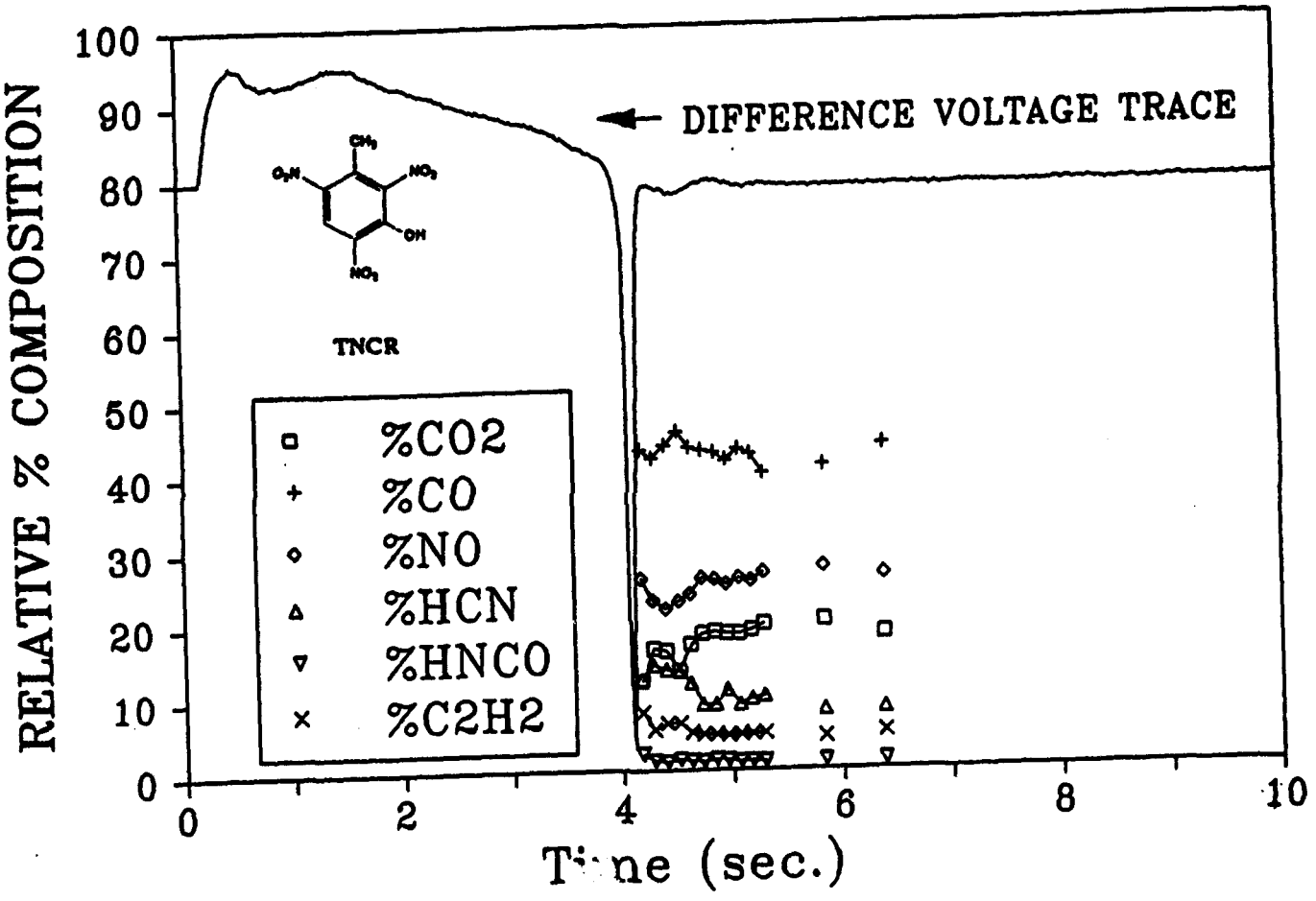

Figure 19. T-Jump/FTIR Data for 2,4,6-Trinitrocresol at 450°C and 10 Atm Ar. Trace CO_2 appears at 2.7 Seconds and Trace H_2O was Present.

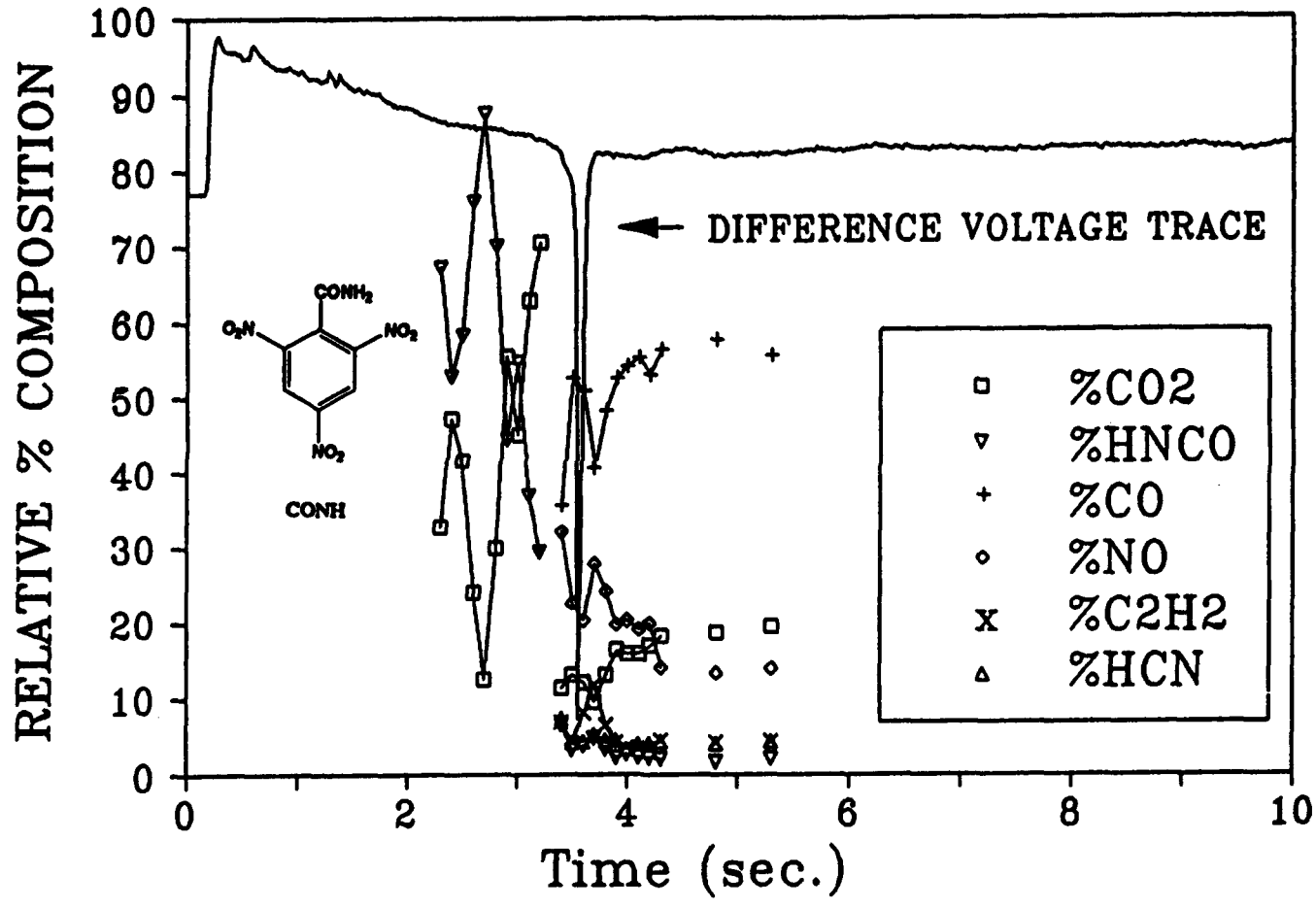

Figure 20. T-Jump/FTIR Data for 2,4,6-Trinitrobenzamide at 457°C and 10 Atm Ar.

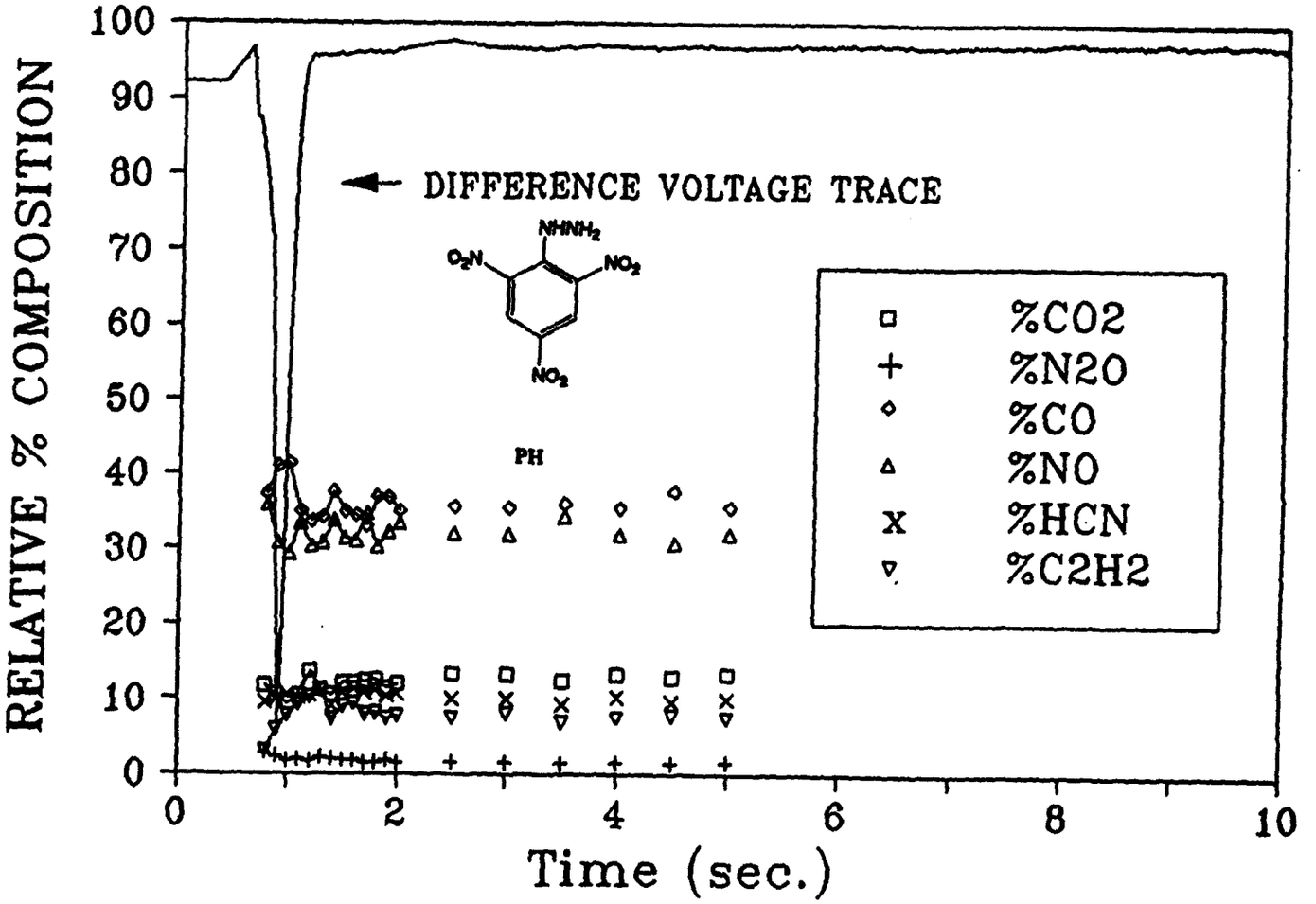

Figure 21. T-Jump/FTIR Data for Picrylhydrazine at 323°C at 10 Atm Ar. HNCO appears at 0.80 Seconds and Trace H_2O was Present.

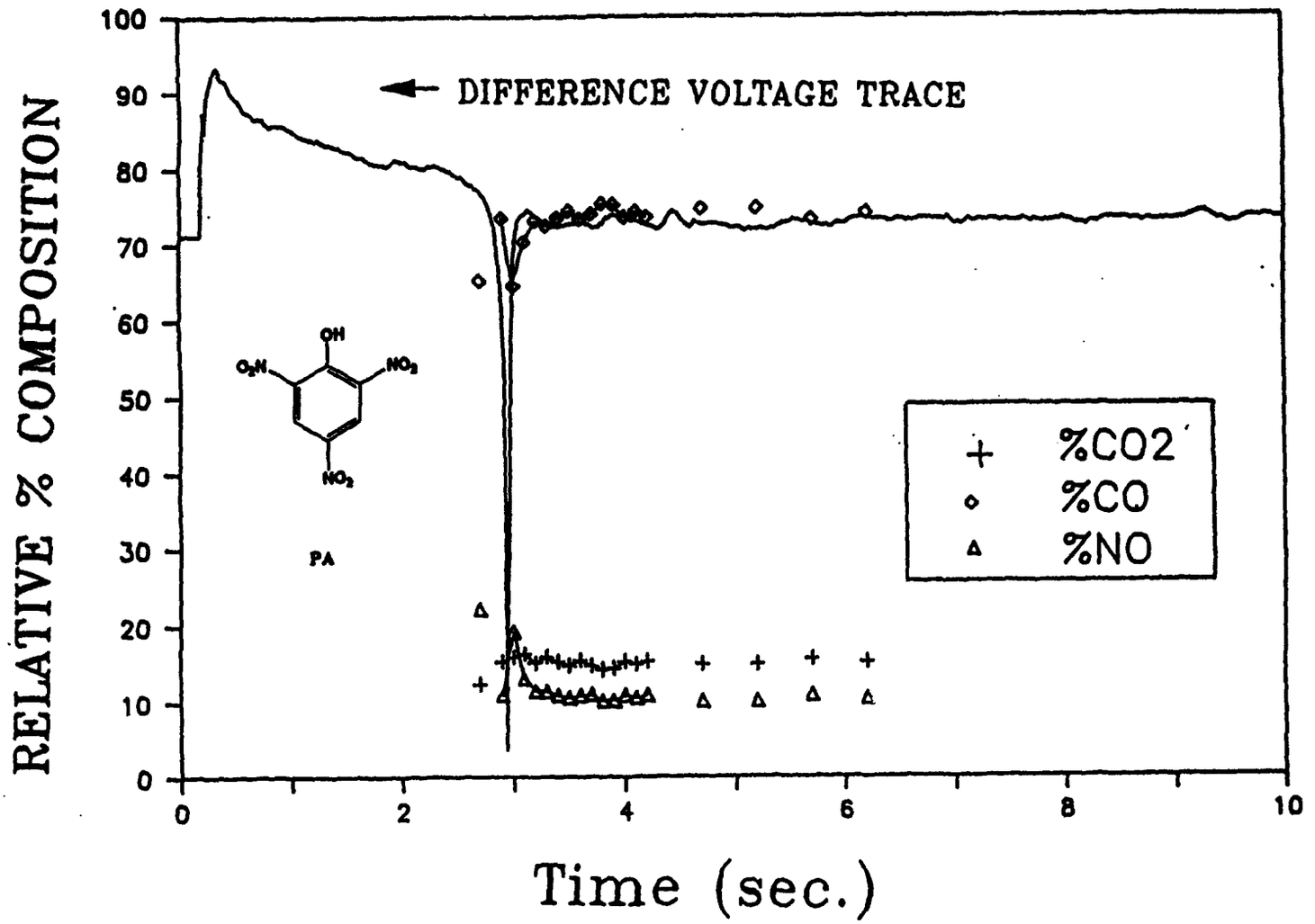

Figure 22. T-Jump/FTIR Data for Picric Acid at 412°C and 20 Atm Ar.

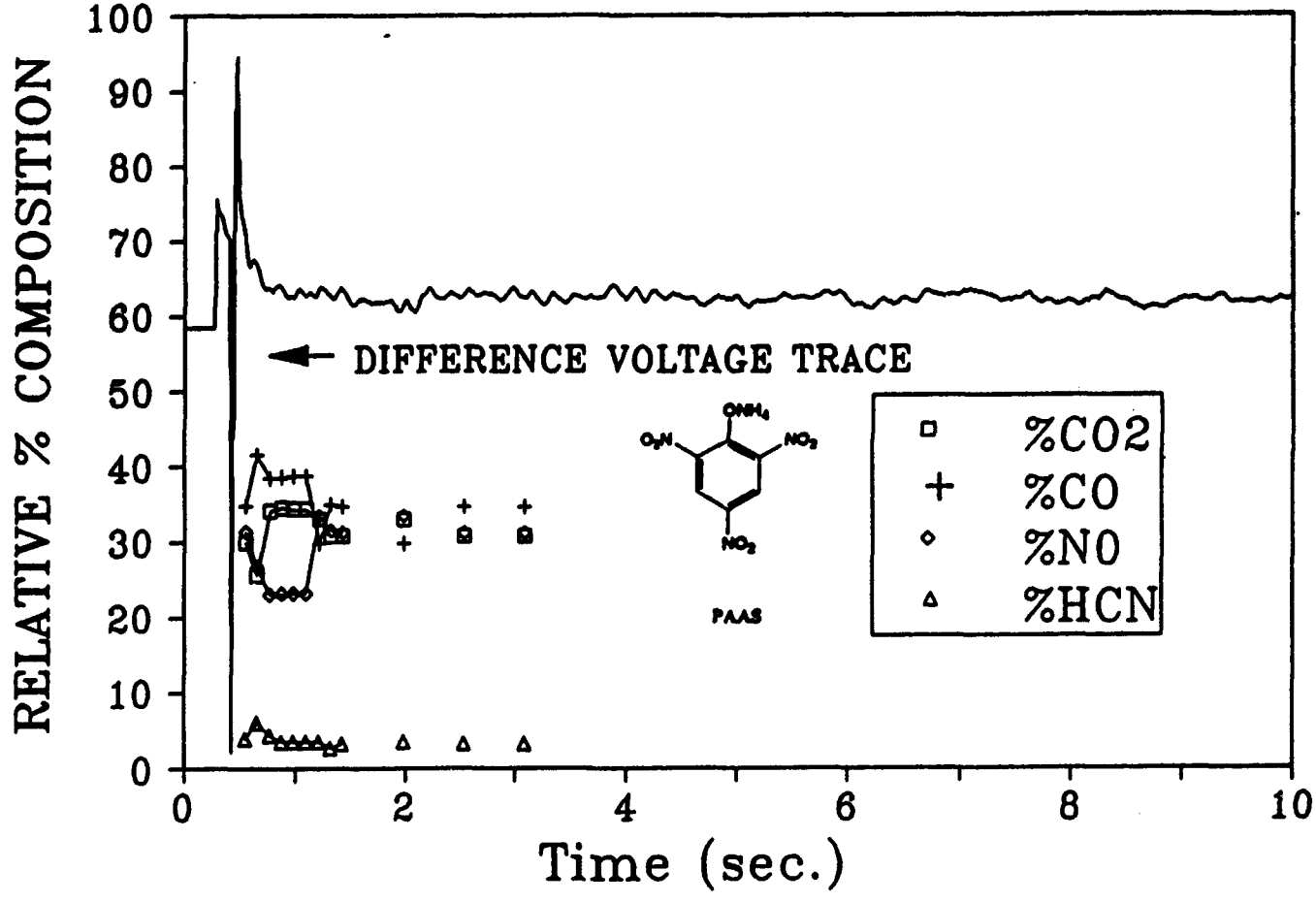

Figure 23. T-Jump/FTIR Data for Picric Acid Potassium Salt at 587°C and 20 Atm Ar.

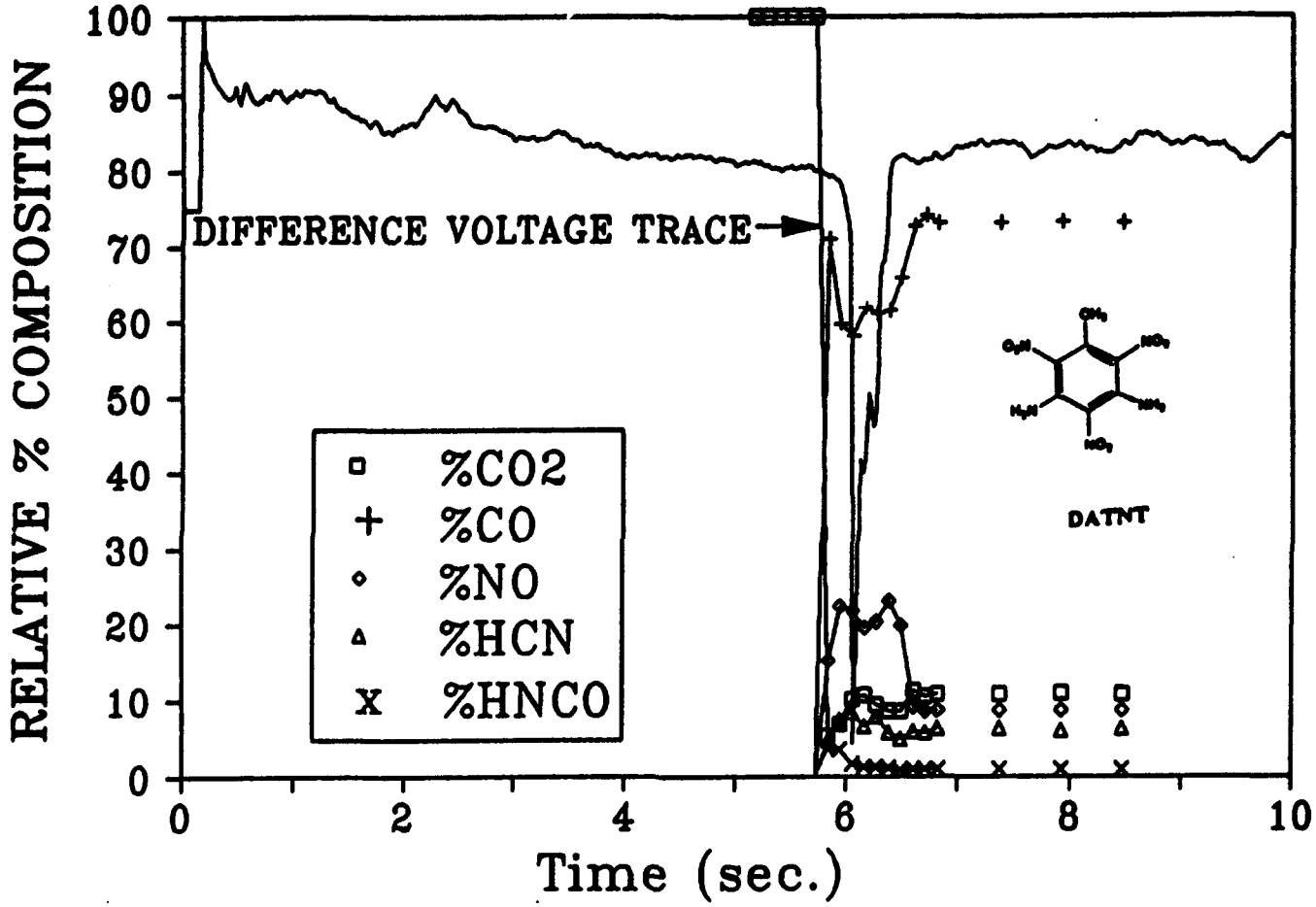

Figure 25. T-Jump/FTIR Data for 1,3-Diamino-2,4,6-trinitrobenzene at 375°C and 20 Atm Ar. Trace H_2O was Present.

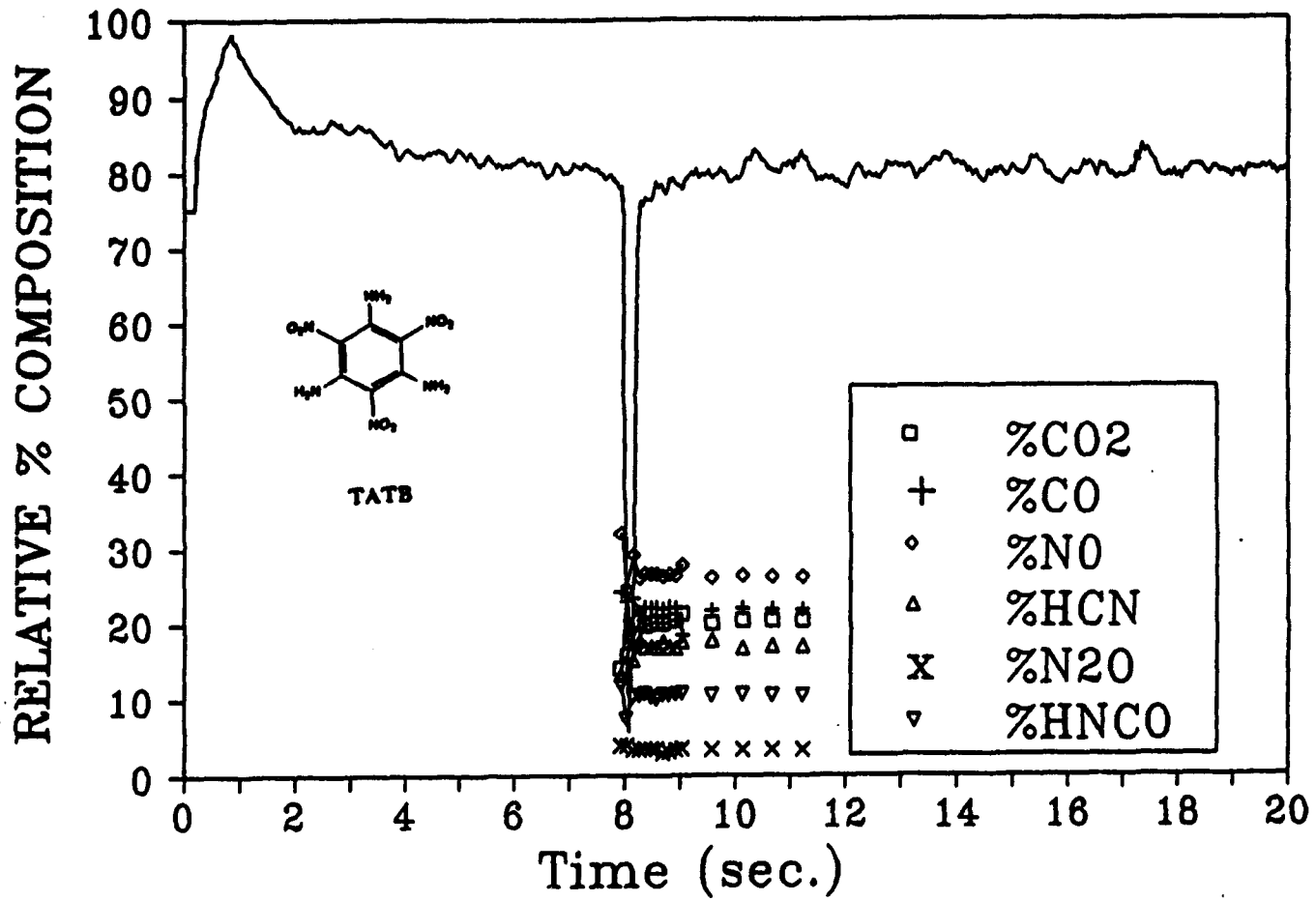

Figure 26. T-Jump/FTIR Data for 1,3,5-Triamino-2,4,6-trinitrobenzene at 402°C and 20 Atm Ar. Trace H_2O was Present.

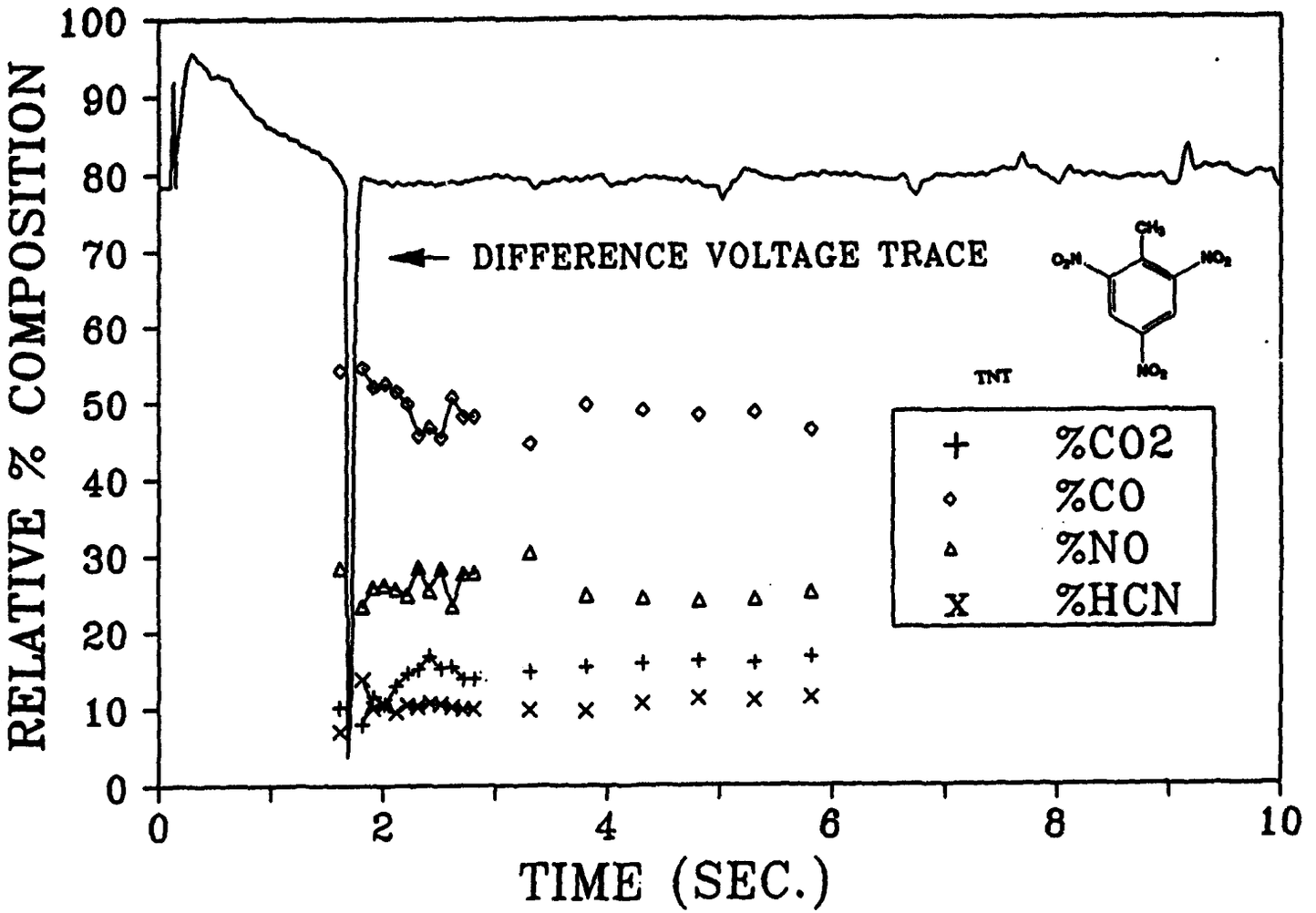

Figure 27. T-Jump/FTIR Data for 2,4,6-Trinitrotoluene at 405°C and 20 Atm Ar. Trace CO_2 appears at 1.1 Seconds.

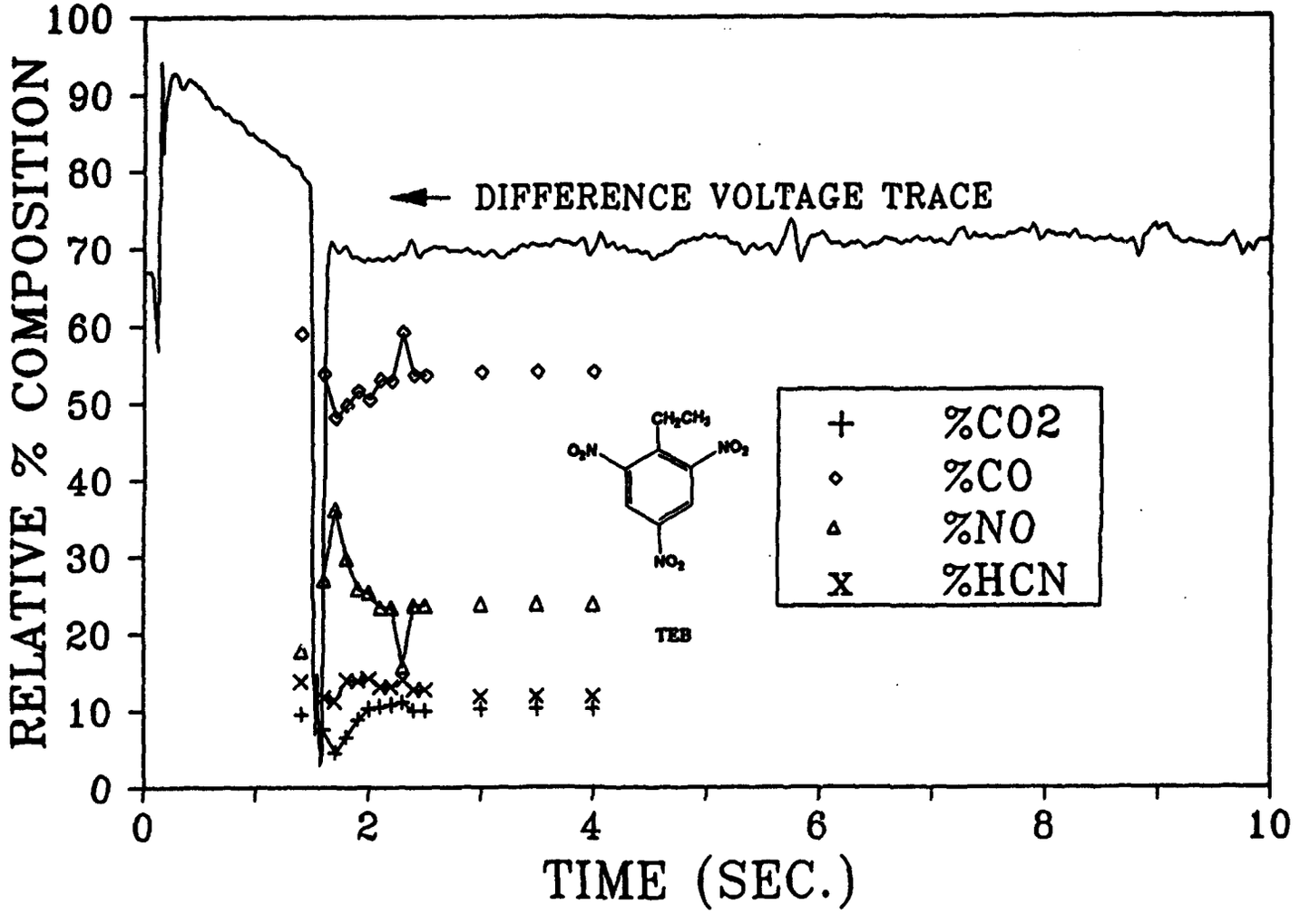

Figure 28. T-Jump/FTIR Data for 2,4,6-Trinitroethylbenzene at 484°C and 20 Atm Ar.

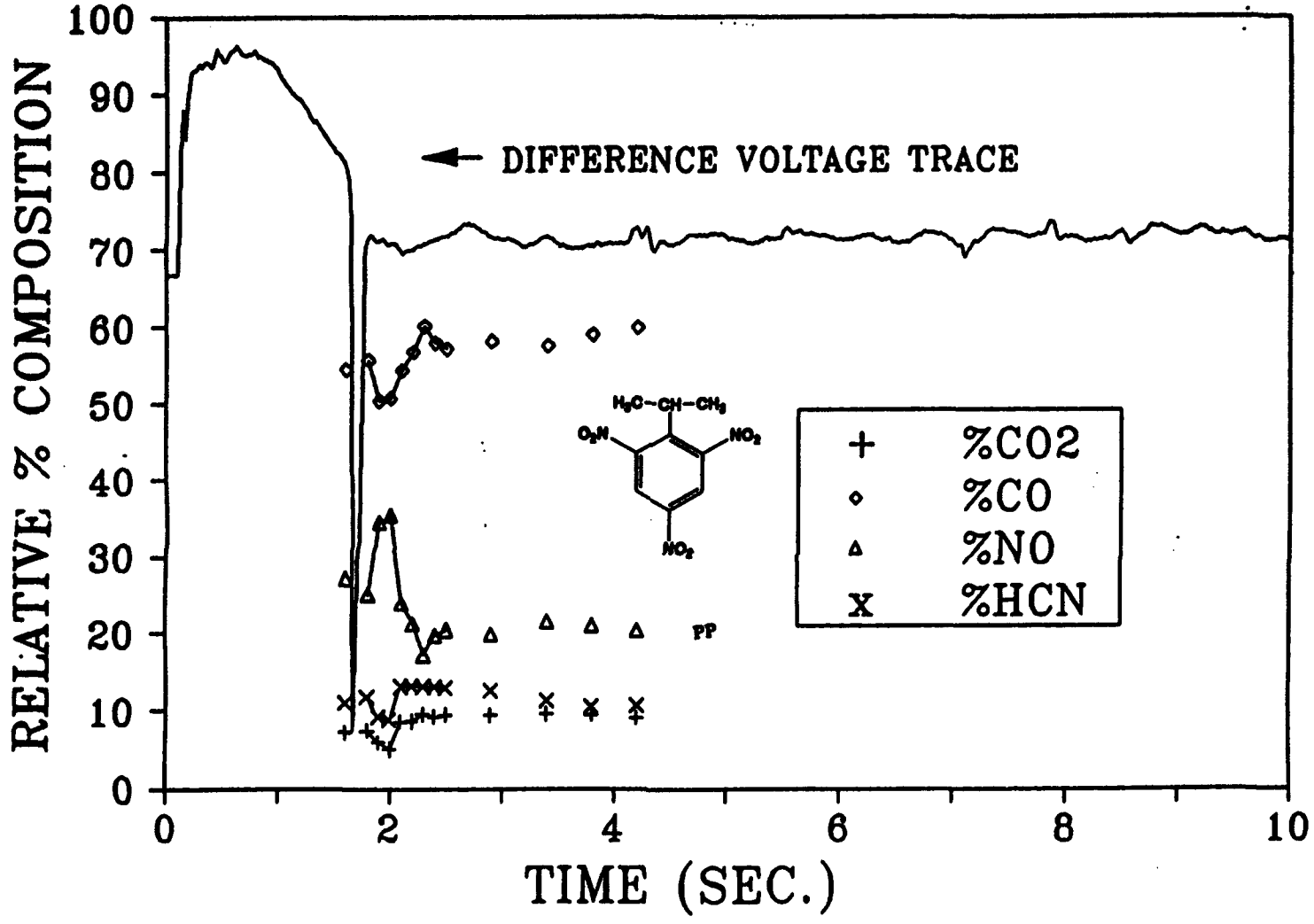

Figure 29. T-Jump/FTIR Data for 2-Picrylpropane at 484°C and 20 Atm Ar.

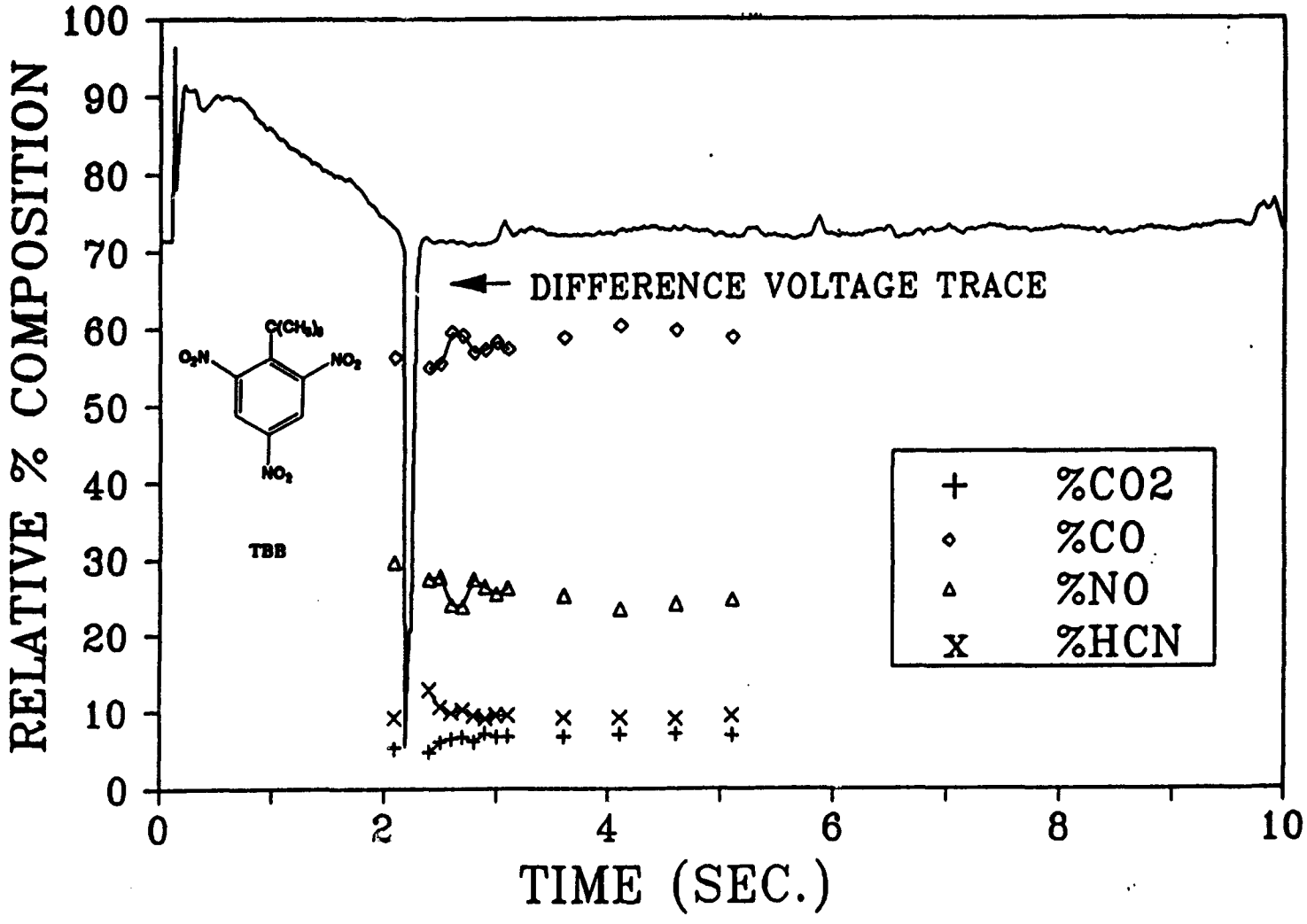

Figure 30. T-Jump/FTIR Data for 2,4,6-Trinitro-t-butylbenzene at 405°C and 20 Atm Ar.

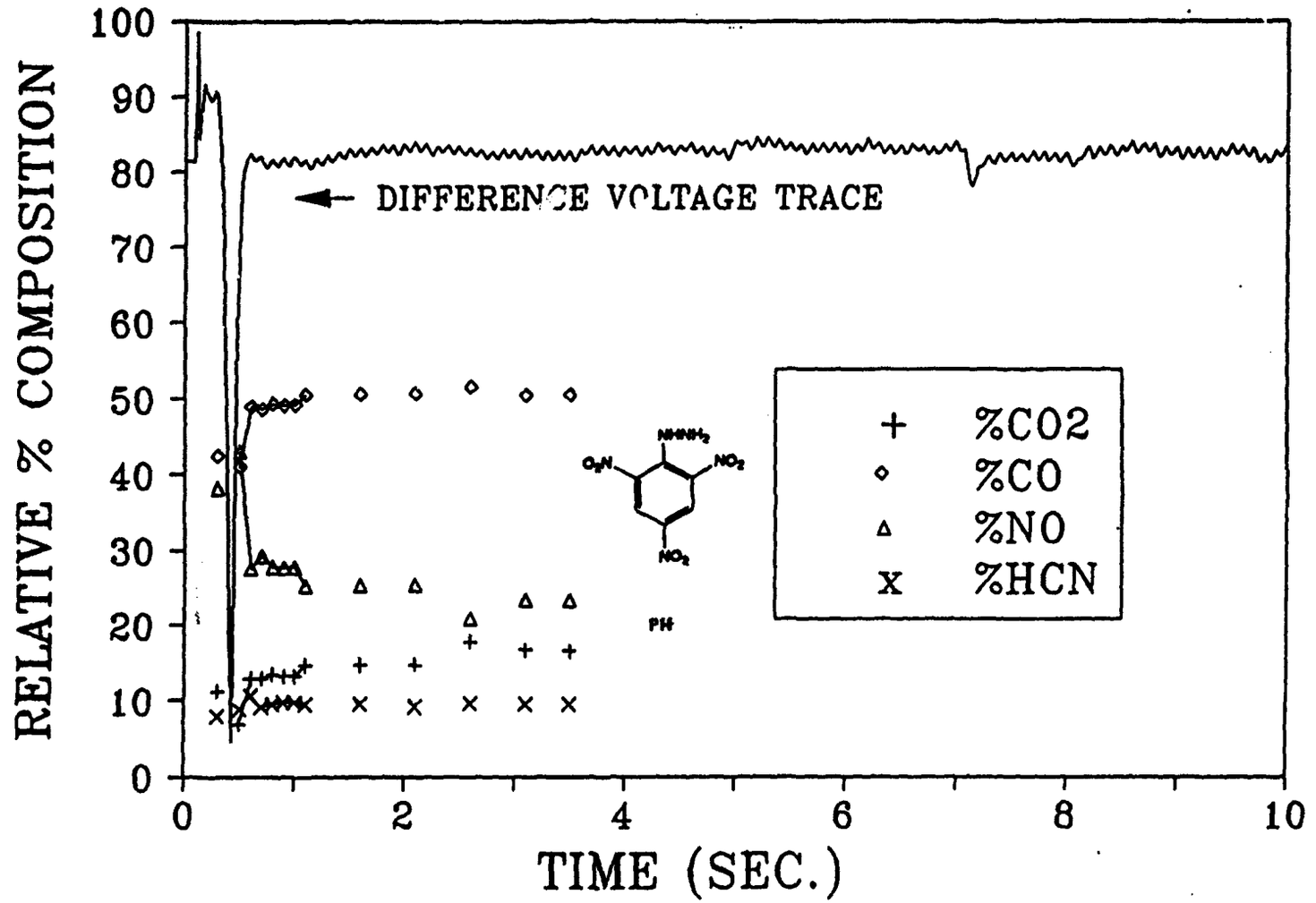

Figure 31. T-Jump/FTIR Data for Picrylhydrazine at 300°C and 20 Atm Ar. Trace H_2O was Present.

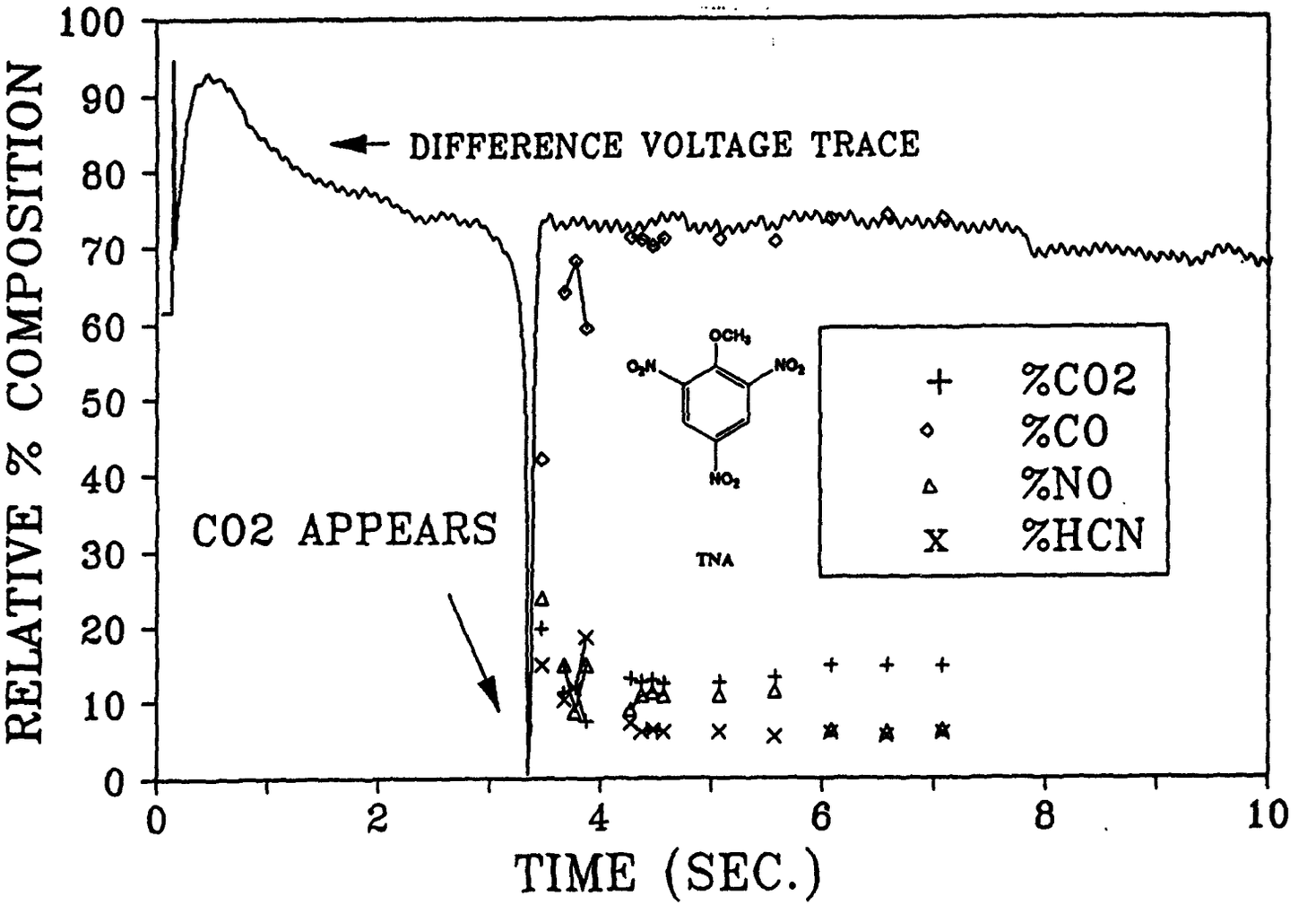

Figure 32. T-Jump/FTIR Data for 2,4,6-Trinitroanisole at 326°C and 20 Atm Ar.

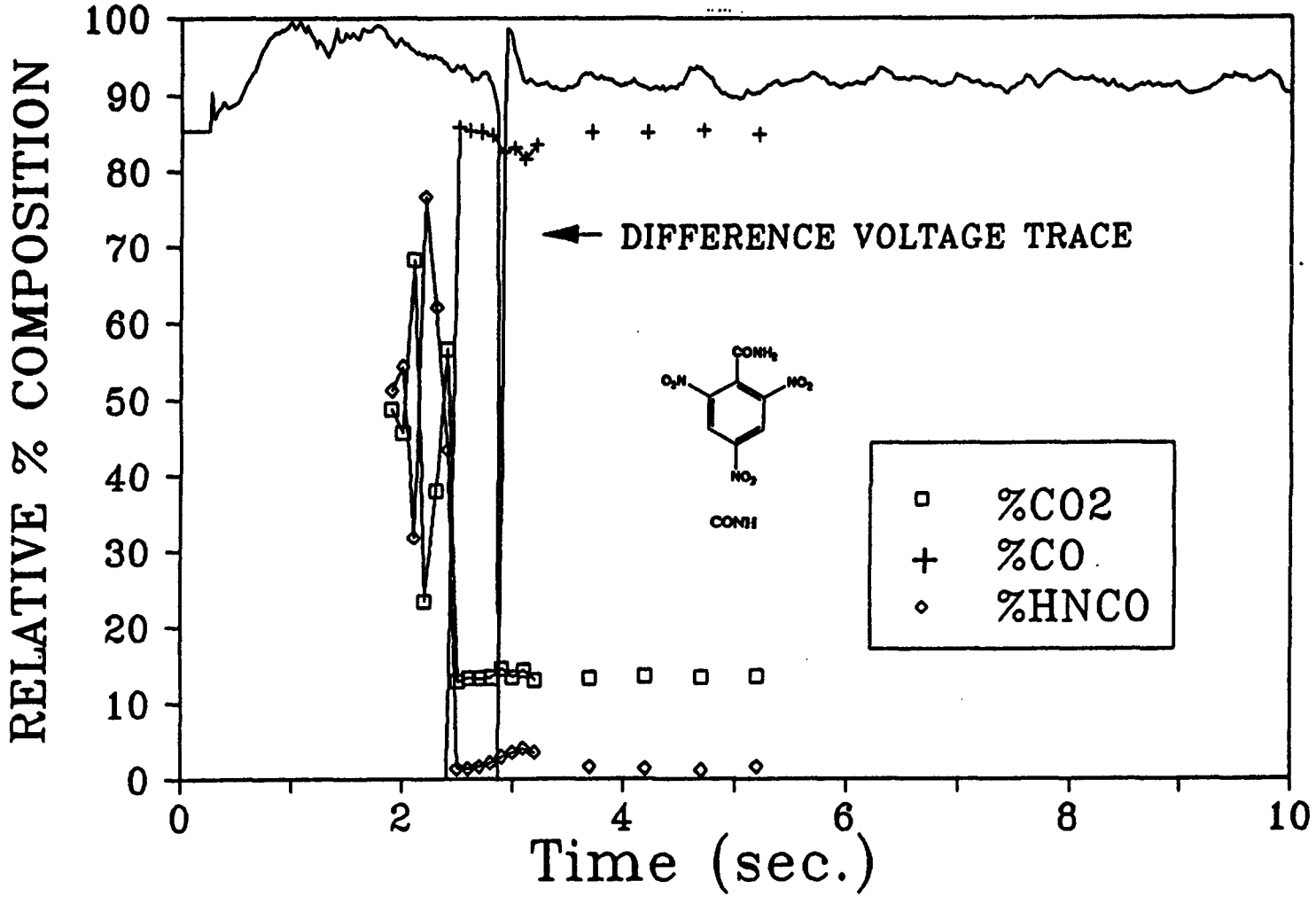

Figure 33. T-Jump/FTIR Data for 2,4,6-Trinitrobenzamide at 510°C and 20 Atm Ar.

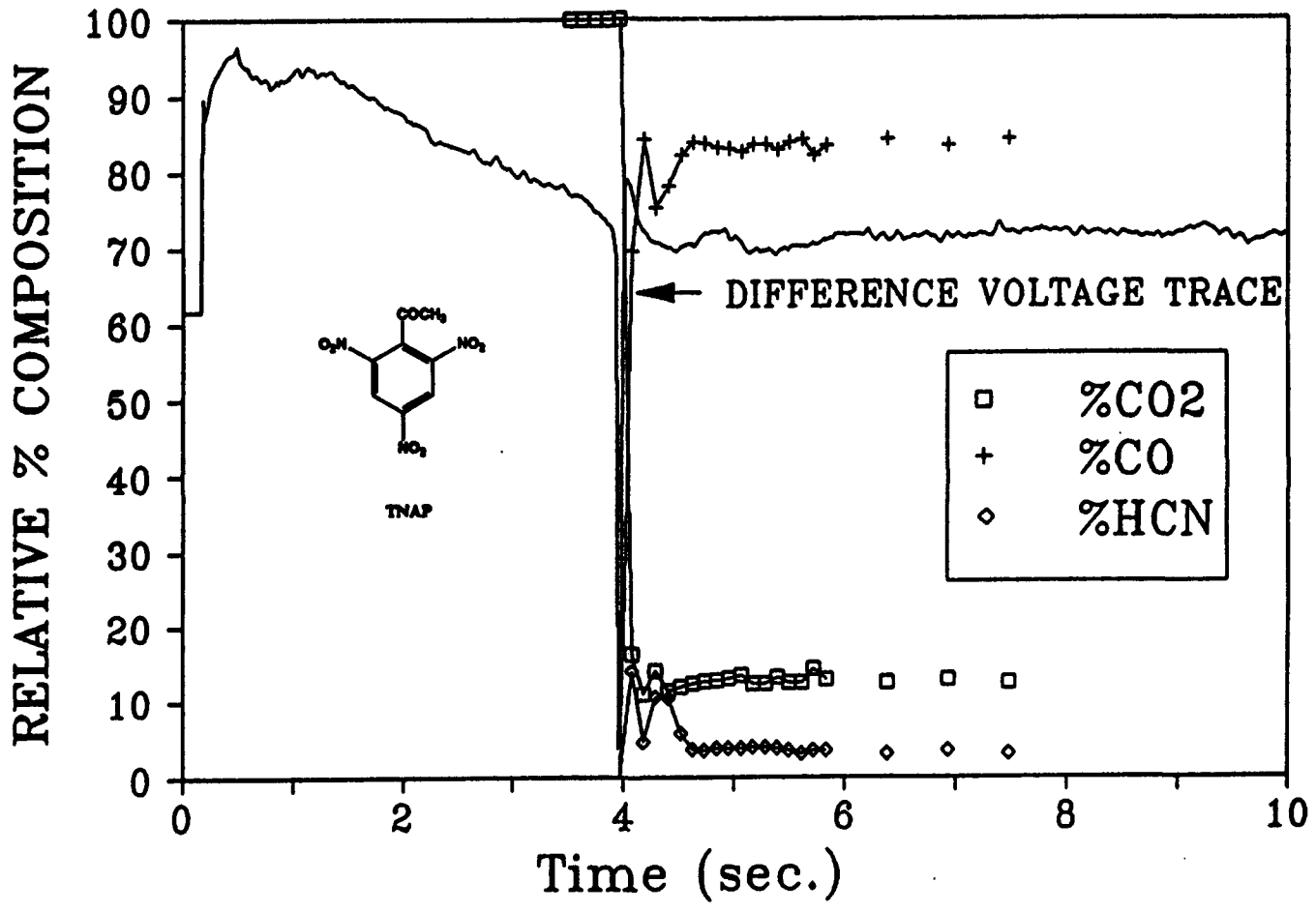

Figure 34. T-Jump/FTIR Data for 2,4,6-Trinitroacetophenone at 506°C and 20 Atm Ar.

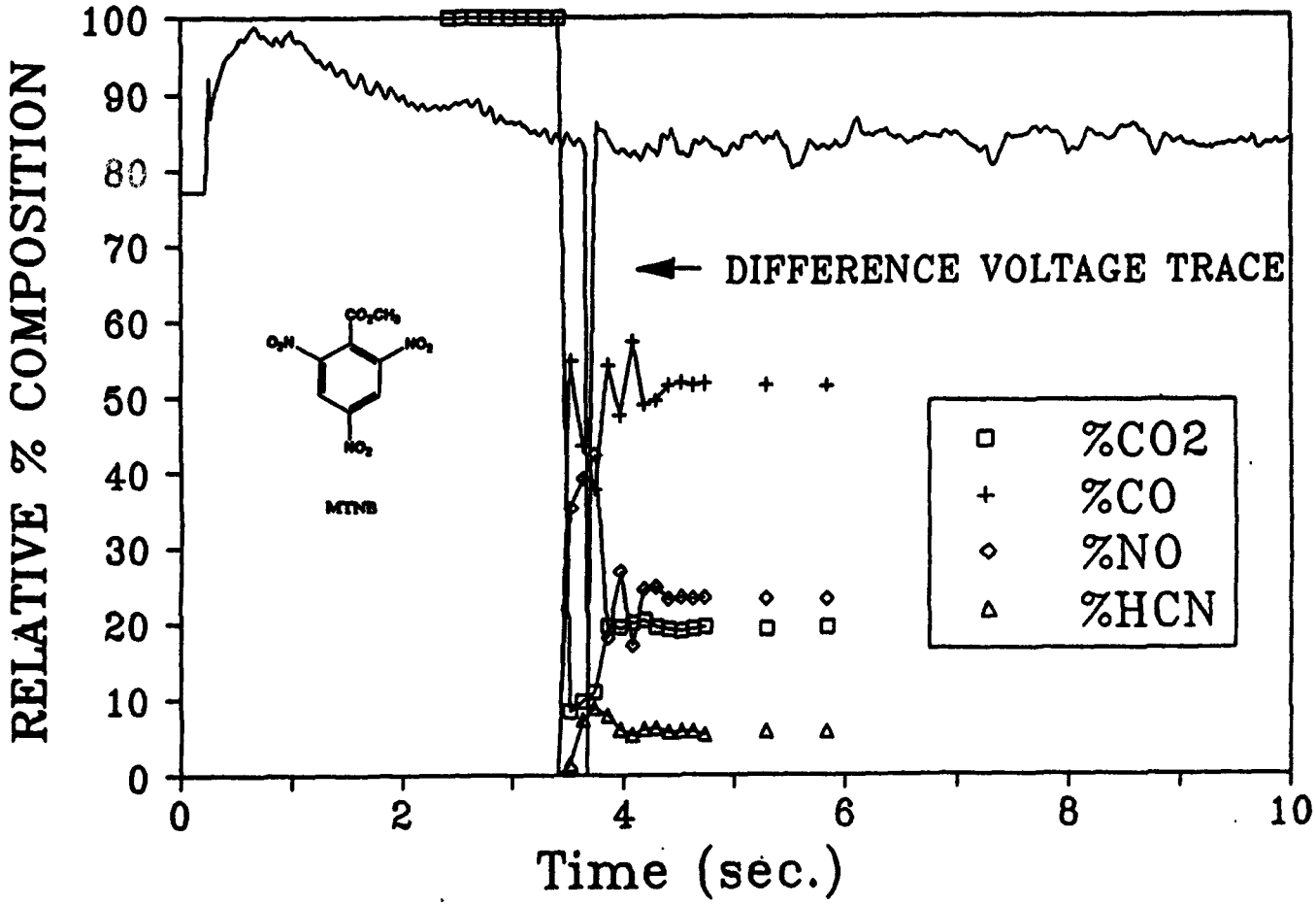

Figure 35. T-Jump/FTIR Data for Methyl 2,4,6-Trinitrobenzoate at 481°C and 40 Atm Ar.

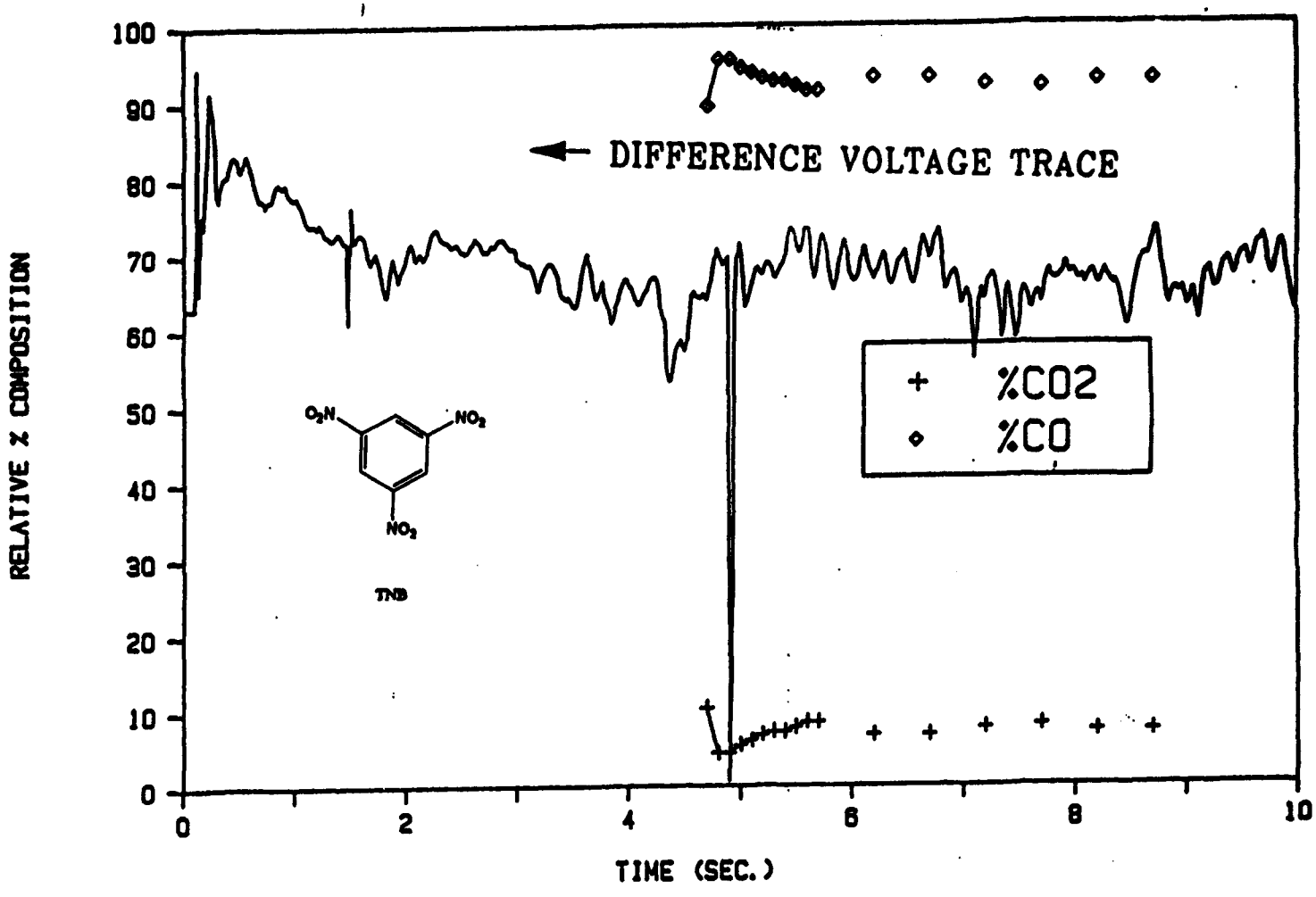

Figure 36. T-Jump/FTIR Data for 1,3,5-Trinitrobenzene at 470°C and 40 Atm Ar.

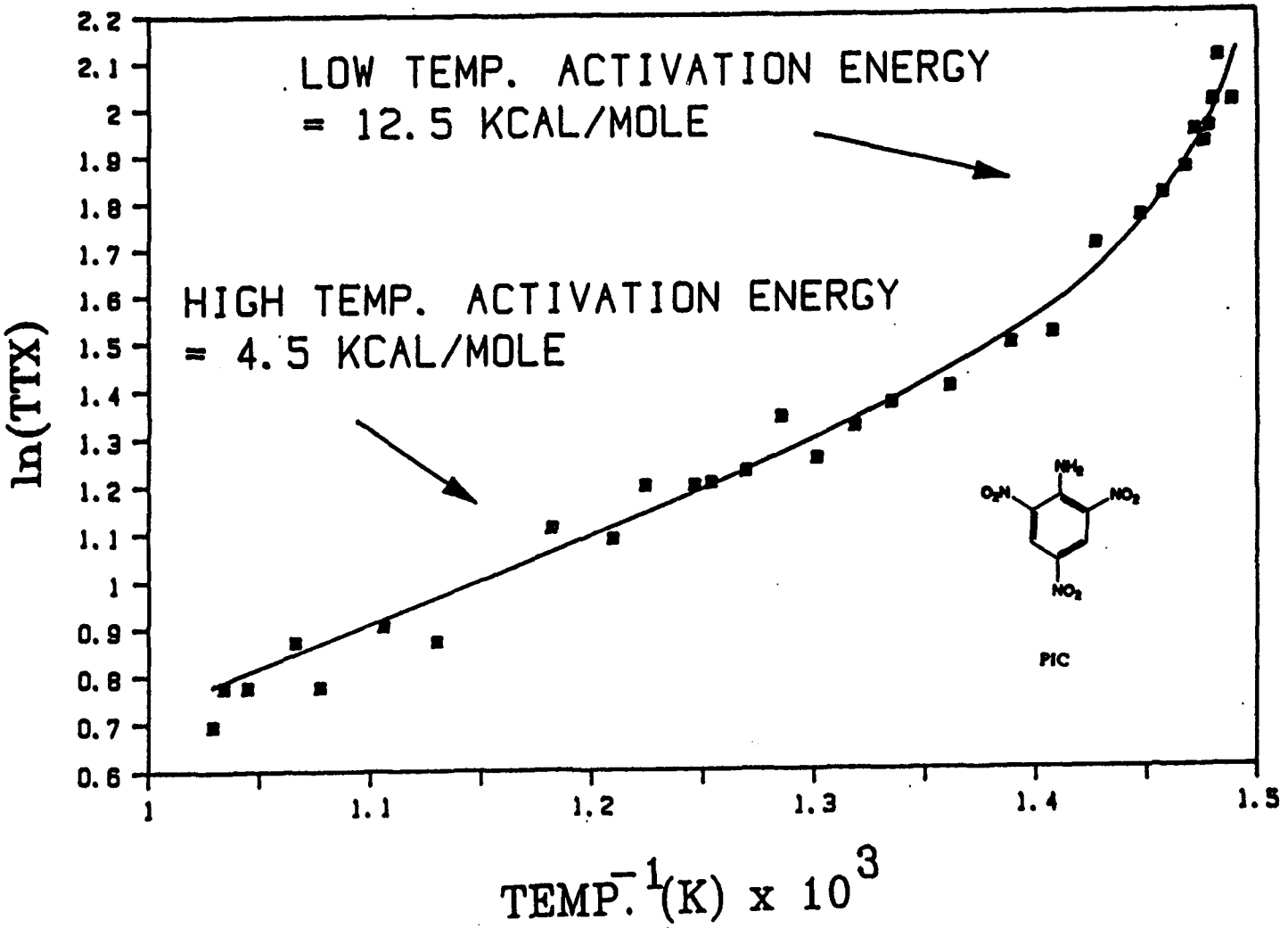

Figure 37. Time-to-Exotherm Data and Apparent Activation Energy of 2,4,6-Trinitroaniline at 10 Atm Ar.

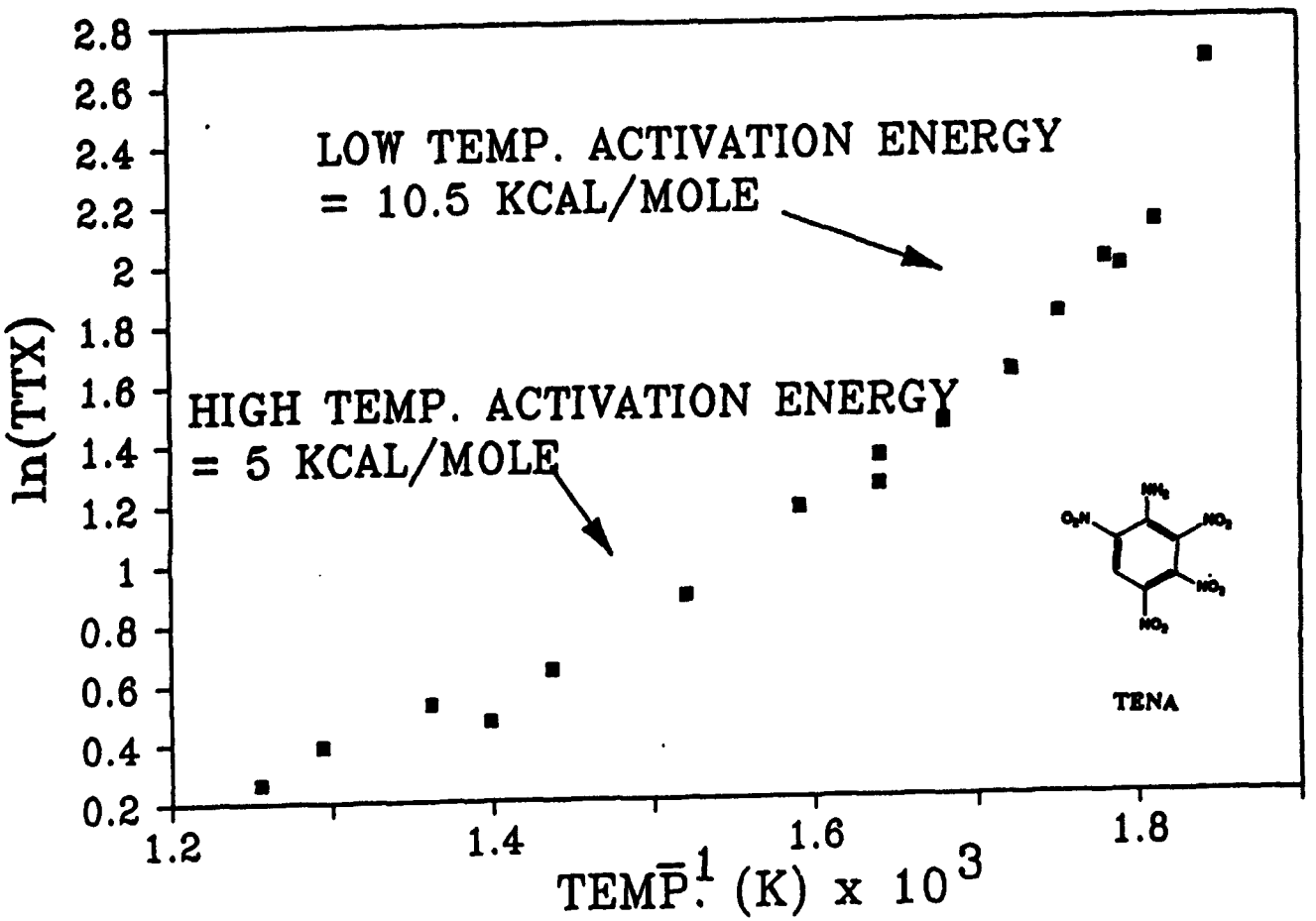

Figure 38. Time-to-Exotherm Data and Apparent Activation Energy of 2,3,4,6-Tetranitroaniline at 10 Atm Ar.

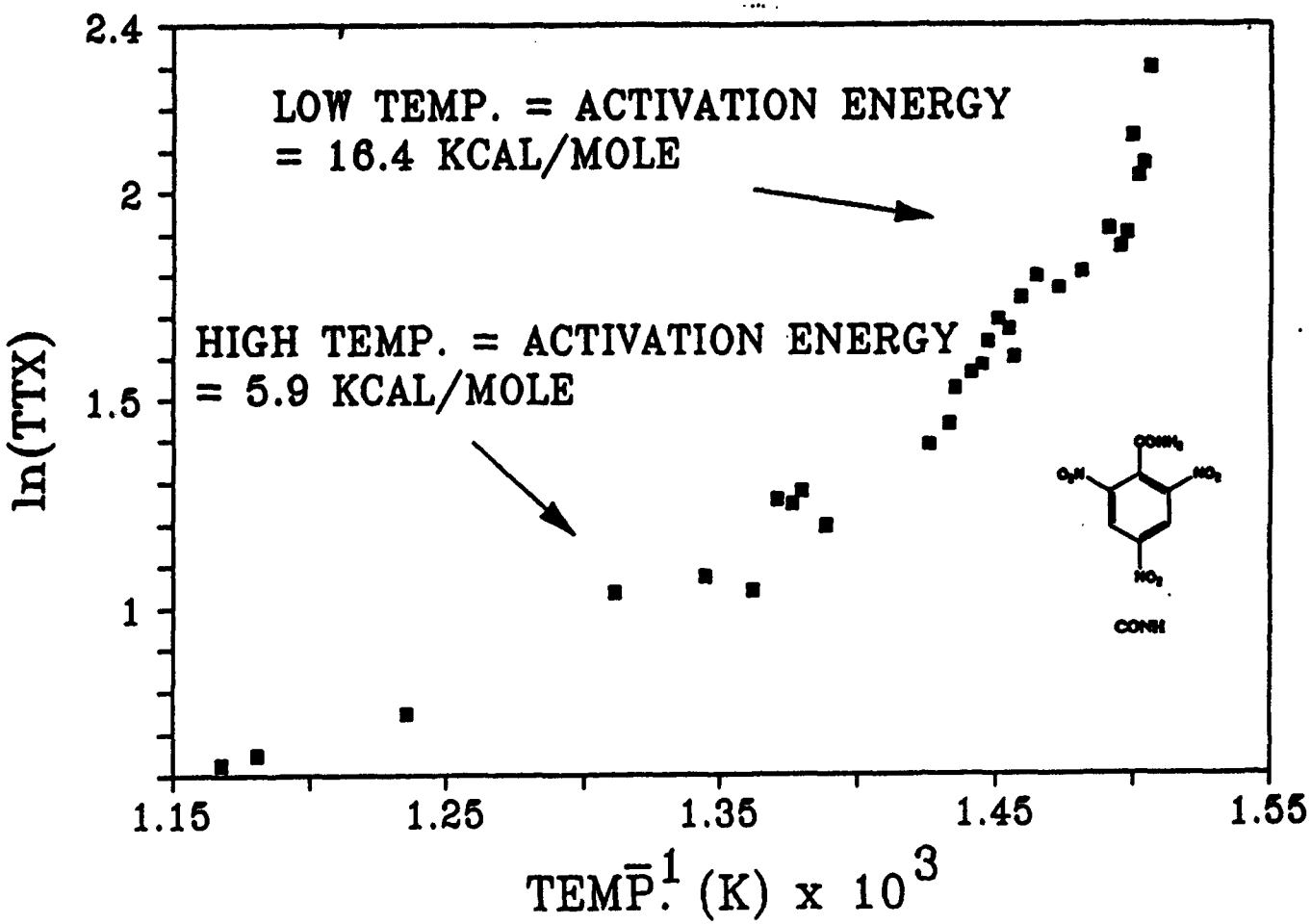

Figure 39. Time-to-Exotherm Data and Apparent Activation Energy of 2,4,6-Trinitrobenzamide at 10 Atm Ar.

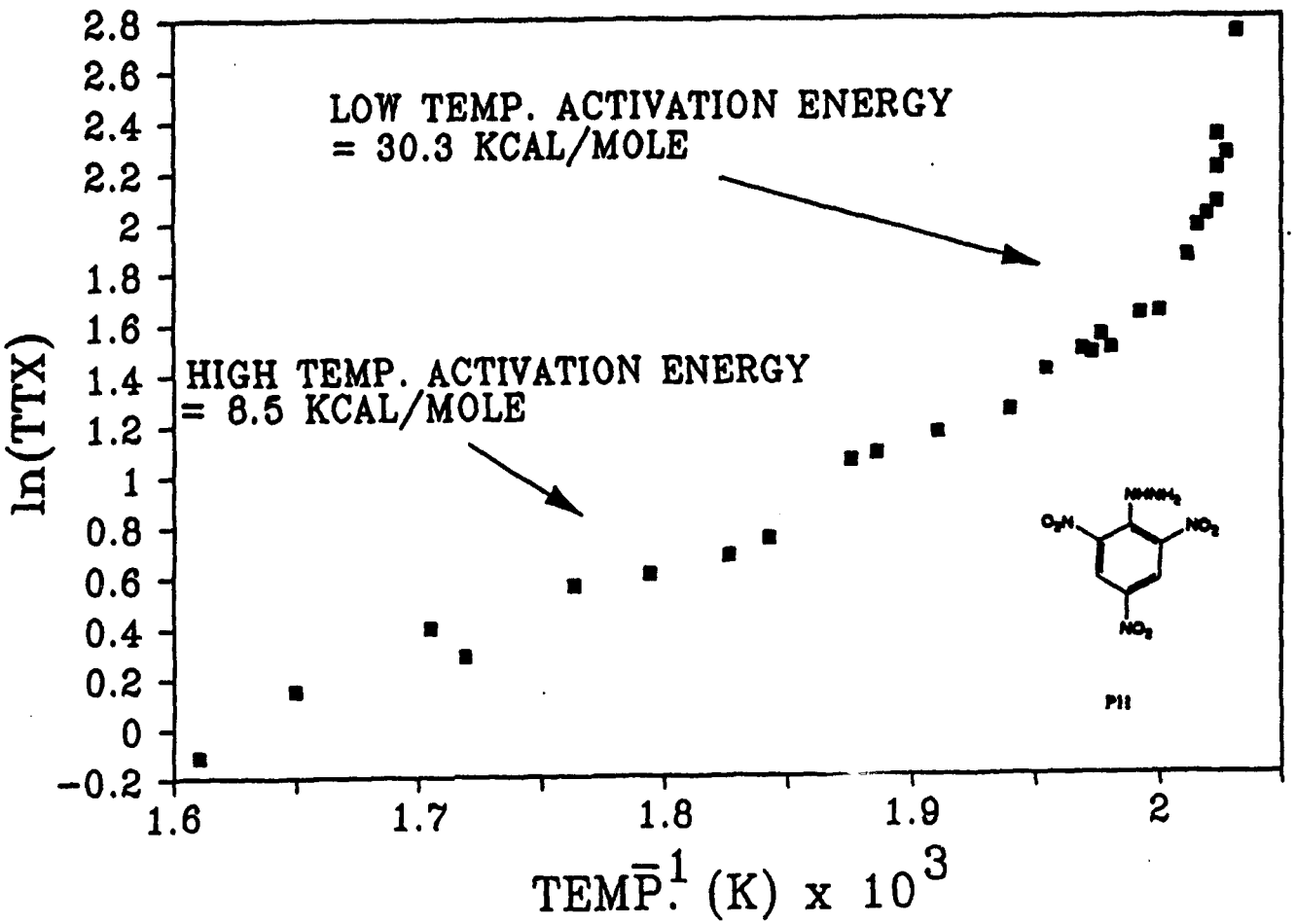

Figure 40. Time-to-Exotherm Data and Apparent Activation Energy of Picrylhydrazine at 10 Atm Ar.

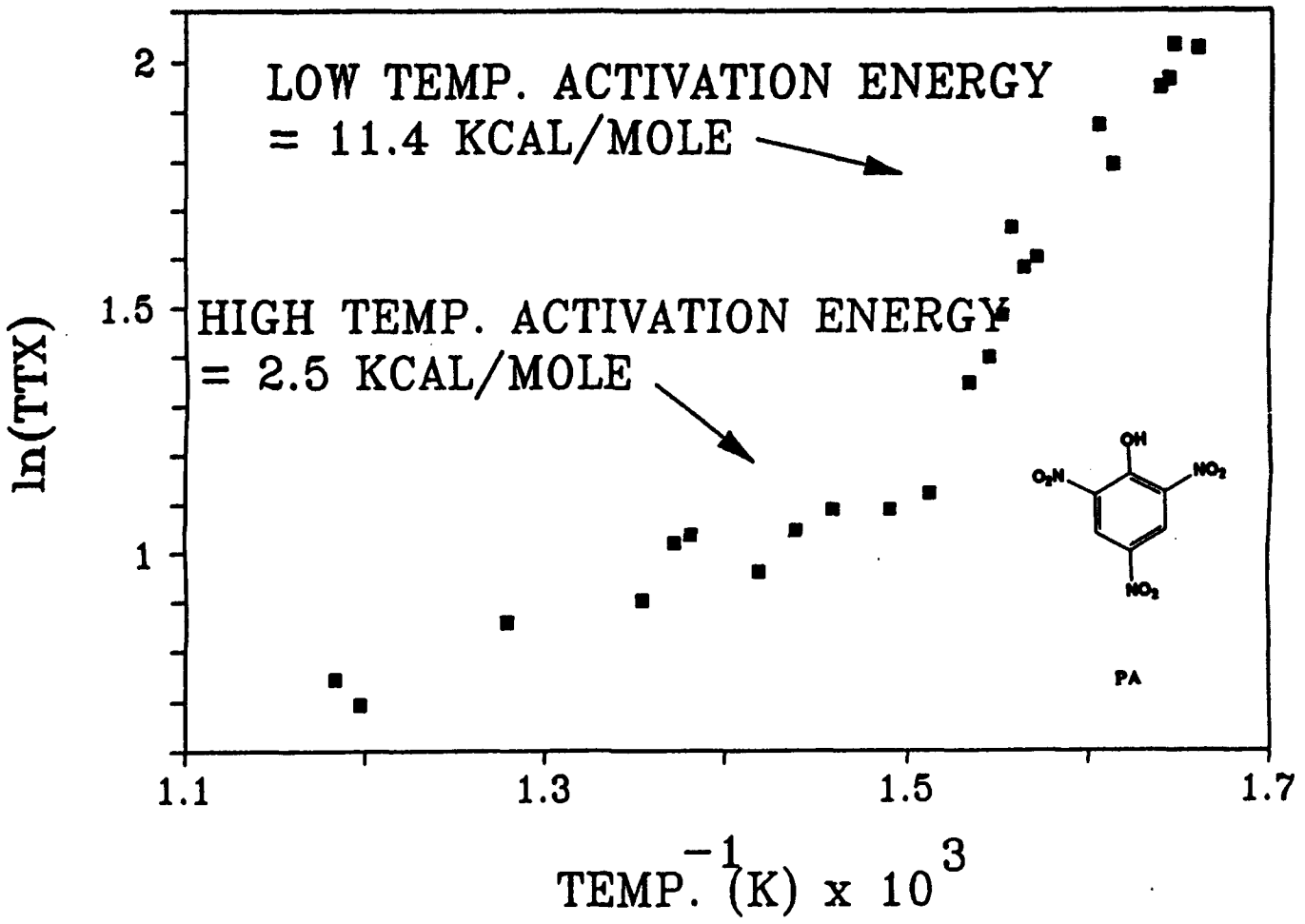

Figure 41. Time-to-Exotherm Data and Apparent Activation Energy of Picric Acid at 10 Atm Ar.

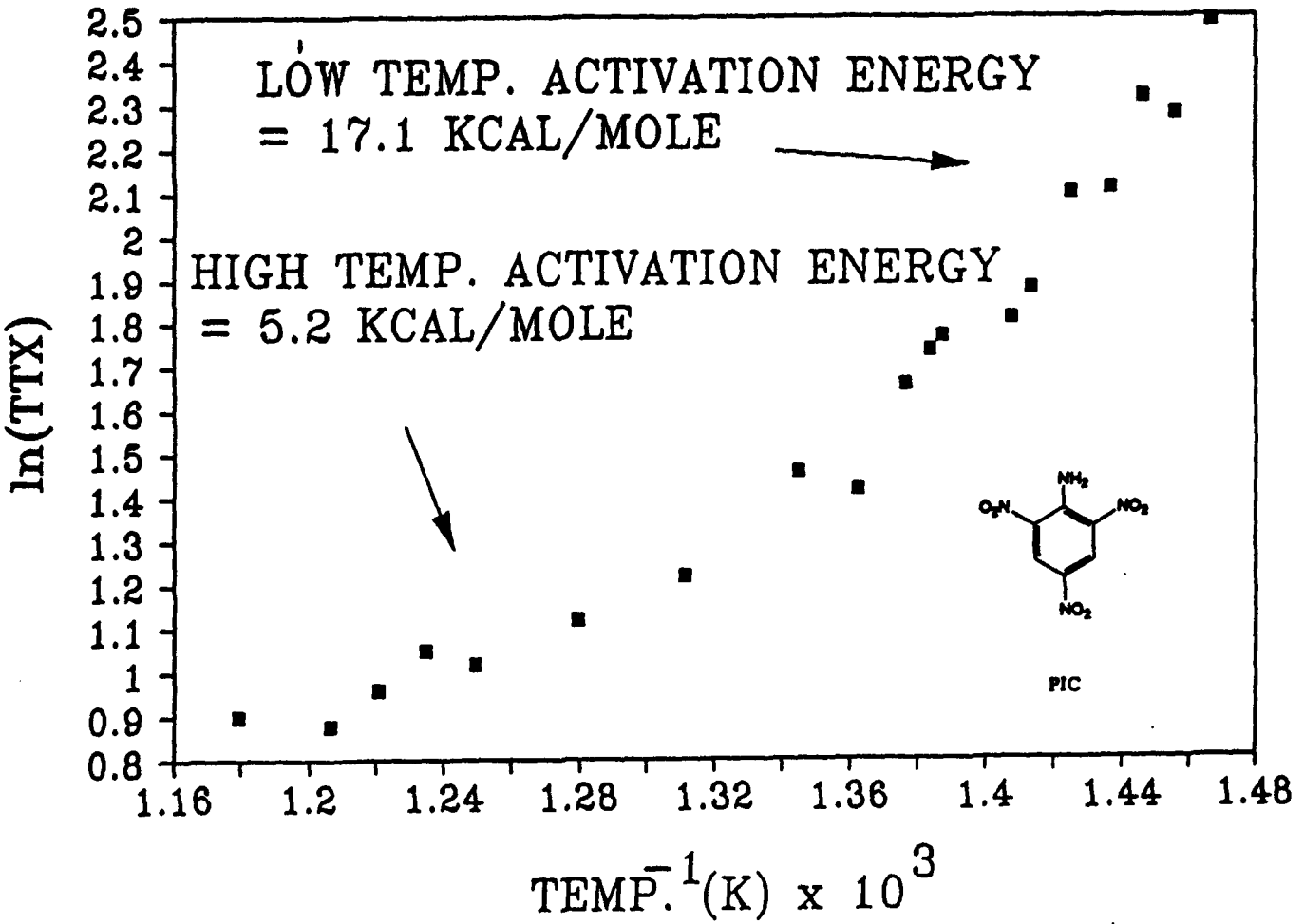

Figure 42. Time-to-Exotherm Data and Apparent Activation Energy of 2,4,6-Trinitroaniline at 20 Atm Ar.

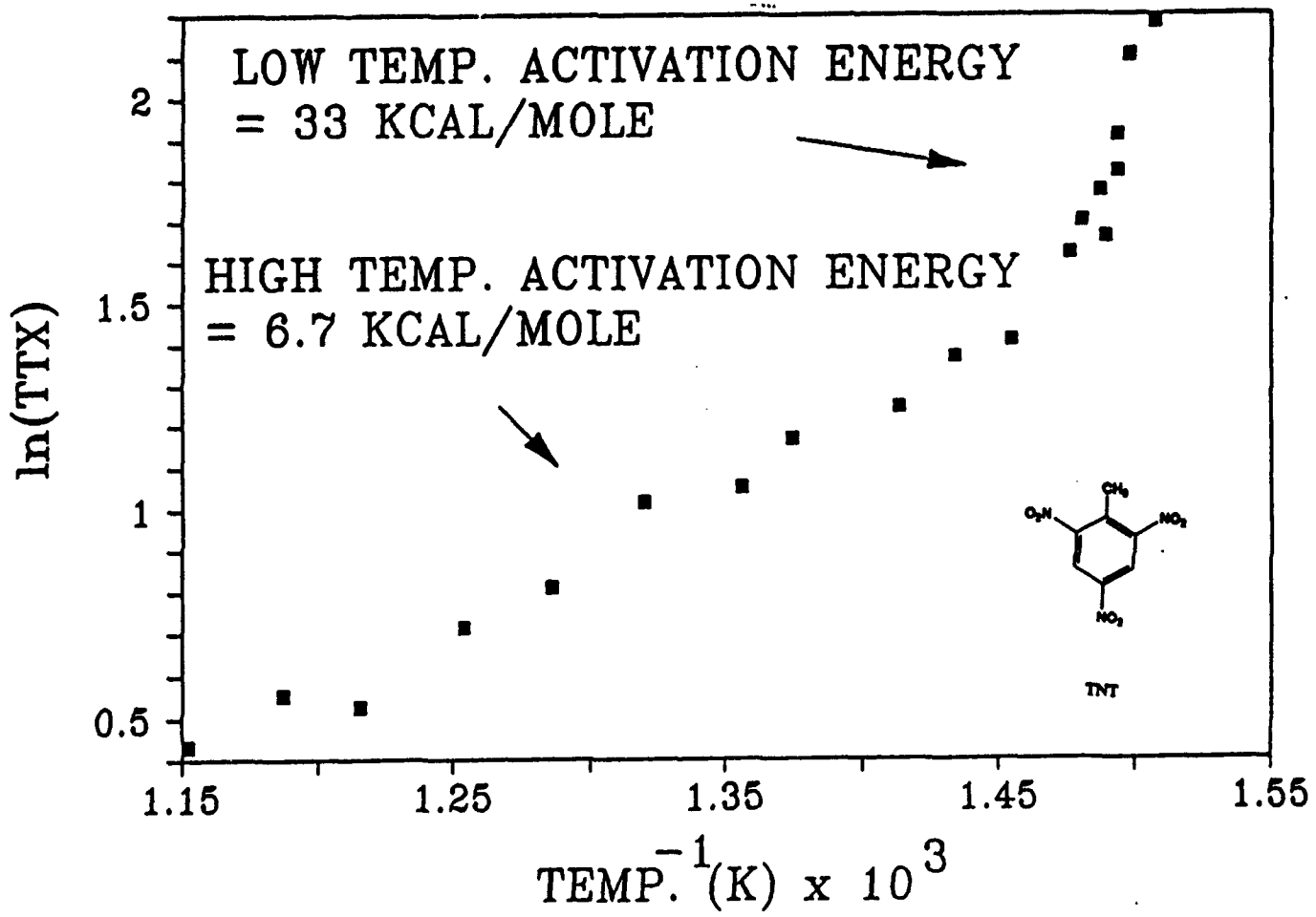

Figure 43. Time-to-Exotherm Data and Apparent Activation Energy of 2,4,6-Trinitrotoluene at 20 Atm Ar.

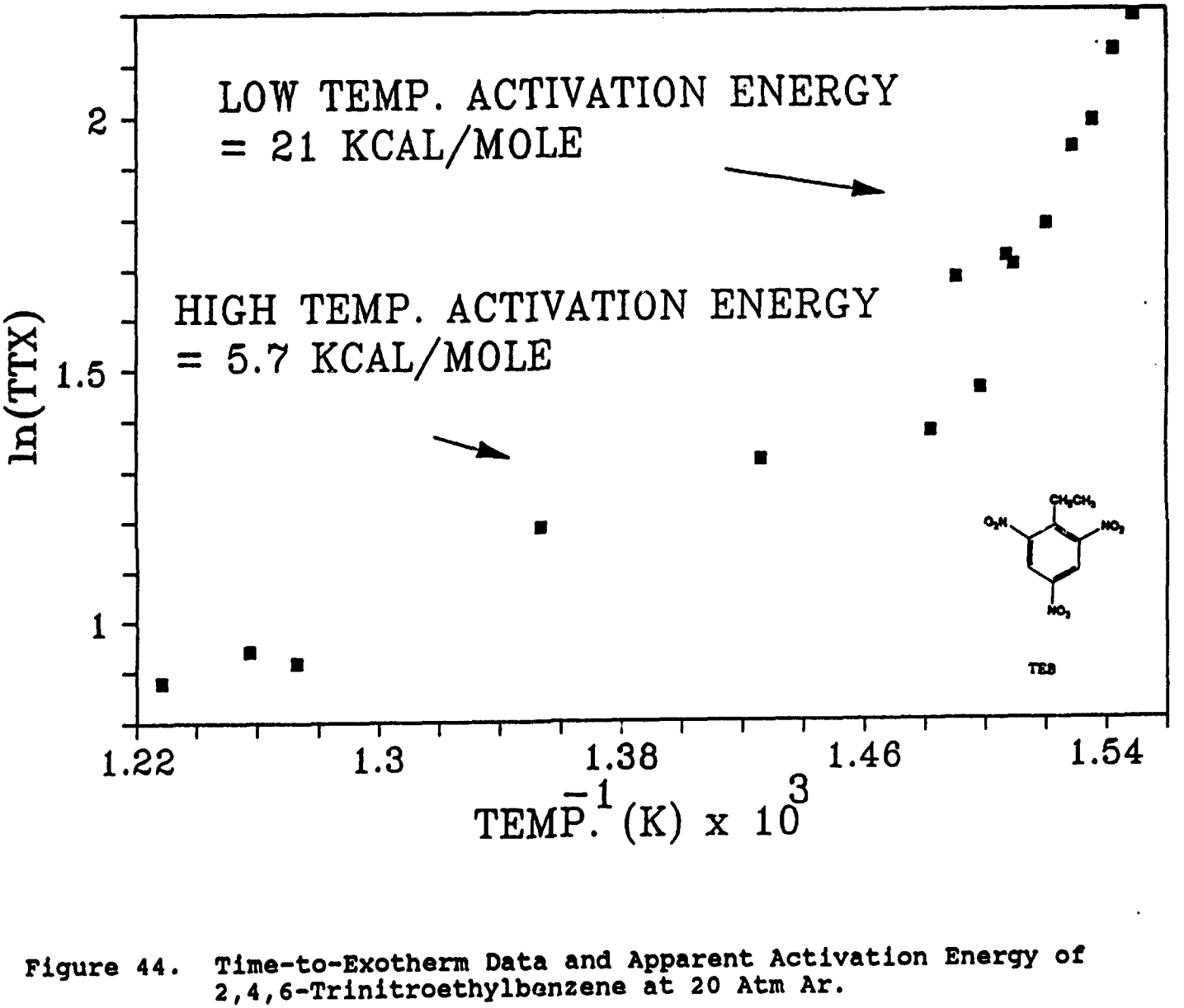

Figure 44. Time-to-Exotherm Data and Apparent Activation Energy of 2,4,6-Trinitroethylbenzene at 20 Atm Ar.

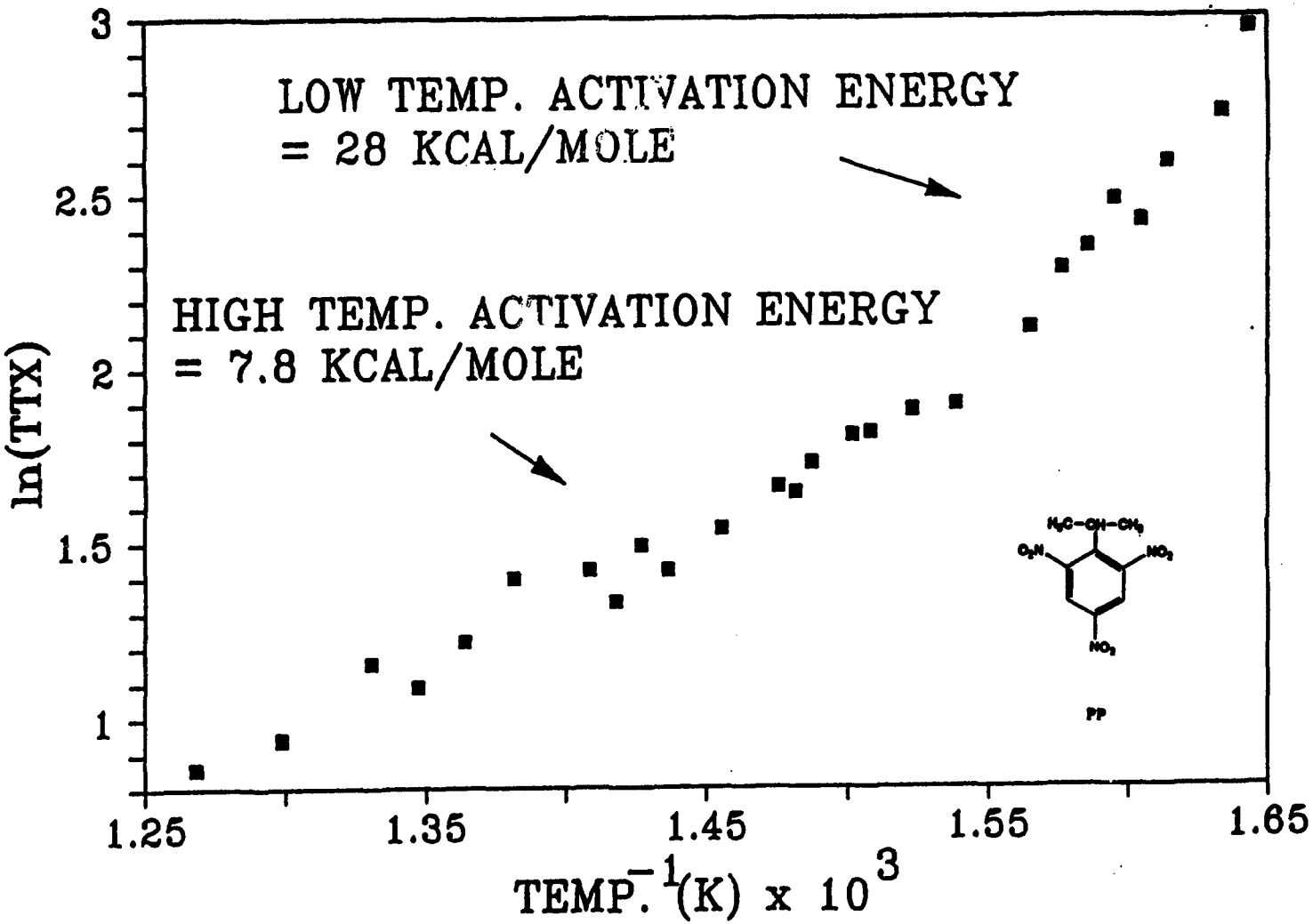

Figure 45. Time-to-Exotherm Data and Apparent Activation Energy of 2-Picrylpropane at 20 Atm Ar.

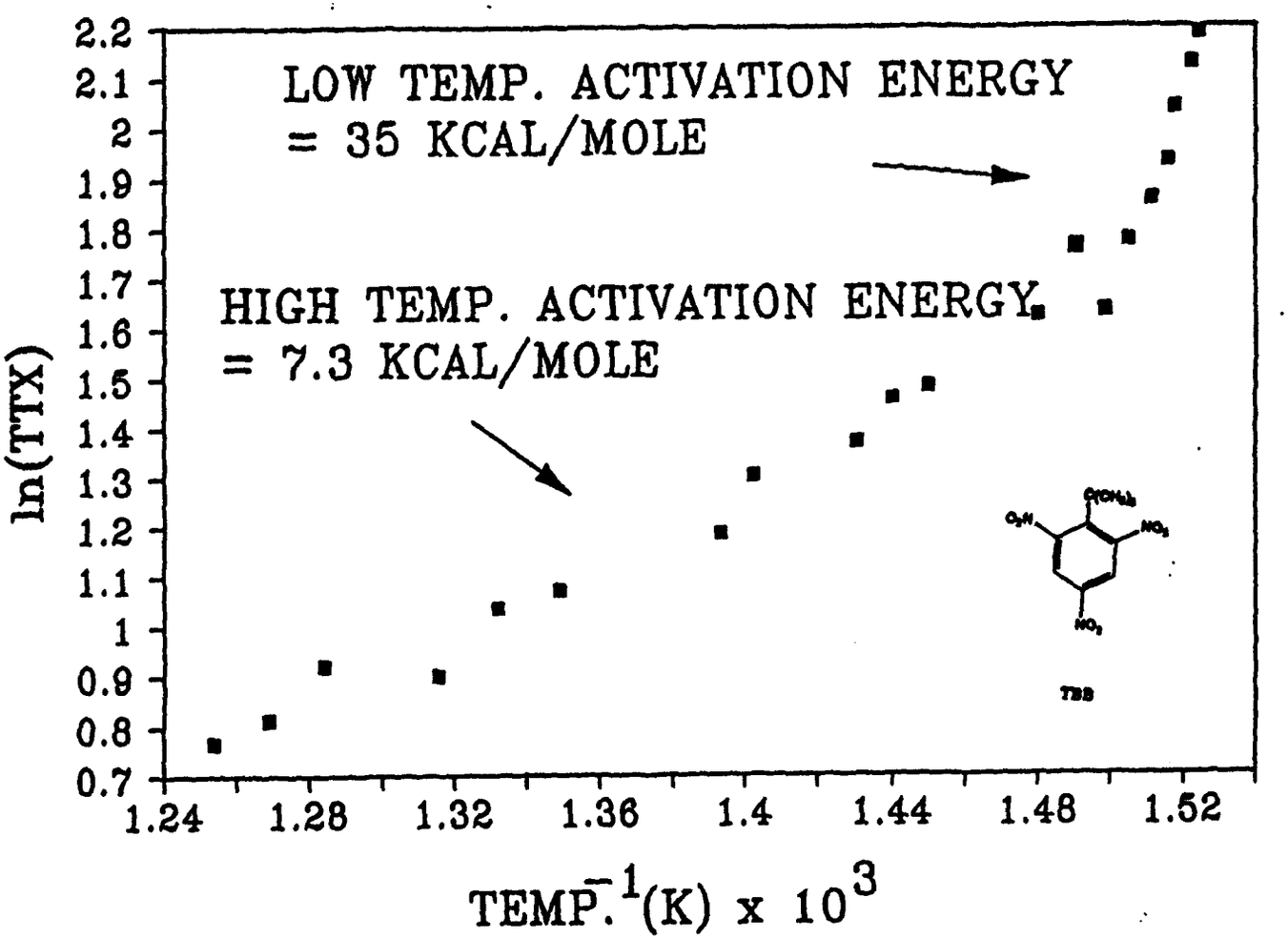

Figure 46. Time-to-Exotherm Data and Apparent Activation Energy of 2,4,6-Trinitro-t-butylbenzene at 20 Atm Ar.

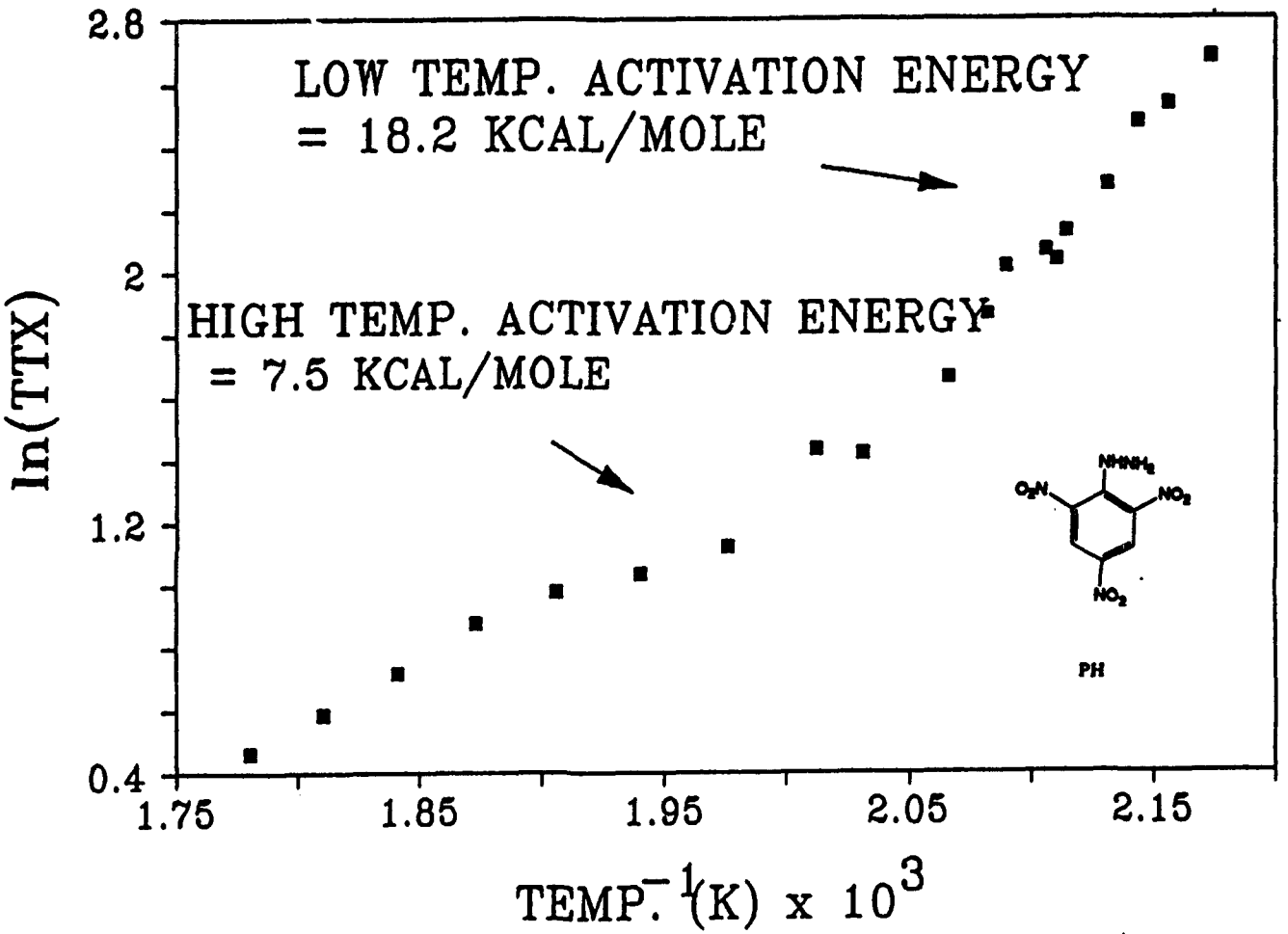

Figure 47. Time-to-Exotherm Data and Apparent Activation Energy of Picrylhydrazine at 20 Atm Ar.

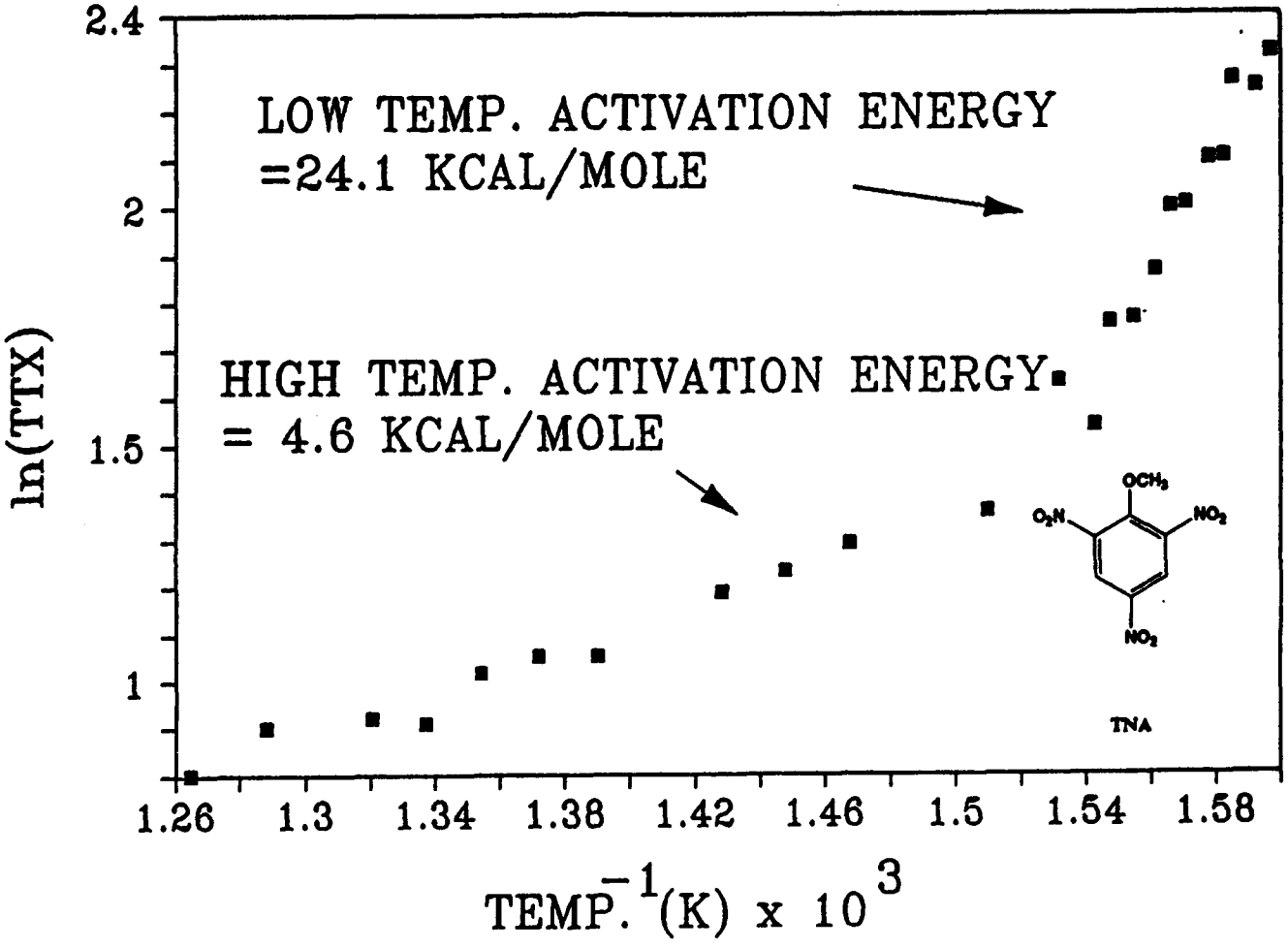

Figure 48. Time-to-Exotherm Data and Apparent Activation Energy of 2,4,6-Trinitroanisole at 20 Atm Ar.

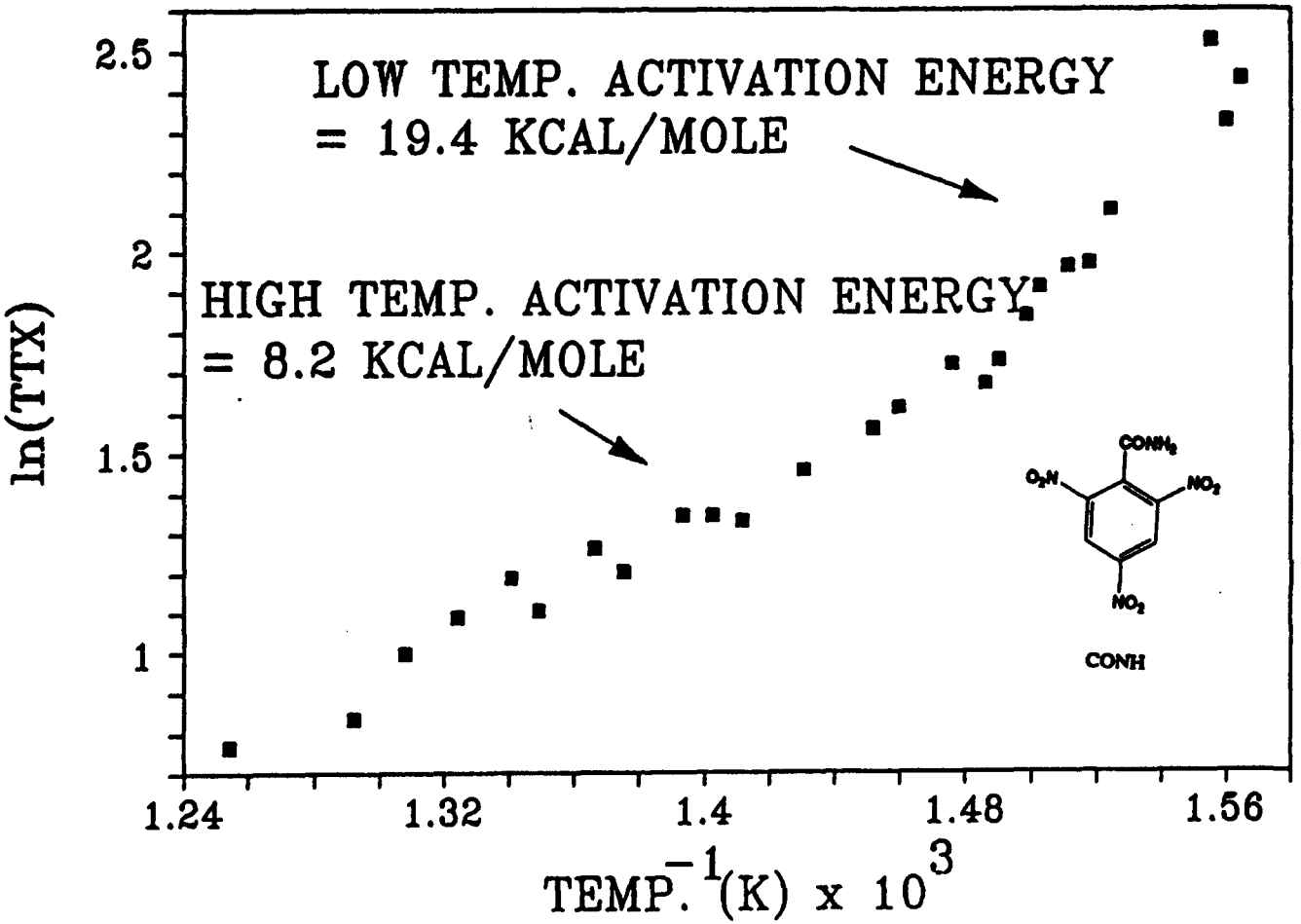

Figure 49. Time-to-Exotherm Data and Apparent Activation Energy of 2,4,6-Trinitrobenzamide at 20 Atm Ar.

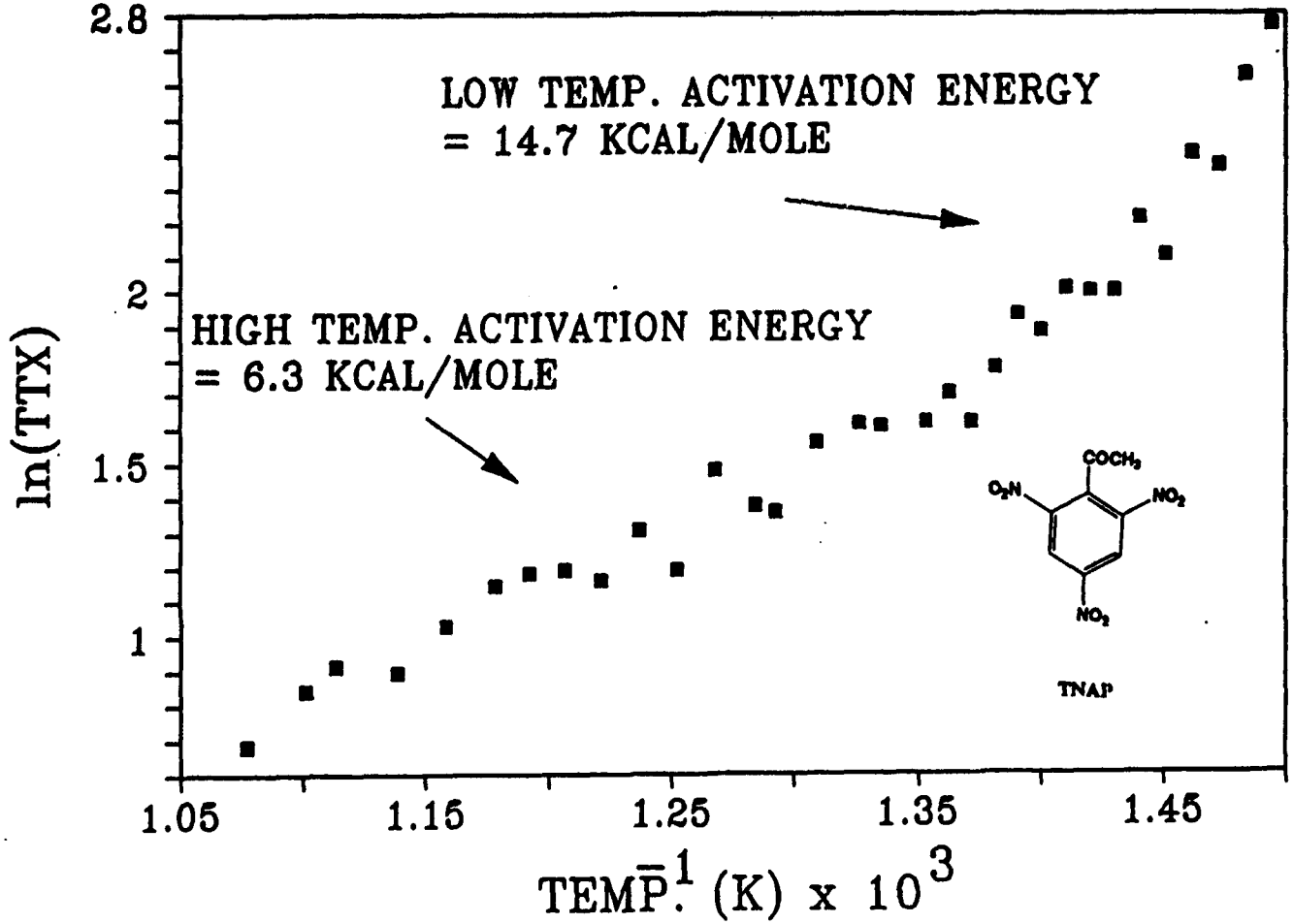

Figure 50. Time-to-Exotherm Data and Apparent Activation Energy of 2,4,6-Trinitroacetophenone at 20 Atm Ar.

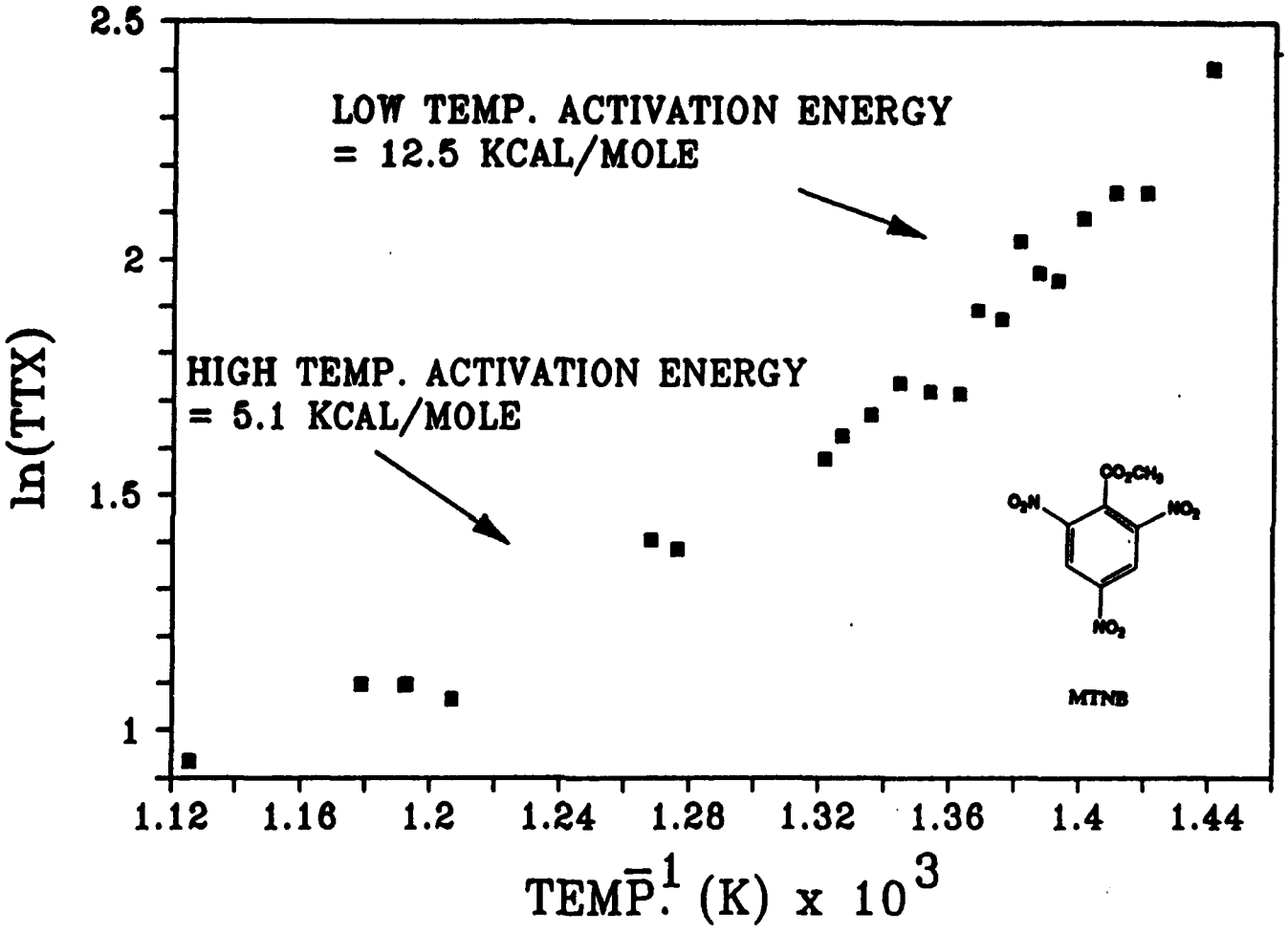

Figure 51. Time-to-Exotherm Data and Apparent Activation Energy of Methyl 2,4,6-Trinitro-t-butylbenzene at 20 Atm Ar.

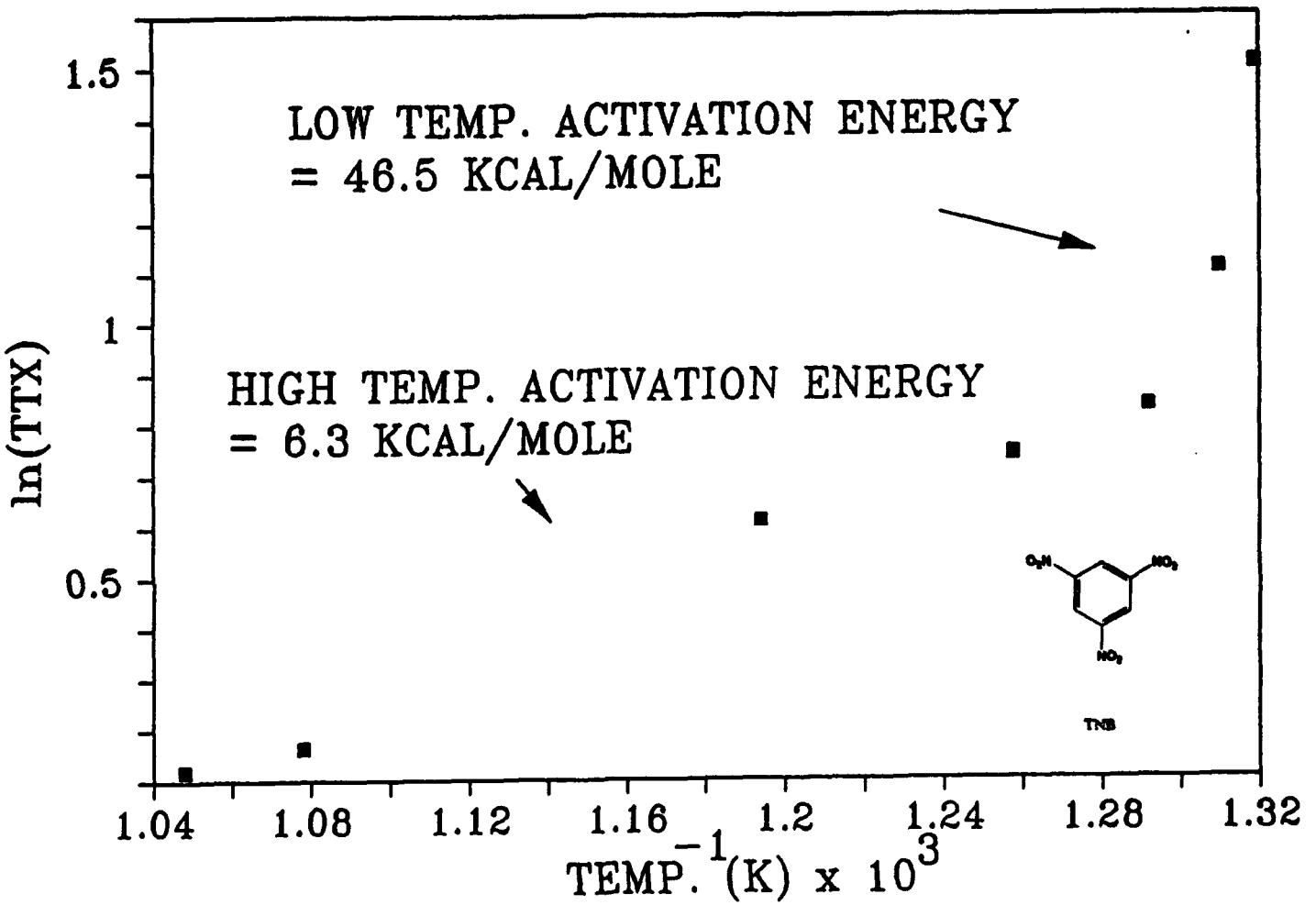

Figure 52. Time-to-Exotherm Data and Apparent Activation Energy of 1,3,5-Trinitrobenzene at 40 Atm Ar.

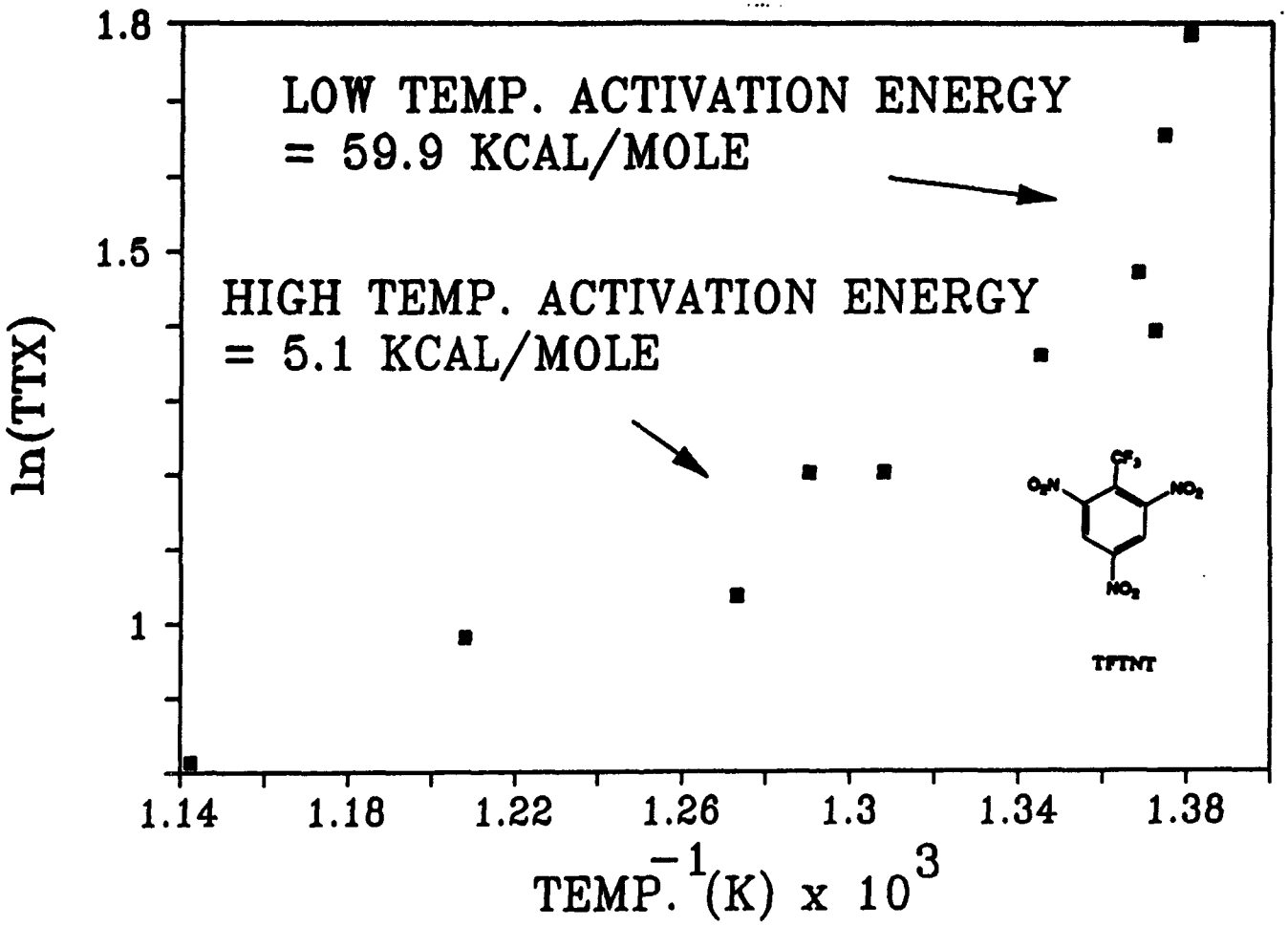

Figure 53. Time-to-Exotherm Data and Apparent Activation Energy of α,α,α,-Trifluoro-2,4,6-trinitrotoluene at 40 Atm Ar.